

Functional replacement of the T-cell receptor in primary human T cells for the treatment of refractory adenovirus infections



Dissertation
der Fakultät für Biologie der
Ludwig-Maximilians-Universität München

vorgelegt von

Tanja Andrea Stief

München 2021

Functional replacement of the T-cell receptor in primary human T cells for the treatment of refractory adenovirus infections

Dissertation

zur Erlangung des Doktorgrades der Naturwissenschaften

Doctor rerum naturalium (Dr. rer. nat.)

an der Fakultät für Biologie

der Ludwig-Maximilians-Universität München

Tag der Abgabe: 07.10.2021

Tag der mündlichen Prüfung: 04.04.2022

Erstgutachter: Prof. Dr. Heinrich Leonhardt

Zweitgutachter: PD Dr. Josef Mautner

Diese Dissertation wurde angefertigt

unter der Leitung von Prof. Dr. Heinrich Leonhardt
im Bereich der Humanbiologie und Biomedizin
an der Ludwig-Maximilians-Universität München

und

unter der Anleitung von Prof. Dr. Tobias Feuchtinger
am Dr. von Hauner'schen Kinderspital,
Klinikum der Universität München

vorgelegt von
Tanja Andrea Stief
aus München
im Jahr 2021

Meinen Eltern

List of contents

1. Abstract	7
2. Zusammenfassung.....	8
3. Introduction	9
3.1. Structure and function of the human T-cell receptor	9
3.2. Human Adenoviruses have highly conserved capsid proteins that can elicit cross-reactive, protective immune responses.....	13
3.3. Treatment of viral infections following stem cell transplantation.....	15
3.4. CRISPR/Cas9-mediated genetic engineering of primary human T cells.....	17
3.5. Identification of two novel LTDL-specific T-cell receptors	20
4. Objective	22
5. Material and Methods.....	23
5.1. Material	23
5.1.1. Antibodies and dyes	23
5.1.2. Reagents.....	24
5.1.3. Cell culture media and reagents	25
5.1.4. Commercial kits.....	26
5.1.5. Oligonucleotides.....	26
5.1.6. Plasmids and templates	27
5.1.7. Equipment	27
5.1.8. Software	28
5.1.9. Consumables	28
5.1.10. Primary cells	28
5.1.11. Stable cell lines.....	29
5.2. Methods	30
5.2.1. Isolation and activation of primary human T cells	30
5.2.2. TCR template design	30
5.2.3. CRISPR/Cas9-mediated TCR editing	31
5.2.4. Retroviral transduction	32
5.2.5. Streptamer and antibody staining.....	32
5.2.6. PCR for TCR editing validation.....	33
5.2.7. Whole-genome analysis	33

5.2.8.	Phenotypic characterization	34
5.2.9.	Effector marker expression	34
5.2.10.	Intracellular cytokine staining	35
5.2.11.	Magnetic isolation of LTDL-specific T cells	35
5.2.12.	Cytotoxic killing assay	36
5.2.13.	T-cell proliferation and cytokine release	36
5.2.14.	Quantification and statistical analysis	37
6.	Results	38
6.1.	Functional disruption of the endogenous T-cell receptor	38
6.2.	Identification of CRISPR/Cas9-induced off-target events	42
6.3.	Highly functional and target-specific LTDL-specific T-cell receptors	49
6.4.	Functional TCR replacement using virus-free CRISPR/Cas9 engineering generates LTDL-specific T cells	52
7.	Discussion	57
7.1.	Safe and highly efficient KO of TCRs in primary human T cells using virus-free CRISPR/Cas9	57
7.2.	Redirecting human T cells towards highly functional LTDL-specific CTLs for adoptive T-cell transfer	61
	References	66
	Appendix	78
	Abbreviations	78
	Sequences	80
	List of figures	83
	List of tables	84
	Eidesstattliche Versicherung	85
	Danksagung	86

1. Abstract

Adenoviral (AdV) infections can cause life-threatening infections, especially in paediatric patients, following haematopoietic stem cell transplantations due to transient lacking T-cell immunity. AdV hexon-protein derived peptide LTDLGQNLLY (LTDL)-specific T cells have proven to induce cross-reactive protection, thus being highly attractive targets for adoptive T-cell transfer (ACT). The aim of this project was to redirect primary human T cells by replacing endogenous T-cell receptors (TCRs) with a LTDL-specific TCR using CRISPR/Cas9 technology. Simultaneous knock out (KO) of the complete endogenous TCR will prevent harmful TCR mispairing and alloreactivity.

Stable and highly efficient genetic KO of the endogenous TCR in primary human T cells was confirmed on protein as well as on genetic level. TCR-KO T cells are phenotypically very similar to unedited cells but fail to produce IFN γ upon stimulation, thereby functionally demonstrating TCR disruption. Whole-genome sequencing of CRISPR/Cas9-edited cells revealed no significant increase of mutations, although analysis of predicted gRNA-dependent off-target sites revealed two putative off-target mutations for the gRNA targeting TCR β chain. Functional analysis of two novel LTDL-specific TCRs revealed strong, target-specific effector functions for both of them. CRISPR/Cas9-mediated knock in (KI) using non-viral delivery of one protective LTDL-specific TCR rescued IFN γ production upon LTDL-specific stimulation and demonstrated LTDL-specific cytotoxic capacity, cytokine secretion and proliferation. The targeted and in-frame integration into the endogenous TCR α chain was combined with an additional KO of the β chain to prevent TCR mispairing and enables expression under the control of the endogenous promoter.

In conclusion, redirecting primary human T cells by replacing endogenous TCRs with a LTDL-specific TCR using CRISPR/Cas9 is feasible, resulting in target-specific cytotoxic T cells with strong effector functions. The combined TCR KO/KI procedure could outcompete transduction based conventional TCR editing strategies and therefore presents a safe and powerful tool for the treatment of refractory viral infections in the immunocompromised host.

2. Zusammenfassung

Fehlende T-Zellimmunität in Folge einer Stammzelltransplantation kann vor allem in pädiatrischen Patienten zu lebensbedrohlichen Infektionen durch Adenoviren (AdV) führen. T-Zellen, die das AdV-spezifische Peptid LTDLGQNLLY (LTDL) erkennen, können vor verschiedenen AdV-Infektionen schützen und sind daher für den adoptiven T-Zell Transfer gut geeignet. Ziel dieser Arbeit war es, mit Hilfe der CRISPR/Cas9-Technologie den endogenen T-Zell Rezeptor (TCR) in primären humanen T-Zellen durch einen LTDL-spezifischen TCR zu ersetzen und somit LTDL-spezifische T-Zellen zu generieren. Gleichzeitiger „Knock-out“ des endogenen TCR verhindert eine potenziell schädliche Kombination aus eingebrachtem und endogenem TCR.

Ein stabiler und sehr effizienter genetischer „Knock-out“ des endogenen TCR in primären humanen T-Zellen wurde sowohl auf genetischer als auch auf Protein-Ebene nachgewiesen. T-Zellen mit TCR „Knock-out“ unterscheiden sich phänotypisch kaum von unbehandelten Zellen, jedoch sind sie nach Stimulation nicht mehr in der Lage IFN γ zu produzieren, was einen „Knock-out“ auch auf funktioneller Ebene bestätigt. Eine Genom-Sequenzierung der bearbeiteten Zellen zeigte keine erhöhte Mutationsrate im Vergleich zu Kontrollzellen. Allerdings hat die Analyse von vorhergesagten „Off-target“ Bereichen zwei Mutationen in Zellen entdeckt, in denen die TCR β -Kette ausgeschaltet wurde. Die funktionelle Charakterisierung zweier neuer LTDL-spezifischer TCRs hat gezeigt, dass beide eine starke und Antigen-spezifische Effektor-Funktion aufweisen. Mit Hilfe der CRISPR/Cas9-Methode wurde ein wirksamer LTDL-spezifischer TCR ohne die Verwendung eines viralen Vektors in T-Zellen eingebaut, welche in Folge einer LTDL-spezifischen Stimulation erfolgreich proliferierten, Zytokine produzierten und zytotoxische Aktivität demonstrierten. Die gezielte und gerichtete Integration in die endogenen TCR α -Kette ermöglicht eine Expression unter der Kontrolle des endogenen Promoters, während die ausgeschaltete β -Kette eine fehlerhafte Kombination der neuen mit endogenen TCR-Ketten verhindert.

Zusammengefasst hat diese Arbeit gezeigt, dass ein Austausch von endogenen TCRs durch einen LTDL-spezifischen TCR mit Hilfe der CRISPR/Cas9-Methode möglich ist und hoch spezifische, zytotoxische T-Zellen generiert. Die Kombination aus TCR „Knock-out“ und erneutem Einbau könnte sich gegenüber herkömmlichen Strategien als vorteilhaft erweisen und stellt damit ein wichtiges Instrument für die sichere Behandlung refraktärer, viraler Infektionen in Patienten mit beeinträchtigtem Immunsystem dar.

3. Introduction

3.1. Structure and function of the human T-cell receptor

The majority of human T-cell receptors (TCRs) are comprised of α and β chains that form heterodimers with one highly specific antigen-binding site. These two chains have short intracellular domains, therefore require additional molecules for intracellular signalling. Dimeric CD3 molecules (CD3 $\delta\epsilon$ and CD3 $\gamma\epsilon$) and the $\zeta\zeta$ homodimer bind non-covalently to the TCR and enable intracellular signal transduction upon activation of the receptor. Together, these molecules form the functional TCR complex, representing all molecules in a 1:1:1:1 ratio (Call et al., 2004, Wucherpfennig et al., 2010) (**Figure 1 A**). The transmembrane parts of the TCR are formed by the constant regions and are encoded by one gene for TCR α chain constant region (*TRAC*) and two genes for the TCR β chain constant region (*TRBC*), which are largely homologous and functionally identical. The variable regions of the TCR are responsible for antigen recognition and gene rearrangement during T-cell development in the thymus enables great diversity of TCR variable regions. On the TCR α locus, 58 variable (V) and 61 joining (J) gene segments undergo rearrangements to form one variable-domain exon. The TCR β locus contains 2 diversity (D) gene segments additionally to the approximately 65 V and 13 J segments (Lefranc et al., 2014). P- and N nucleotides in the junctions between rearranged V(D)J elements further increase diversity (**Figure 1 B**). The variable regions of α and β chains form hypervariable three-dimensional complementarity determining regions (CDR) which form the antigen-binding pocket. CDR1 and CDR2 are encoded by the V gene segments and are at the outer site, while the highly specific CDR3 loop depends on D and J segments and forms the centre of the binding pocket (Janeway et al., 2001). The TCR complex recognizes its cognate antigen when it is presented on a major histocompatibility complex (MHC) on the cell surface of an antigen-presenting cell (APC). In humans, the MHC complexes are also called human leucocyte antigen (HLA) complexes. There are three HLA types (A, B and C) that correspond to MHC class I, presenting endogenously derived and cross-presented exogenous peptides to CD8⁺ T cells. In contrast, HLAs of MHC class type II (DP, DM, DQ and DR) present exogenously derived peptides to CD4⁺ T cells.

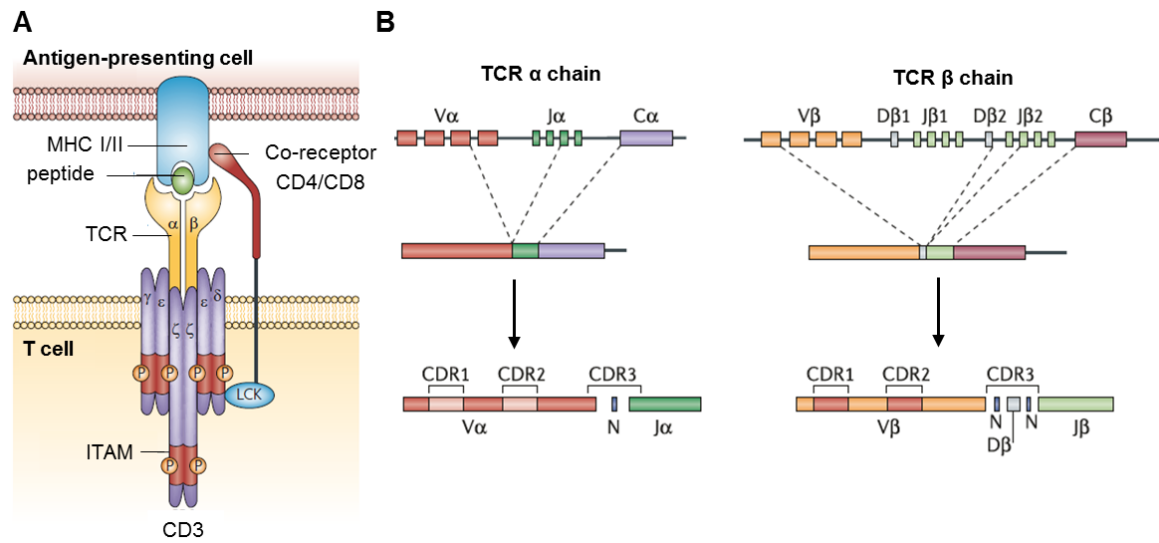


Figure 1: T-cell receptor structure and diversity due to gene rearrangement

A T-cell receptor (TCR) alpha and beta chains form a functional complex with CD3 molecules and $\zeta\zeta$ chains. The cognate antigen is presented on major histocompatibility complex (MHC). Upon recognition, intracellular phosphorylation starts the signal cascade and induces T-cell activation (adapted from Gascoigne, 2008).

B Gene rearrangement of variable (V), joining (J) and diversity (D) elements. Three-dimensional complementarity determining regions (CDR) form the highly specific antigen-binding pocket (adapted from Turner et al., 2006).

TCR = T-cell receptor; ITAM = tyrosine-based activation motif, LCK = LCK kinase, CDR = complementarity determining regions, MHC = major histocompatibility complex, V = variable, j = joining, D = diversity, N = nucleotide

Once the TCR recognized its cognate peptide : MHC (pMHC) ligand, the co-receptor CD4 or CD8, respectively, transports the LCK kinase into close proximity to the TCR complex. Subsequently, 10 immunoreceptor tyrosine-based activation motifs (ITAMs) within the cytoplasmic domains of CD3 and ζ chains get phosphorylated, thus initializing the intracellular signalling cascade (Weiss and Littman, 1994). After phosphorylation of downstream MAP kinases cascade, they translocate into the nucleus where they in turn activate transcription factors. TCR signalling is enhanced by binding of CD4 and CD8 co-receptors as well as co-stimulatory molecules like CD28 (Salomon and Bluestone, 2001). Activation of T cells by the TCR elicits T-cell responses which are characterised by cytokine secretion, target cell killing and proliferation.

These mechanisms are crucial for the control of viral infections but require the presentation of immunogenic virus-derived peptides on MHC molecules by professional APCs, like dendritic cells (DCs). Infected DCs can present endogenously synthesised viral proteins as well as exogenous antigens upon uptake and cross presentation on MHC class I. Uptake by endocytosis is followed by proteasomal degradation of the viral protein (van Montfoort et

al., 2014). Degraded viral peptides are then transported into the endoplasmic reticulum, where they are loaded on MHC class I molecules. Stable pMHC I complexes are subsequently translocated to the cell surface where the viral peptides are presented to CD8⁺ cytotoxic T cells (CTLs) (Hansen and Bouvier, 2009).

Upon pMHC I complex recognition CD8⁺ T cells form an immunological synapse with the antigen-presenting target cell (Grakoui et al., 1999). Subsequently, the cytotoxic granules containing perforin, granzymes, and granulysin translocate from the cytosol to the synapse where the cytotoxic granules are directed towards the target cell. A membrane pore that enables release of granzymes from endosomes into the target cell's cytosol is formed by perforin (Kagi et al., 1994, Lowin et al., 1994). Additionally, granulysin increases membrane permeability and induces apoptosis (Kaspar et al., 2001, Pardo et al., 2001). Once released into the cytosol, Granzyme B activates a caspase-dependent apoptosis pathway as well as caspase-independent cell death (Trapani et al., 1998) (**Figure 2 A**).

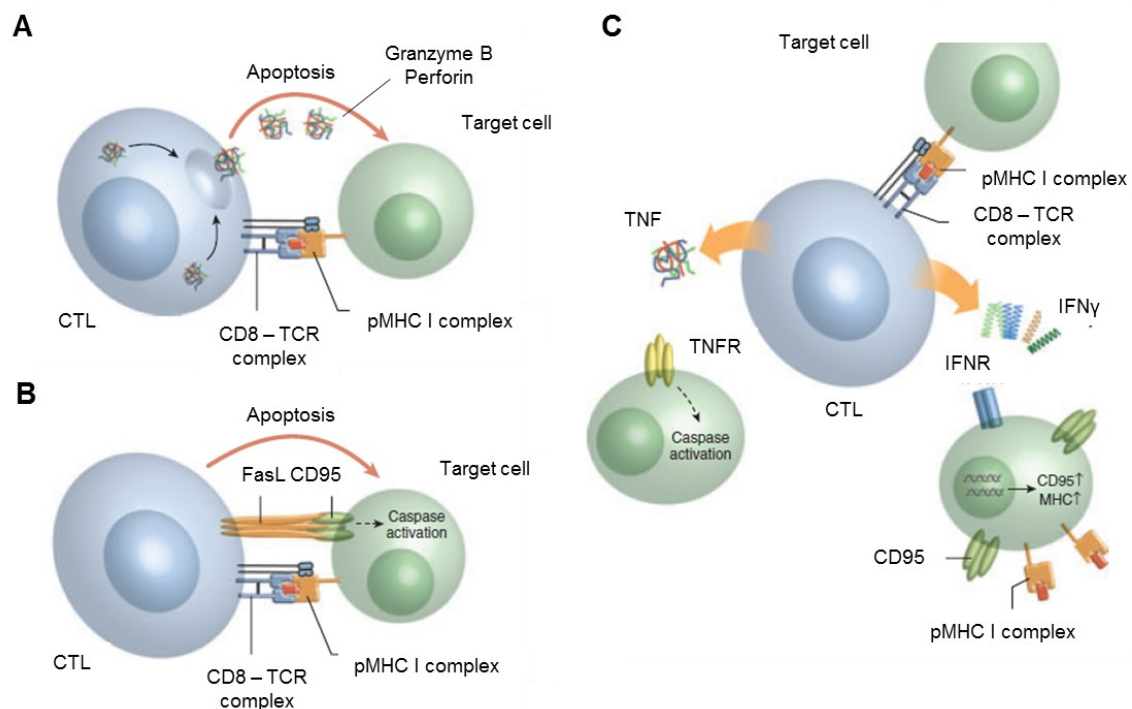


Figure 2: Cytotoxic capacities of cytotoxic T cells

A Direct killing of the target cell after recognition of the peptide : MHC complex on target cells. Release of perforin and granzymes into the immunological synapse induces cell death. **B** Death-receptor (Fas, CD95) activation induces cell death by inducing the caspase cascade. **C** Cytokines like TNF α and IFN γ further contribute to cell death by caspase activation or death-receptor upregulation in target cells (adapted from Andersen et al., 2006).

CTL = cytotoxic T lymphocyte; TCR = T cell receptor; TNFR = tumor necrosis factor receptor; IFNR = interferon receptor; pMHC I complex = peptide : MHC class I complex, FasL = Fas ligand, CD95 = Fas receptor

Granzyme A induces cell death as well, by inducing single-stranded DNA nicks (Beresford et al., 2001) and pro-inflammatory activation (Irmiler et al., 1995). The cytotoxic granules also contain CD107a, which can be measured on CD8⁺ T cells upon antigen stimulation and degranulation. Therefore, CD107a can be used as an effector marker for cytotoxic activities in CTLs (Betts et al., 2003, Aktas et al., 2009). CTLs can induce cell death also by the interaction of Fas ligand (FasL) with the Fas protein, which is also called death receptor or CD95 (**Figure 2 B**). Its activation in turn activates a cascade of caspases which induce cell death by destruction of proteins and membranes accompanied by DNA fragmentation (McIlwain et al., 2013). Additionally, cytokines like IFN γ and TNF α contribute to CTL-mediated apoptosis. While TNF α activates the caspase cascade upon receptor binding, IFN γ enhances the pMHC class I presentation pathway and Fas expression (Andersen et al., 2006) (**Figure 2 C**).

Interleukins (IL) further contribute to the immune response following initial T-cell activation *via* the TCR. Many of them have pleiotropic characteristics, thus inducing pro-inflammatory as well as anti-inflammatory processes throughout different cell types and conditions. An important key role in the regulation of the immune system plays IL-2, by controlling differentiation and proliferation of inflammatory as well as anti-inflammatory T cells. It promotes CD4⁺ T cell fate decisions and induces the production of IFN γ , TNF α , Granzyme B, and perforin and promotes target cell killing in antigen stimulated CD8⁺ T cells. IL-2 further shapes T cell differentiation: while high levels of IL-2 support terminally differentiated effector T cells, lower doses induce rather memory phenotypes (Ross and Cantrell, 2018). Another pleiotropic cytokine is IL-4 which is amongst others secreted by CD4⁺ type 2 helper T cells (Th cells) and NK-T cells. IL-4 supports CD4⁺ T cell differentiation into Th2 cells, a subpopulation that supports humoral immune responses, and strengthens cytotoxic activities of CD8⁺ T cells (Silva-Filho et al., 2014). IL-4 and IL-6 can also reduce FasL and Fas receptor upregulation upon TCR stimulation, thereby protecting CD8⁺ T cells from activation-induced cell death (Silva-Filho et al., 2014, Ayroldi et al., 1998). IL-6 is also crucial for the differentiation of Th17 cells, which produce pro-inflammatory IL-17A that in turn induces cytokine and chemokine expression from myeloid cells, thereby linking innate and adaptive immune responses (Xu and Cao, 2010). It also synergizes with TNF α to sustain pro-inflammatory immune responses (Gu et al., 2013). The anti-inflammatory cytokine IL-10 inhibits Th1 and NK cell activities during infection, thus also lowering the secretion of IL-2, IL-4, IL-6, IFN γ , and TNF α , and thereby regulating pro-inflammatory CD4⁺ T cell responses (Couper et al., 2008). In conclusion, these complex interactions, together with

neutralizing antibodies, control viral infections by destruction of infected cells, thus limiting viral spread.

3.2. Human Adenoviruses have highly conserved capsid proteins that can elicit cross-reactive, protective immune responses

Due to the still premature adaptive immunity in early childhood, adenoviral infections prevail in younger children, where they usually cause asymptomatic infections. Human Adenoviruses (AdVs) are lytic, non-enveloped, double-stranded linear DNA viruses which are about 90 nm in diameter. The genome is 30 – 35 kilo base pairs (bp) long and the central part of the genome is highly conserved throughout human AdV species. Multiple open reading frames and alternative splicing allow the expression of 23 - 46 protein-coding genes. The viral DNA together with additional viral proteins including viral protease, are enclosed by a nucleocapsid with a rounded icosahedral shape, composed of hexon proteins, penton proteins and fibers. Within the hexon, 720 subunits are arranged in 240 trimers and 12 hexon trimers together with a penton on each vertex form one facet of the capsid (**Figure 3**). Each of the 12 penton-base pentamers is associated with fiber trimers which form spikes that initiate receptor-mediated endocytosis of the virus. Additional minor or accessory proteins complete the capsid structure (Burnett, 1985, Liu et al., 2010, Reddy et al., 2010).

Recombination between the three major capsid genes affects species diversity as well as tissue tropism and pathogenicity (Walsh et al., 2009, Dhingra et al., 2019). AdV can be grouped into seven species (A-G) and 51 serotypes according to hemagglutination and serum neutralization reactions. Current approaches for the identification of new types rely on genotyping which can distinguish between 103 different types of AdV (<http://hadv.wg.gmu.edu/>). With different prevalences among the seven different species, AdV can cause a variety of infectious diseases including pharyngitis, pneumonia, conjunctivitis, gastroenteritis, urinary infections and myocarditis (Bennett et al., 2014, Ghebremedhin, 2014).

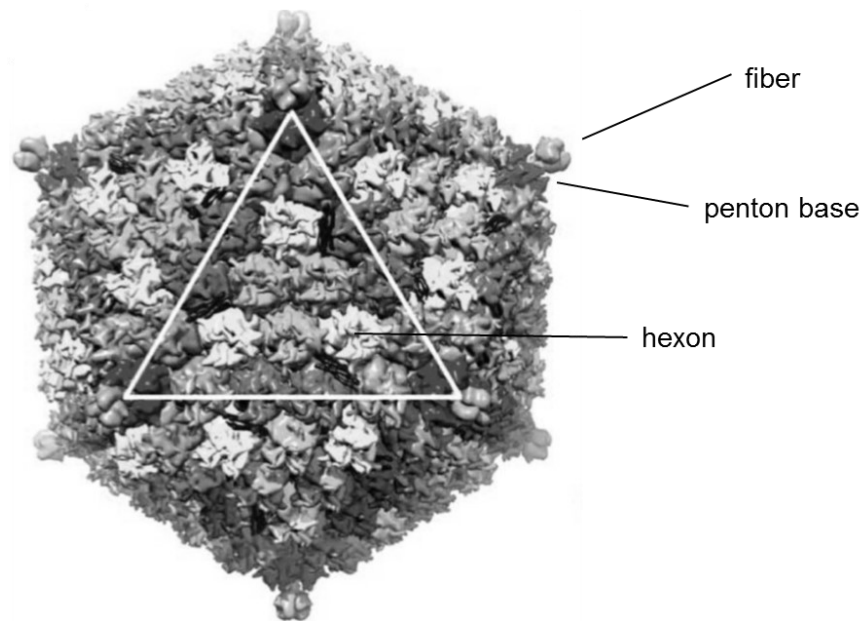


Figure 3: Three major capsid proteins form the icosahedral shape of adenovirus capsid

Crystal structure at 3.5 Å resolution of the capsid of recombinant human AdV-5 (subgroup C) with a short fiber protein derived from AdV-35 (subgroup B). Five penton bases are associated with a trimeric fiber protein at the vertices of a facet. In the center of each of the 20 facets 12 hexon trimers are located. White triangle highlights one facet (adapted from Reddy et al., 2010).

Besides acute and lytic infections, AdV can also establish persistent and partially latent infections in selected host cells. Following acute infection of the upper and lower respiratory tract, AdV species C can persist in lymphoid cells of the mucosal lymphoid tissue (Zhang et al., 2010). During persistence, infected cells continue to produce the viral genome but only few infectious viruses, therefore maintaining the virus over a long period of time. AdV sequences can be detected in human tonsils in the absence of infectious virus particles, indicating viral latency (Neumann et al., 1987, Garnett et al., 2009). Also, interferons (IFN) contribute to viral persistence. Both IFN α and IFN γ impede the transcription of *E1A*, a gene that is early transcribed during infection and required for the expression of later genes, thus inhibiting productive AdV replication (Zheng et al., 2016). High frequencies of latent AdV infections occur in children (almost 80% of examined children, (Garnett et al., 2002)), but the amount of viral DNA decreases with age. Although young children have been challenged with several serotypes already by the age of 10, the majority of infections proceed asymptomatic or with a mild clinical course, thus being rarely documented. In these immunocompetent individuals, distinct frequencies of AdV-specific cytotoxic T cells control viral spread (Sukdolak et al., 2013). The hexon protein has shown to be highly conserved among different AdV serotypes and cytotoxic T cells directed against hexon-derived

antigens elicit cross-reactive, protective immune responses (Heemskerk et al., 2006, Tang et al., 2006, Leen et al., 2004, Veltrop-Duits et al., 2006). The hexon-derived and HLA-A*01:01 restricted epitope (L)TDLGQNLLY, (amino acids 886 to 894 in AdV-5 of species C), has been shown to be cross-reactive with serotypes from subgroups B, C, E and D (Leen et al., 2004). Although subgroup A, B, E and F viruses have an amino acid exchange on position 7 (Leucine → Methionine) the TCR-binding motif is not affected. The presence of (L)TDLGQNLLY-specific T cells is therefore likely to be crucial to control the viral burden of different AdV subgroups.

3.3. Treatment of viral infections following stem cell transplantation

Hematopoietic stem cell transplantation (HSCT) is a common treatment strategy for a variety of malignancies and hematopoietic diseases (Craddock, 2000, Ljungman et al., 2006). However, immune reconstitution is impaired after HSCT and recovery can take 3 to 6 months (Bahceci et al., 2003, Federmann et al., 2010, Small et al., 1999). This period of transient severe immune deficiency gives rise to infections that become major causes for non-relapse-related morbidity and mortality in those patients (Gratwohl et al., 2005, Lin and Liu, 2013, Baldwin et al., 2000). Among viral infections persistent viruses like cytomegalovirus, Epstein-Barr virus and AdV are mainly prevalent (Özdemir et al., 2007, Xuan et al., 2013). In immunocompetent individuals, these life-long, chronic infections are controlled by virus-specific T cells but will re-occur with life-threatening replication rates after HSCT with abrogated T cell immunity (Runde et al., 2001, van Tol et al., 2005b, de Mezerville et al., 2006). In immunocompromised paediatric patients AdV species B and C are highly prevalent and cause life-threatening, opportunistic infections due to reactivation of persistent viruses as well as *de novo* infections (Lion et al., 2010, Al Qurashi et al., 2011). The presence of serotype-specific antibodies prior to SCT can predict reactivation of persistent endogenous AdV (Veltrop-Duits et al., 2011). AdV-related infections have a very high incidence in paediatric patients that is also affected with higher mortality rates than in adult patients (Feuchtinger et al., 2007, Flomenberg et al., 1994). Pharmacological treatments against AdV infections are limited and controlled clinical trials to prove *in vivo* efficacy are still lacking. Antiviral therapy shows limited efficacy for ribavirin but relevant toxicity with cidofovir, thus rather trigger the development of resistances and therefore highlight the urgent need for alternative treatment strategies (Leen et al., 2006, Ljungman, 2004). Since viral complications following SCT can be associated with absence of virus-

specific T cells, treatment with *ex vivo* derived CTLs is an alternative approach. Adoptive T-cell transfer (ACT) with virus-specific T cells from the stem-cell donor is capable to restore T-cell immunity and to control established viral infections in HSCT patients (Walter et al., 1995, Feucht et al., 2015, Feuchtinger et al., 2006, Bollard et al., 2004). At the beginning of ACT in the 1990s, donor lymphocyte infusions were used for the transfer of virus-specific T cells. Since low frequencies of virus-specific but high frequencies of allo-reactive T cells promote graft-versus-host disease (GvHD), the isolation and enrichment of virus-specific T cells was required (Leen et al., 2010). *Ex vivo* expansion of virus-specific T cells by co-culture with infected or pulsed APCs resulted in sufficient T cell numbers without significant side effects (Walter et al., 1995). Nevertheless, time consuming production and an undefined antigen repertoire required further improvement. Direct isolation of virus-specific T cells upon antigen exposure can be done by cytokine-capture technique (Feuchtinger et al., 2010, Kállay et al., 2018) or MHC I-multimer binding (Freimüller et al., 2015, Schmitt et al., 2011). AdV hexon-specific T cells isolated by the cytokine-capture technique from seropositive donors have shown to induce viral clearance in paediatric patients with refractory AdV infection following HSCT in a clinical trial (Feucht et al., 2015). Magnetically labelled pMHC Streptamers allow direct isolation of epitope-specific CD8⁺ T cells, which can be removed from the Streptamer by ligand competition, thus remaining negligibly manipulated with maintained phenotype and functionality (**Figure 4**) (Knabel et al., 2002).

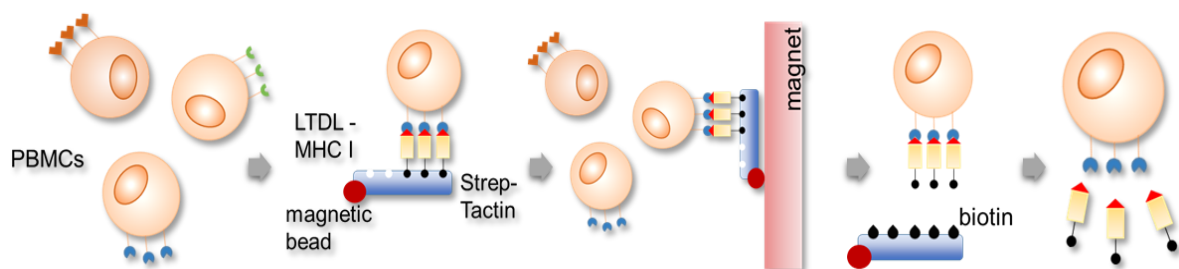


Figure 4: Magnetic isolation of LTDL-specific T cells using pMHC I Streptamer

Peptides form stable complexes with MHC I molecules by multimerization with a Strep-Tactin backbone. Strep-Tactins can be either labelled with fluorochromes for flow cytometry analysis or magnetic beads for magnetic isolation of cells. pMHC I Streptamers bind their cognate TCRs with high specificity which enables magnetic separation of these cells. The Strep-Tactin backbone can be removed by ligand competition with biotin (adapted from IBA, GmbH, Göttingen, Germany).

LTDL-specific T cells isolated by pMHC I Streptamer technique proliferate upon recognition of their cognate antigen and showed cytotoxic activity across different AdV species (Chakupurakal et al., 2013, Gunther, 2015), thus being a highly attractive target for ACT (Dörrie et al., 2014, Geyeregger et al., 2013). Although smaller amounts of virus-specific T cells are obtained with this method, the cells effectively expand *in vivo* and achieve viral protection (Stemberger et al., 2014, Neuenhahn et al., 2017, Schmitt et al., 2011).

Nevertheless, these approaches are limited by donor availability, time-consuming procedures, presence of virus-specific T cells and GvHD mediated through alloreactive TCRs. Genetic engineering allows to overcome these hurdles by generating recombinant T cells with defined TCR specificities also from seronegative HSCT donors in a short period of time. This is commonly achieved by retro- or lentiviral transduction of virus-specific TCRs into primary human T cells yielding in functional, target-specific T cells with high efficacy (Berdien et al., 2013). Transduction of transgenic TCRs can redirect T cells towards a new antigen specificity but is still associated with considerable limitations. First, the transgenic TCRs compete with endogenous TCRs for CD3 molecules to form functional TCR complexes on the cell surface (Ahmadi et al., 2011). Second, mispairing of transgenic with endogenous TCR chains can create TCRs with unknown specificity, thus inducing GvHD by alloreactive T cells (van Loenen et al., 2010, Bendle et al., 2010, Provasi et al., 2012). Third, retroviral vectors use strong viral promoters for transgene transcription and thereby prevent physiological TCR expression following stimulation with the cognate pMHC-complex (van Loenen et al., 2011, Eyquem et al., 2017, Schober et al., 2019). Fourth, random integration of retroviral vectors into the host genome and good-manufacturing process (GMP)-conform production of corresponding cell products is strongly regimented due to potential safety issues. Highly attractive alternatives are targeted, virus-free methods like CRISPR/Cas systems which allow seamless integration of a gene of interest into a target locus *via* homologous-directed repair, thus utilizing endogenous promoters for transgene expression (Roth et al., 2018, Eyquem et al., 2017, Schober et al., 2019).

3.4. CRISPR/Cas9-mediated genetic engineering of primary human T cells

Clustered regularly interspaced short palindromic repeats (CRISPR) are characterized by short repetitive sequences that are interrupted by unique spacer sequences. They were first described in *Escherichia coli* (Ishino et al., 1987) and later demonstrated to provide adaptive

immunity against bacteriophages in prokaryotes through integrated viral spacers (Barrangou et al., 2007). In bacteria, foreign nucleic acids get integrated at the CRISPR locus together with proximal protospacer adjacent motives (PAM). CRISPR-associated (cas) genes identify those foreign sequences due to downstream PAMs and transcribe RNA precursors into non-coding CRISPR RNA (crRNA). Together with an additional trans-activating CRISPR RNA (tracrRNA) the crRNA forms a single guide RNA (gRNA) that recruits the Cas9 endonuclease to form a ribonucleoprotein complex (RNP) (**Figure 5**) (Brouns et al., 2008). Cas9 is an endonuclease derived from *Streptococcus pyogenes* that requires a 5'-NGG-3' PAM sequence downstream of the target sequence, which is identified by complementary binding of the crRNA (Gasiunas et al., 2012). Subsequently, the Cas9 endonuclease cleaves nucleic acids three to four nucleotides upstream of the PAM sequence, thereby generating a DNA double-strand break (DSB) (Sternberg and Doudna, 2015, Jinek et al., 2012). Accordingly, this pathway is referred to as CRISPR/Cas9 system.

By 2013 the CRISPR/Cas system was demonstrated to be applicable for targeted gene editing in human cells (Cho et al., 2013, Jinek et al., 2013). Therefore, a single crRNA of 20 nucleotides in length, which is complementary within the gene of interest and followed by NGG, must be designed. Lentiviral transduction, injection, transfection, or electroporation can be used to deliver gRNA and Cas9 RNA or the complete RNP complex into the target cell. From the cytosol, the RNP translocates into the nucleus where the endonuclease induces a DSB three base pairs upstream of the PAM sequence (Jinek et al., 2012). In mammalian cells, most DSBs are repaired either by non-homologous end-joining (NHEJ) or less frequent by homology-directed repair (HDR) (**Figure 5**). NHEJ is an error-prone mechanism that uses small insertions and deletions (INDELS) to repair the DSB. This often causes frameshifts within the open-reading frame which is predetermined to cause genetic knock outs (KO). DSBs can also be repaired using DNA templates that can be derived from sister chromatids as well as transgenes with homologous sequences flanking the target sequence. This pathway is referred to as homology-directed repair (HDR). This mechanism enables the seamless integration of genes of interest into a targeted locus, which is further referred to as knock in (KI) (Liang et al., 2017). Genetic-engineering using CRISPR/Cas systems allows precise and highly efficient on-target gene editing with very high knock-out rates and lower KI efficiencies (Schumann et al., 2015, Wu et al., 2018). Nevertheless, specificity depends on the 20-nucleotide crRNA sequence and mismatches with other genomic regions can cause DSB events apart from actual target sequences, so-called off-target events. Especially regarding clinical applications, CRISPR/Cas-mediated gene editing has to be further investigated in order to evaluate possible side effects.

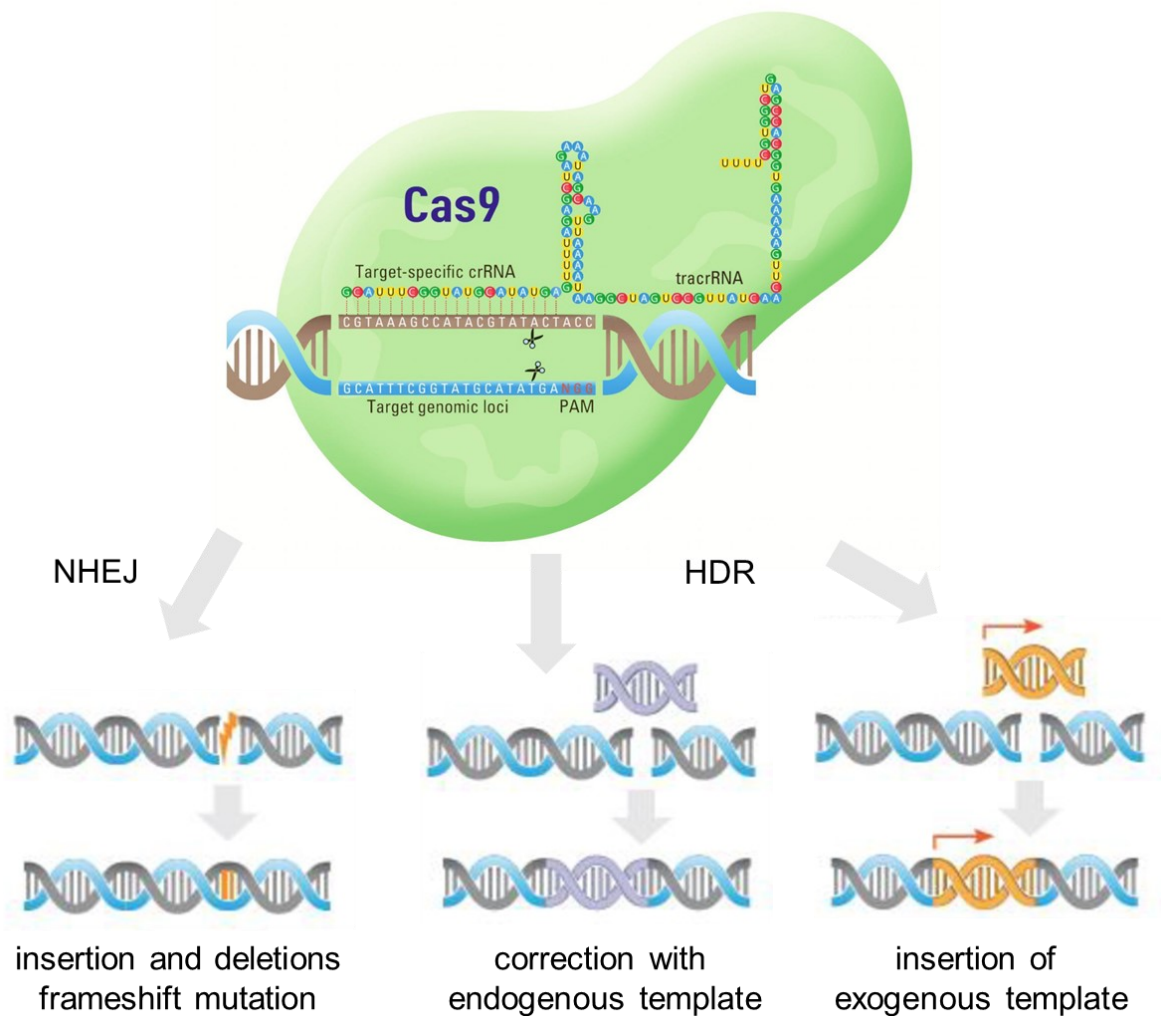


Figure 5: CRISPR/Cas9-mediated genome engineering

Target specific crRNA together with tracrRNA direct the Cas9 nuclease towards the target sequence proximal to the protospacer adjacent motive (PAM). The endonuclease induces a double strand break (indicated by scissors) which will be repaired by host cell mechanisms. Error-prone non-homologous end-joining (NHEJ) uses nucleotide insertions and deletions (INDELs), causing frameshifts with frequent knock-out mutations. In contrast, homology-directed repair (HDR) uses templates to repair the gap. DNA templates can be derived from sister chromatins as well as provided transgenes for genetic knock in (adapted from ThermoFisher, Waltham, MA, USA). NHEJ = non-homologous end-joining, HDR = homology-directed repair

First studies, using human cancer cell lines presume considerable off-target events with up to five nucleotide mismatches for a small subset of potential off-target sites (Fu et al., 2013, Hsu et al., 2013). In contrast, a study using human stem cells reports only low levels of off-target events (Schwank et al., 2013). These findings are limited to a small panel of predicted off-target sites and unbiased whole-genome sequencing observed only few mutations in human stem cells (Smith et al., 2014, Veres et al., 2014). These findings illustrate that

detailed investigation of the edited cell type and used gRNAs is required to assess the safety of CRISPR/Cas-mediated genetic engineering. However, this technique could be a highly attractive alternative for the generation of virus-specific T cells from HSCT donors with lacking virus-specific T cells, thereby overcoming limitations of commonly used procedures.

3.5. Identification of two novel LTDL-specific T-cell receptors

A 17-year-old, male patient suffering from Ewing-Sarcoma was treated with allogeneic stem cell transplantation using TCR $\alpha\beta$ /CD19 depleted leukaphereses (3.6×10^6 CD34⁺ cells/kg) from a haploidentical parent (Stief et al., 2022). He developed AdV viremia with life-threatening systemic infection and enteritis with up to 1.5×10^8 viral copies/ml peripheral blood 156 days *post* HSCT. Since infection was refractory to antiviral therapy with cidofovir the patient received virus-specific T cells directed against AdV hexon protein. The hexon-specific T cells were isolated from the haploidentical stem cell donor using cytokine-capture technique upon stimulation with a pool of overlapping oligopeptides covering the complete sequence of the AdV hexon protein. Subsequently, viral loads decreased but the patient did not develop a sustained T-cell population of LTDL-specific T cells and viral clearance could not be achieved. For this reason, immunomagnetic pMHC-Streptamer isolation (Schmitt et al., 2011, Knabel et al., 2002, Neuenhahn et al., 2017) of LTDL-specific T cells from the stem cell donor was performed and 1.75×10^3 LTDL-specific cytotoxic T cells/kg body weight were infused into the patient on day 0 (**Figure 6**). *In vivo*, the frequency of LTDL-specific T cells increased from background level (0.02%) up to 12.6% on day 28 after ACT with LTDL-specific T cells as detected by flow cytometric analysis from the peripheral blood of the patient. Increasing frequencies of LTDL-specific T cells were associated with virus clearance and viral copies were below PCR threshold by day 36 *post* ACT. Two and a half years following ACT the patient was still free of AdV infections and a sustained population of LTDL-specific T cells could be detected in the patient's peripheral blood.

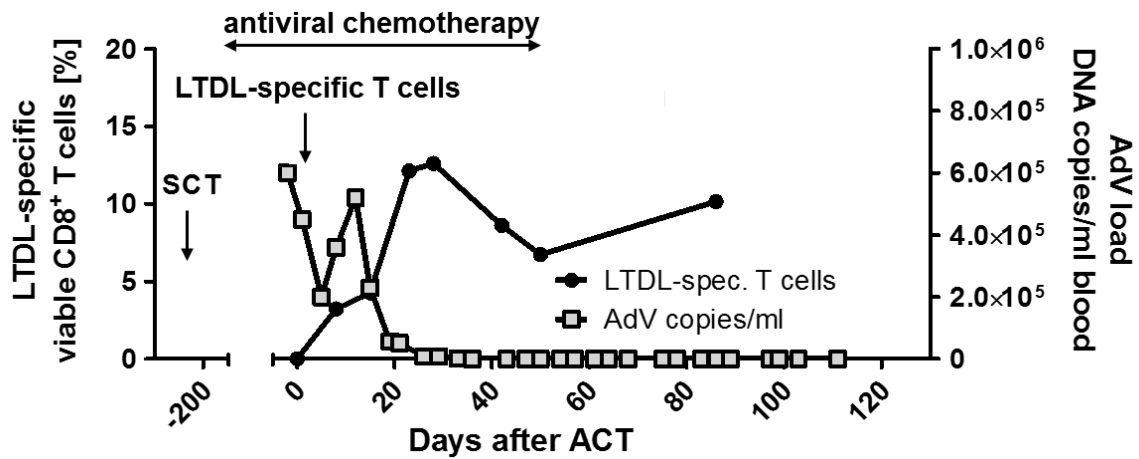


Figure 6: Adoptive transfer of LTDL-specific T cells controls AdV infection *in vivo*

A paediatric patient developed severe AdV infection following stem cell transplantation (SCT) which was refractory to antiviral treatment. He received adoptive T-cell transfer (ACT) with LTDL-specific T cells on day 0. Increasing frequencies of LTDL-specific T cell in the peripheral blood correlated with viral clearance (adapted from Stief et al., 2022)

In order to identify the protective TCRs, CD8⁺ LTDL-specific T cells were re-isolated from the patient and two different, full α/β TCRs were identified by TCR-SCAN RACE PCR (Dössinger et al., 2013) (**Table 1**). Both TCRs are restricted to HLA A*01:01 and have very similar CDR3 regions. The β chains of these TCRs vary in their diversity (TRBD) and joining (TRBJ) elements, thus causing slightly different CDR3 β regions (Ala10Thr and Tyr14Phe). The α chains have identical variable regions but also differ in their CDR3 α regions due to two amino acid substitutions (Met4Ile and Thr5Arg) (**Table 1**). These novel TCRs, that were most likely capable to establish viral protectivity *in vivo*, are highly attractive targets for the therapeutic use with genetically engineered T cells.

Table 1: Structure of protective LTDL-specific TCRs

	HLA	TRBV	TRBD	TRBJ	CDR3 β	TRAV	TRAJ	CDR3 α
LTDL TCR_1	A*01:01	5-1	2	2-7	CASSLEGQTAGEQYF	21	24	CAVMTTDSWGKIQF
LTDL TCR_2	A*01:01	5-1	1	2-1	CASSLEGQTTGEQFF	21	24	CAVIRTDSWGKIQF

4. Objective

The aim of this study was to establish a CRISPR/Cas9-mediated procedure for the genetic replacement of T-cell receptors (TCRs) in order to redirect primary human T cells with any specificity towards highly functional Adenovirus-derived hexon-specific T cells. This would provide a new strategy for the generation of virus-specific T cells for the treatment of refractory viral infections in immunocompromised hosts, using adoptive transfer of genetically engineered T cells.

First, a protocol for the CRISPR/Cas9-mediated genetic knockout (KO) of endogenous TCRs in human T cells will be developed to prevent mispairing with subsequently introduced virus-specific TCR chains. TCR-KO T cells will be investigated regarding their phenotypical characteristics and functionality in detail. Whole-genome sequencing and analysis of predicted off-target sites in TCR-KO T cells will be performed to evaluate on-target specificity and therefore safety of the CRISPR/Cas9-technique and the used gRNAs. Within the second part of this project, *in vivo* protective Adenovirus-specific TCRs will be retrovirally transduced into primary human T cells with high endogenous TCR-KO frequencies in order to confirm their effector function *in vitro*. Third, the established CRISPR/Cas9 protocol will be further exploited for integration of a LTDL-specific TCR into the endogenous TCR locus. Simultaneous KO of the endogenous TCR will be performed to prevent TCR mispairing. Primary human T cells with replaced LTDL-specific TCR and endogenous TCR KO will be functionally characterized regarding virus-specific cytokine secretion, proliferation and cytotoxic activities.

This proof-of-concept study could open the way for redirecting primary human T cells from seronegative donors towards protective virus-specific T cells in a single editing step. These recombinant T cells will prevent alloreactivity and random integration of the transgene into the host genome, thereby providing a safe and effective approach for the treatment of refractory viral infections in the immunocompromised host.

5. Material and Methods

5.1. Material

5.1.1. Antibodies and dyes

Product	Clone	Manufacturer	Catalogue #
7AAD Viability Staining Solution		Biolegend, San Diego, CA, USA	420404
CD107a – APC	REA792	Miltenyi Biotec, Bergisch Gladbach, Germany	130-111-847
CD14 – APC	TÜK4	Miltenyi Biotec, Bergisch Gladbach, Germany	130-091-243
CD14 – FITC	M5E2	Biolegend, San Diego, CA, USA	301804
CD154- VioBlue	REA238	Miltenyi Biotec, Bergisch Gladbach, Germany	130-113-615
CD19 – PE/Vio770	REA675	Miltenyi Biotec, Bergisch Gladbach, Germany	130-113-647
CD20 – APC	2H7	Biolegend, San Diego, CA, USA	302310
CD20 – FITC	2H7	Biolegend, San Diego, CA, USA	302304
CD3 – APCVio-770	REA613	Miltenyi Biotec, Bergisch Gladbach, Germany	130-113-136
CD3 – FITC	REA613	Miltenyi Biotec, Bergisch Gladbach, Germany	130-113-138
CD4 – PE/Cy7	SK3	Biolegend, San Diego, CA, USA	344612
CD4 – VioBright-FITC	REA623	Miltenyi Biotec, Bergisch Gladbach, Germany	130-113-229
CD4 – VioGreen	REA623	Miltenyi Biotec, Bergisch Gladbach, Germany	130-113-230
CD45 – VioBlue	5B1	Miltenyi Biotec, Bergisch Gladbach, Germany	130-092-880
CD45RO – PE	UCHL1	Biolegend, San Diego, CA, USA	304206
CD56 – APC	NCAM16.2	BD Biosciences, San Jose, CA, USA	341027
CD56 – FITC	NCAM16.2	BD Biosciences, San Jose, CA, USA	345811
CD56 – PE	REA196	Miltenyi Biotec, Bergisch Gladbach, Germany	130-113-312
CD62L –FITC	DREG-56	Biolegend, San Diego, CA, USA	304803
CD8 – APC	SK1	BD Biosciences, San Jose, CA, USA	345775
CD8 – APC/Cy7	SK1	Biolegend, San Diego, CA, USA	344714
CD8 – APC/Vio770	REA734	Miltenyi Biotec, Bergisch Gladbach, Germany	130-110-681
CD8 – VioBlue	REA734	Miltenyi Biotec, Bergisch Gladbach, Germany	130-110-683
CellTrace™ Violet Cell Proliferation		ThermoFisher Scientific	C34557
eBioscience Fixable Viability Dye eFluor™ 780		Thermo Fisher	65-0865-18
IFN γ – APC (BD)	25723.11	BD Biosciences, San Jose, CA, USA	341117

IFN γ – PE	25723.11	BD Biosciences, San Jose, CA, USA	340452
IFN γ – PE	45-15	Miltenyi Biotec, Bergisch Gladbach, Germany	130-113-493
MHC I-Strep HLA-A*0101; ADV hexon (885-894); LTDLGQNLly		Lothar Germeroth, Juno Therapeutics, Göttingen Germany	
Propidium Iodide Solution		Miltenyi Biotec, Bergisch Gladbach, Germany	130-093-233
Strep-Tactin®-PE		IBA GmbH, Göttingen, Germany	6-5000-001
TCR α/β – FITC	IP26	Biolegend, San Diego, CA, USA	306705
TCR α/β – PE	IP26	Biolegend, San Diego, CA, USA	306708
TNF α – PE/Vio770	cA2	Miltenyi Biotec, Bergisch Gladbach, Germany	130-120-492
Viability Dye 405/520		Miltenyi Biotec, Bergisch Gladbach, Germany	130-110-206

5.1.2. Reagents

Product	Manufacturer	Catalogue #
100 bp DNA Ladder Ready to Load	Solis BioDyne, Tartu, Estonia	01-11-00050
AccuPrime™ Taq DNA Polymerase	Invitrogen, Thermo Fisher Scientific Corp., Waltham, Massachusetts, USA	12346-086
Albomin 5 % infusion solution human albumin (HSA)	Biotest AG, Dreieich, Germany	623 050
Alt-R® Cas9 Electroporation Enhancer	Integrated DNA Technologies, Leuven, Belgium	1075916
Alt-R® HDR Enhancer	Integrated DNA Technologies, Leuven, Belgium	1081073
Alt-R® S.p. Cas9 Nuclease V3	Integrated DNA Technologies, Leuven, Belgium	1081059
Anti-Mouse Ig, κ /Negative Control Compensation Particles Set	BD Biosciences, San Jose, California, USA	552843
Biocoll 1,077g/ml	Biochrom GmbH, Berlin, Germany	L6115
Brefeldin A solution	Miltenyi Biotec, Bergisch Gladbach, Germany Sigma-Aldrich®, Merck KG	130-097-343 B5936
CD56 MicroBeads, human	Miltenyi Biotec, Bergisch Gladbach, Germany	130-050-401
CD8 MicroBeads, human	Miltenyi Biotec, Bergisch Gladbach, Germany	130-045-201
Dimethylsulfoxid	Carl Roth GmbH + Co. KG, Karlsruhe, Germany	4720.4
DNA Gel Loading Dye (6X)	Thermo Fisher Scientific Corp., Waltham, Massachusetts, USA	R0611
dNTP Mix (10 mM each)	Thermo Scientific	R0192
Dynabeads™ Human T-Activator CD3/CD28	GIBCO, Thermo Fisher Scientific Corp., Waltham, Massachusetts, USA	11131D

eBioscience™ Phytohemagglutinin-L (PHA-L) Solution (500X)	Invitrogen, Thermo Fisher Scientific Corp., Waltham, Massachusetts, USA	00-4977-93
Ethidium bromide	Carl Roth GmbH + Co. KG, Karlsruhe, Germany	2218.1
FIX & PERM™ Cell Permeabilization Kit	Invitrogen, Thermo Fisher Scientific Corp., Waltham, Massachusetts, USA	GAS004
GSEELRSLY (GSEE) peptide	Provided by Stefan Stevanovic University of Tübingen	
Human IL-15, premium grade	Miltenyi Biotec, Bergisch Gladbach, Germany	130-095-765
Human IL-7, premium grade	Miltenyi Biotec, Bergisch Gladbach, Germany	130-095-363
IL -2 Proleukin®S	Novartis Pharma GmbH, Nürnberg, Germany	
Inside Stain Kit	Miltenyi Biotec, Bergisch Gladbach, Germany	130-090-477
Lipofectamine™ 2000 Transfection Reagent	Invitrogen, Thermo Fisher Scientific Corp., Waltham, Massachusetts, USA	11668-030
LTDLGQNLly (LTDL) peptide	Provided by Stefan Stevanovic University of Tübingen	
MACS Comp Bead Kit anti-mouse/ anti-REA	Miltenyi Biotec GmbH, Bergisch Gladbach, Germany	130-097-900 130-104-693
Q5® High-Fidelity DNA Polymerase	New England Biolabs GmbH, Frankfurt am Main, Germany	M0491S
RetroNectin®	Takara Bio, Saint-Germain-en- Laye, France	CL T100A
Seakem Le Agarose	DMA, Rockland, Maine, USA	50004
Staphylococcal enterotoxin B	Merck KGaA, Darmstadt, Germany	S 4881
Strep-Tactin® Magnetic Microbeads	IBA GmbH, Göttingen, Germany	6-5510-050
Streptamer® Solution Set Standard for washing und dissociation	IBA GmbH, Göttingen, Germany	6-5603-005
TAE Buffer (50x)	Applichem GmbH, Darmstadt, Germany	A4686
Trypan Blue Solution, 0.4	Thermo Fisher Scientific Corp., Waltham, Massachusetts, USA	15250061

5.1.3. Cell culture media and reagents

Product	Manufacturer	Catalogue #
Fetal Bovine Serum, Research Grade	Merck KGaA, Darmstadt, Germany	F0804
Human AB serum	Ramin Lotfi, Institut für Klinische Transfusionsmedizin und Immungenetik Ulm (IKT Ulm), Germany	

L-Glutamine (200 mM)	Biochrom GmbH, Berlin, Germany	K 0283
PBS Dulbecco's phosphate-buffered saline	Thermo Fisher Scientific Corp., Waltham, Massachusetts, USA	14190144
Penicillin-Streptomycin (10,000 U/mL)	GIBCO, Thermo Fisher Scientific Corp., Waltham, Massachusetts, USA	15140-122
TexMACS (GMP grade, w/o phenol red)	Miltenyi Biotec, Bergisch Gladbach, Germany	170-076-307
TexMACS (research grade)	Miltenyi Biotec, Bergisch Gladbach, Germany	130-097-196
VLE Dulbecco's MEM	Biochrom GmbH, Berlin, Germany	FG1445
VLE RPMI 1640	Biochrom GmbH, Berlin, Germany	F 1415

5.1.4. Commercial kits

Product	Manufacturer	Catalogue #
QIAamp DNA Mini Kit	QIAGEN, Hilden, Germany	51304
DNA Clean & Concentrator-5	Zymo Research Europe GmbH, Freiburg, Germany	D4014
EasySep™ Human T-Cell Enrichment Kit	STEMCELL Technologies, Grenoble, France	19051
LEGENDplex™ Human CD8/NK Panel (13-plex)	Biolegend, San Diego, CA, USA	740267

5.1.5. Oligonucleotides

Oligonucleotide	Sequence	Supplier
TRAC crRNA	5'- GAGAATCAAATCGGTGAAT-3'	Integrated DNA Technologies, Leuven, Belgium (Osborn et al., 2016)
TRAC fwd	5'-ATCACGAGCAGCTGGTTTCT-3'	metabion international AG, Planegg, Germany (Osborn et al., 2016)
TRAC HDRT KI fwd	5'- CCCAACTTAATGCCAACATACCA-3'	metabion international AG, Planegg, Germany
TRAC HDRT KI rev	5'- GAAGTACTGCTCCCCCGC-3'	metabion international AG, Planegg, Germany
TRAC rev	5'- CCCGTGTCATTCTCTGGACT-3'	metabion international AG, Planegg, Germany (Osborn et al., 2016)
HDRT fwd	5'- CTGCCTTTACTCTGCCAGAG-3'	metabion international AG, Planegg, Germany

HDRT rev	5'- CATCATTGACCAGAGCTCTG-3'	metabion international AG, Planegg, Germany
tracrRNA		Integrated DNA Technologies, Leuven, Belgium
TRBC crRNA	5'- GGAGAATGACGAGTGGACCC-3'	Integrated DNA Technologies, Leuven, Belgium (Ren et al., 2017)
TRBC fwd	5'- TACCAGGACCAGACAGCTCTTAGA-3'	metabion international AG, Planegg, Germany (Ren et al., 2017)
TRBC rev	5'- TCTCACCTAATCTCCTCCAGGCAT-3'	metabion international AG, Planegg, Germany (Ren et al., 2017)

5.1.6. Plasmids and templates

Product	Supplier	Comments
LTDL-TCR_1 pMP71	Dirk Busch, Institute for Medical Microbiology, Immunology and Hygiene, Technische Universität München, Munich, Germany (Engels et al., 2003)	LTDL-TCR_1 with murine constant regions and full-length α chain
LTDL-TCR_2 pMP71	Dirk Busch, Institute for Medical Microbiology, Immunology and Hygiene, Technische Universität München, Munich, Germany (Engels et al., 2003)	LTDL-TCR_2 with murine constant regions and full-length α chain
LTDL-TCR_1 Puc57-Bsal-free	BioCat GmbH, Heidelberg, Germany	LTDL-TCR_1 with human constant regions and short α chain
LTDL-TCR_1 gBlock	Integrated DNA Technologies, Leuven, Belgium	LTDL-TCR_1 with human constant regions and short α chain

5.1.7. Equipment

Device	Product	Manufacturer
Flow cytometry unit	MACSQuant Analyzer 10	Miltenyi Biotec, Bergisch Gladbach, Germany
Flow cytometry unit	BD Canto™ II Flow Cytometer	BD Biosciences, San Jose, CA, USA
Magnetic cell separator	DynaMAG™ -2	Thermo Fisher Scientific Corp.; Waltham, Massachusetts, USA

Magnetic cell separator	QuadroMACS™ MACS MultiStand	Miltenyi Biotec, Bergisch Gladbach, Germany
Nucleofector	Nucleofector™ 2b Device	Amata Biosystems GmbH, Cologne, Germany

5.1.8. Software

Software	Manufacturer
BD FACSDiva Version 6	BD Biosciences, San Jose, California, USA
Cas-OFFinder	Molecular Genome Engineering Lab, Hanyang University, Korea
FlowJo 10.0.7r2	FlowJo LLC, Ashland, Oregon, USA
GraphPad Prism 5.0	GraphPad Software Inc., San Diego, California, USA
Integrative genomic viewer	Robinson et al., 2011
TIDE	Bas van Steensel lab and Desktop Genetics Ltd., London, UK

5.1.9. Consumables

Product	Manufacturer	Catalogue #
LS separation columns	Miltenyi Biotec, Bergisch Gladbach, Germany	130-042-401
2mm Cuvettes for electroporation	Biolabproducts GmbH, Bebensee, Germany	75-EP-202

5.1.10. Primary cells

Primary cells were obtained from healthy voluntary donors after informed consent was obtained and approved according to national law by the local Institutional Review Board (ethics committee of Ludwig-Maximilian university hospital in Munich). The work was done in accordance with the declaration of Helsinki.

Primary human T cells were cultured in TexMACS medium (Miltenyi Biotec) with 2.5% human AB serum, 10ng ml⁻¹ IL-7 and 10ng ml⁻¹ IL-15 (Miltenyi Biotec), unless indicated otherwise.

Autologous feeder PBMCs (PHA blasts) were cultured in VLE RPMI 1640 (Biochrom) with 10% fetal bovine serum (Sigma) and 1% L-Glutamine (Biochrom).

5.1.11. Stable cell lines

K32 cell lines expressing HLA-A*01 linked to LTDLGQNLLY or FSECNALGSY, respectively, were grown in VLE Dulbecco's MEM (Biochrom) supplemented with 10% fetal bovine serum (Sigma) and penicillin-streptomycin (10.000 U/mL) (GIBCO) at 37°C and 5% CO₂. Cells were kindly provided by Kevin. M. Dennehy from German Centre for Infection Research (DZIF), partner site Tübingen.

293Vec-Galv cells (BioVec Pharma Inc., Quebec, Canada) were cultured in VLE Dulbecco's MEM (Biochrom) with 10% fetal bovine serum (Sigma), penicillin-streptomycin (10.000 U/mL) (GIBCO) and 2% L-Glutamine (Biochrom) at 37°C and 5% CO₂.

293Vec-RD114 cells (BioVec Pharma Inc., Quebec, Canada) were cultured in VLE Dulbecco's MEM (Biochrom) with 10% fetal bovine serum (Sigma), penicillin-streptomycin (10.000 U/mL) (GIBCO) and 2% L-Glutamine (Biochrom) at 37°C and 5% CO₂.

5.2. Methods

Parts of the methods section were previously published (Stief et al., 2022).

5.2.1. Isolation and activation of primary human T cells

PBMCs were isolated from whole blood using Ficoll-density centrifugation (Biocoll, Biochrom). T cells were enriched from PBMCs using untouched magnetic separation (EasySep™ Human T-cell Enrichment Kit, Stemcell). Subsequently, T cells were cultured in TexMACS medium (Miltenyi Biotec) with 2.5% human AB serum, 10ng ml⁻¹ IL-7 and 10ng ml⁻¹ IL-15 (Miltenyi Biotec). T cells were activated with magnetic CD3/CD28 Dynabeads (GIBCO) in a bead to cell ratio of 1:4 and 30 IU ml⁻¹ IL-2 (Novartis) for two to three days.

5.2.2. TCR template design

DNA templates for CRISPR/Cas9-mediated HDR were designed *in silico* and synthesized as double stranded gBlock (Integrated DNA Technologies) or plasmid (Puc57-Bsal-free vector, biocat). The HDR template had the following structure: 5' homology arm (370 base pairs (bp)), P2A, complete TCR β chain with human *TRBC*, T2A, variable region of TCR α chain and first *TRAC* exon until Cas9-induced double strand break, 3' homology arm (280 bp). PAM sequences of *TRAC* and *TRBC* were mutated to prevent CRISPR/Cas9-mediated cleavage of the template. The HDR template was designed together with Kilian Schober, TUM.

The HDR template was amplified by PCR using Q5 high-fidelity DNA polymerase (NEB) and HDRT primer pairs (5.1.5). After initial denaturation at 98°C for 30 seconds, 40 cycles with the following conditions were performed: denaturation was performed at 98°C for 10 sec, followed by primer annealing at 59°C for 20 sec and elongation at 72°C for 70 sec. Final elongation was done at 72°C for 2 minutes. PCR products were purified using Clean&Concentrator-5 Kit (Zymo) according to manufacturer's instructions.

DNA constructs for retroviral transduction had the following structure: human Kozac sequence, followed by TCR β chain with murine *TRBC* with an additional cysteine bridge.

A subsequent P2A sequence is followed by TCR α chain including murine *TRAC* with an additional cysteine bridge (Cohen et al., 2007), cloned into pMP71 vectors (provided by Dirk Busch, TUM) (Engels et al., 2003).

5.2.3. CRISPR/Cas9-mediated TCR editing

80 μ M target-specific crRNA (Integrated DNA Technologies) was mixed with 80 μ M universal tracrRNA (Integrated DNA Technologies) and incubated at 95°C for 5 min to form the gRNA. Cas9 nuclease (Integrated DNA Technologies) was diluted to 40 μ M with PBS and slowly added to the cooled down gRNA. If only one gRNA was used Cas9 to gRNA ratio was 0.6 : 1, in case of two gRNAs 2 : 1 : 1. Electroporation Enhancer (Integrated DNA Technologies) was added to a final concentration of 20 μ M and the ribonucleoprotein complex (RNP) was incubated for 15 min at room temperature.

5'- GAGAATCAAATCGGTGAAT-3' TRAC crRNA (Osborn et al., 2016)

5'- GGAGAATGACGAGTGGACCC-3' TRBC crRNA (Ren et al., 2017)

CD3/CD28 Dynabeads were magnetically removed from activated T cells prior to electroporation. 1×10^6 activated T cells were re-suspended in 100 μ l pre-cooled Buffer M (5 mM KCl, 15 mM MgCl₂, 120 mM Na₂HPO₄/NaH₂PO₄, 50 mM Mannitol pH = 7.2 (Chicaybam et al., 2013)) and 10.4 μ l RNP with one gRNA or 26 μ l RNP with two gRNAs were added to the cells, respectively. For CRISPR/Cas9-mediated KI 2 - 3 μ g PCR amplified, purified HDR template was added to the RNP complex. Cells were electroporated in 2 mm cuvettes with pulse code T-023 in an Amaxa Nucleofector IIb (Lonza). After electroporation, cells were cultured in 500 μ l TexMACS medium (Miltenyi Biotec) without interleukins for 30 min in an incubator. Subsequently, 500 μ l TexMACS medium with 20 ng ml⁻¹ IL-7 and 20 ng ml⁻¹ IL-15 (Miltenyi Biotec) and 10 μ l HDR Enhancer (Integrated DNA Technologies) for HDR KI were added. HDR Enhancer was removed after 24 h and 1 ml of fresh complete medium was added to all samples. For MOCK controls, cells were electroporated without CRISPR/Cas reagents.

5.2.4. Retroviral transduction

Primary human T cells with high TCR KO frequencies were retrovirally transduced with the respective TCRs using stable 293Vec-RD114 producer cell lines. To generate stable producer cell lines 293Vec-Galv cells were transfected with 3 µg pMP71 expression vector (containing the TCR construct) using Lipofectamine 2000 (Invitrogen) according to manufacturer's instructions. 293Vec-RD114 packaging cells were transduced by adding virus-containing supernatant from transfected 293Vec-Galv cells. Virus supernatant from stable transduced 293Vec-RD114 cells was coated on retronectin (TaKaRa)-treated well plates and 1×10^6 T cells were transduced *via* spinoculation (3000 g, 90 min, 32°C) on virus-coated plates two days after electroporation.

5.2.5. Streptamer and antibody staining

0.3 µg pMHC I molecules with a Strep-tag were multimerized using 1.5 µl Strep-Tactin®-PE (IBA) to form a fluorescent Streptamer in a total volume of 15 µl with FACS buffer (PBS + 1% FCS) per 1×10^6 cells. T cells were stained for 45 min at 4°C in the dark with LTDL-Streptamers followed by antibody staining with 7AAD (Biolegend), CD56 – APC (BD), CD20 – APC (Biolegend), CD14 – APC (Miltenyi Biotec), CD8 – APC/Cy7 (Biolegend), CD4 – PE/Cy7 (Biolegend) and human TCR α/β – FITC (Biolegend). For analysis of CD3 re-expression CD3 – FITC (Miltenyi Biotec) instead of TCR α/β – FITC was used. Flow cytometric analysis was done on a BD Canto II (BD Biosciences). Since CD3 is a commonly used marker for T-cell identification but absent in TCR-KO T cells, lack of surface markers characteristic for other cell types (CD20 for B cells, CD56 for NK (T) cells, and CD14 on monocytes) in the presence of CD4 or CD8 were used to identify T cells by flow cytometry.

Alternatively, T cells were stained with eFlour780 (eBioscience) for life/dead discrimination, CD56 – FITC (BD), CD20 – FITC (Biolegend), CD14 – FITC (Biolegend), CD8 – APC (BD), CD4 – PE/Cy7 (Biolegend) and human TCR α/β – PE (Biolegend) for 10min at 4°C. BD Canto II (BD Biosciences) was used for flow cytometric analysis.

5.2.6. PCR for TCR editing validation

Genomic DNA was isolated (QIAamp DNA Mini Kit, Qiagen) seven days after electroporation. PCR was performed using TRAC and TRBC primer pairs (5.1.5) and AccuPrime polymerase system (Invitrogen). Human serum albumin (HSA) was added to the reaction mix in final concentration of 0.05%. Targeted integration of the HDRT into the endogenous TRAC locus was examined by designed primers, that bind upstream of the left homology arm (forward primer) and within the variable region of the transgenic β chain (reverse primer).

After initial denaturation at 95°C for 2 min, 45 cycles with denaturation at 95°C for 40 sec, followed by primer annealing at 55°C for TRAC/TRBC and 59°C for TRAC HDRT KI, respectively, for 40 sec and elongation at 68°C for 60 sec were performed. Final elongation was done at 68°C for 10 min. For TCR KO validation PCR products were purified (Clean&Concentrator-5, Zymo), sent for Sanger sequencing (eurofins) with forward and/or reverse primers and analysed using TIDE software (Brinkman et al., 2014).

5.2.7. Whole-genome analysis

Four days after electroporation with Cas9 and TRAC or TRBC gRNA, respectively, genomic DNA from samples with high TCR KO efficiency (> 93% TCR⁻ T cells, analysed by flow cytometry) was isolated (QIAampDNA Mini Kit, Qiagen) and sent for whole-genome sequencing (GATC/eurofins). Sequences were aligned to hg19 reference genome and genome-wide variant calling using GATK was done by GATC/eurofins.

Off-target events were predicted using Cas-OFFinder (Bae et al., 2014). Predicted off-target candidates were analysed using Integrative Genomics Viewer (Robinson et al., 2011) by comparing sequences of edited and control cells. For each off-target candidate a region spanning 20 nucleotides up- and 20 nucleotides downstream of a possible DSB site, including the predicted position, was analysed. Possible off-target DSB sites are between nucleotide three and four upstream of a PAM motive and within a gRNA complementary sequence with up to four nucleotide mismatches. Off-target events were defined as INDELS, which appear only in sequences of treated cells of two donors, but not in respective control cells.

5.2.8. Phenotypic characterization

Cellular composition was determined by surface staining of CD45 – VioBlue, CD19 – PE/Vio770, CD14 – APC, CD3 – FITC, CD56 – PE, CD4 – VioGreen, CD8 – APC/Vio770 (all antibodies are from Miltenyi Biotec). 7AAD (Biolegend) staining was used for live/dead discrimination. Flow cytometric analysis was performed on MACSQuant (Miltenyi Biotec).

For categorisation in different T-cell phenotypes cells were stained with CD56 – APC (BD Biosciences), CD20 – APC (Biolegend), CD14 – APC (Biolegend), CD4 – PE/Cy7 (Biolegend), CD8 – APC/Cy7 (Biolegend), CD45RO – PE (Biolegend) and CD62L – FITC (Biolegend). 7AAD staining (Biolegend) was performed for live/dead discrimination. Flow cytometric analysis was performed on BD Canto II (BD Biosciences). T-cell phenotypes were defined as naïve T cells: CD45RO⁻ CD62L⁺; stem cell-like T cells: CD45RO⁻ CD62L⁺; central memory T cells: CD45RO⁺ CD62L⁺; effector memory T cells: CD45RO⁺ CD62L⁻; effector T cells CD45RO⁻ CD62L⁻.

5.2.9. Effector marker expression

One week after genetic engineering 5×10^5 cells were cultured without interleukins overnight, followed by stimulation with 0.5 µg peptide and addition of brefeldin A and CD107a – APC antibody. After 6h cells were stained with CD4 – VioGreen, CD3 – FITC, and CD8 – APC/Vio770. Subsequently, cells were fixated, permeabilized, and intracellularly stained with IFN γ – PE, TNF α – PE/Vio770 and CD154 – VioBlue antibodies (all reagents were obtained from Miltenyi Biotec, stimulation and staining was performed according to manufacturer's instructions). Flow cytometric analysis was performed on MACSQuant (Miltenyi Biotec).

T cells were either stimulated with LTDLGQNLLY or GSEELRSLY, a non-immunogenic human immunodeficiency virus (HIV) Type 1-derived and HLA A*01:01-restricted peptide.

5.2.10. Intracellular cytokine staining

Two weeks after genetic engineering cells were co-cultured with K32 cells, expressing HLA A*01:01 linked to LTDLGQNLLY in a 1:1 ratio or stimulated with *Staphylococcus* enterotoxin B (SEB, 10 µg per 1×10^6 cells) for 6 h at 37°C. After 2 hours 10 µg/ml Brefeldin A (Sigma-Aldrich®, Merck KG) was added. Live/dead discrimination was done with 7AAD (Biolegend). For surface marker staining CD56 – FITC (BD), CD20 – FITC (Biolegend), CD14 – FITC (Biolegend), CD8 – APC/Cy7 (Biolegend), CD4 – PE/Cy7 (Biolegend) and LTDL-Streptamer-PE were used (Panel A). Subsequently, cells were fixated and permeabilized using Cytofix/Cytoperm (BD Biosciences) and intracellularly stained with IFN γ – APC (BD). Alternatively, cells were stained with CD8 – VioBlue, CD4 – VioBright-FITC, CD3 – APCVio-770 and IFN γ -PE. For live/dead discrimination Viobility Dye was used (all reagents from Miltenyi Biotec, Panel B). Flow cytometric analysis was performed on BD Canto II (BD Biosciences, for Panel A) or MACSQuant (Miltenyi Biotec, Panel B).

K32 cells presented either LTDLGQNLLY or non-immunogenic FSECNALGSY in the context of HLA A*01:01 on the cell surface.

5.2.11. Magnetic isolation of LTDL-specific T cells

3 µg LTDL – MHC I molecules with a Strep-tag were labelled with 30 µl Strep-Tactin® magnetic microbeads (IBA) for 30 min at 8°C. Subsequently, 2×10^7 cells were incubated with the magnetic Streptamers for 20 min. After magnetic separation of the unbound negative fraction the positive fraction was incubated with 1 mM D-biotin to remove the Strep-Tactin® magnetic microbeads by dissociation. Supernatant containing LTDL-specific T cells was washed and resuspended in TexMACS medium w/o phenol red (Miltenyi Biotec). All steps were performed according to manufacturer's instructions and at 4 – 8°C to avoid uncontrolled dissociation of the Streptamers.

5.2.12. Cytotoxic killing assay

Frozen autologous PBMCs were thawed and cultured in VLE RPMI 1640 (Biochrom) with 10% fetal bovine serum (Sigma) and 1% L-Glutamine (Biochrom). Cells were incubated with phytohemagglutinin (PHA, Invitrogen) for 3 days according to manufacturer's recommendations. Subsequently, medium was replaced and supplemented with 200 IU ml⁻¹ IL-2. After 3 days, medium was again replaced with 100 IU ml⁻¹ IL-2 for one day. 1x10⁶ PHA blast were pulsed with 1 µg of respective peptide over night at 37°C. On the next day, cells were labelled with CellTrace™ Violet (Invitrogen). Two weeks after genetic engineering, T cells were magnetically depleted for CD56⁺ cells (CD56 microbeads, Miltenyi Biotec) to avoid masking effects of LTDL-specific NK (T) cells and enriched for LTDL-Streptamer⁺ cells (magnetic Streptamers see 5.2.11, IBA). For MOCK controls CD8⁺ T cells were magnetically isolated using CD8 microbeads (Miltenyi Biotec). After one week, T cells were co-cultured with autologous, pulsed PHA blasts in the respective effector-to-target ratios in TexMACS medium w/o phenol red (Miltenyi Biotec) for 48 h. Cells were stained with propidium iodide (Miltenyi Biotec) for live/dead discrimination. Cytotoxic killing capacity was assessed by determination of CTV negative, lysed target cells in co-cultures compared to target cell-only controls. Each experiment was performed in technical triplicates.

Target cells were either pulsed with LTDLGQNLYY or GSEELRSLY, a non-immunogenic, but also HLA A*01:01-restricted peptide.

5.2.13. T-cell proliferation and cytokine release

Frozen autologous PBMCs were thawed and cultured in VLE RPMI 1640 (Biochrom) with 10% fetal bovine serum (Sigma) and 1% L-Glutamine (Biochrom). Cells were cultured with PHA (Invitrogen) according to manufacturer's recommendations for 3 days. Subsequently, medium was replaced and supplemented with 200 IU ml⁻¹ IL-2. After 3 days, 1x10⁶ PHA blast were pulsed with 10 µg peptide over night at 37°C, followed by irradiation at 30 Gy. T cells were magnetically depleted of CD56⁺ cells (CD56 microbeads, Miltenyi Biotec) two weeks after genetic engineering. T cells were labelled with CellTrace Violet™ (Invitrogen) and co-cultured with pulsed autologous PHA blasts in a 1:1 ratio in TexMACS medium w/o phenol red (Miltenyi Biotec). After three days cells were stained with LTDL-Streptamer-PE

followed by surface staining with CD56 – FITC (BD), CD20 – FITC (Biolegend), CD14-FITC (Biolegend), CD8 – APC (BD), CD4 – VioGreen (Miltenyi Biotec) and 7AAD (Biolegend) for live/dead discrimination. Specifically proliferated cells were determined as 7AAD⁻ LTDL-Streptamer⁺ T cells with reduced fluorescent intensity for CTV, as the dye dilutes with every cell division. Supernatants were harvested after six days by centrifugation and secreted cytokines were analysed in a bead-based immunoassay (LegendPlex, Biolegend) in technical duplicates.

PHA blasts were either pulsed with LTDLGQNLYY or GSEELRSLY, a non-immunogenic, but also HLA A*01:01-restricted peptide.

5.2.14. Quantification and statistical analysis

FlowJo software (FlowJo, LLC) was used for the analysis of flow cytometric data. GraphPad Prism (Version 5, GraphPad Software Inc.) was used for all statistical analyses. All experiments were performed at least two times, except the cytotoxic killing assay with GSEE-pulsed PHA-blasts which was done once in technical triplicates. Statistical analysis was carried out by paired/unpaired Student's t test, respectively (GraphPad Prism). P value < 0.05 was considered statistically significant. Statistical information for each experiment can be found in figure legends.

6. Results

6.1. Functional disruption of the endogenous T-cell receptor

Transgenic TCR chains are capable of binding endogenous TCR chains, thus causing TCR mispairing. This would not only reduce stoichiometric expression of correctly assembled TCRs but create TCRs with unknown specificity. Therefore, primary human T cells with a CRISPR/Cas9-mediated KO of the endogenous TCR were generated to prevent mispairing with subsequent introduced LTDL-specific TCRs. KO efficiency was evaluated on protein as well as on genetic level and both, phenotypic and functional characteristics were analysed.

One week after electroporation of Cas9 nuclease and target-specific gRNA as ribonucleoprotein complex (RNP, 5.2.3), TCR KO efficiency was evaluated on protein level by flow cytometric analysis (5.2.5). KO of either the TCR α chain (*TRAC*) or β chain (*TRBC*) constant region is sufficient to disrupt the complete TCR complex surface expression (**Figure 7 A**). Mean editing efficiencies of 87.3% ($p < 0.0001$) TCR⁻ T cells for TRAC gRNA and 79.2% ($p < 0.0001$) TCR⁻ T cells for TRBC gRNA were obtained, respectively (**Figure 7 B**). Using both gRNAs simultaneously increased the KO efficiency to 96.4% ($p < 0.0001$) TCR⁻ T cells (**Figure 7 B**). MOCK cells, which were electroporated but without CRISPR/Cas9 reagents, and untreated cells served as controls.

TCR KO efficacy was also evaluated on genetic level by comparing DNA sequences of edited and MOCK control cells at the targeted locus using TIDE (5.2.6). For TRAC and TRBC gRNA 87.1% ($p = 0.0007$) and 78.0% ($p = 0.0031$) total editing efficiencies, displayed as frequency of appearing insertions and deletions (INDELs) at the targeted locus, were observed, respectively (**Figure 7 C**). Of note, the application of both gRNAs simultaneously did not significantly affect the editing efficacy (83.6% in *TRAC* and 77.2% in *TRBC*). Mutational load due to electroporation was rather low (5%), as comparison of MOCK with untreated samples revealed (**Figure 7 C**). Each gRNA shaped an individual, donor-independent INDEL pattern which was maintained when both gRNAs were used simultaneously. While TRAC gRNA mainly induced deletions of eight nucleotides, smaller deletions and insertions were caused by TRBC gRNA (**Figure 7 D**).

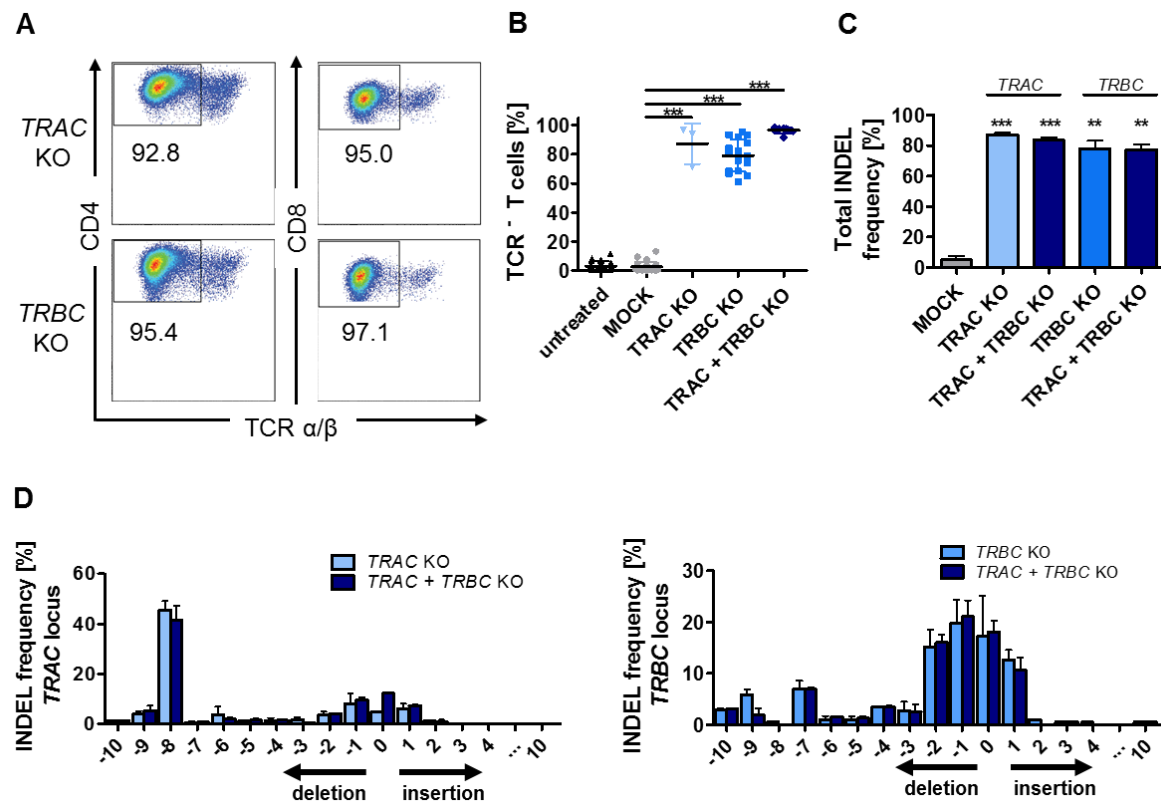


Figure 7: Highly efficient TCR KO in primary human T cells

Analysis of TCR-KO efficiency on protein and genetic level in primary human T cells. **A** Representative dot plots showing TCR⁻ T cells after treatment with Cas9 and TRAC or TRBC gRNA, respectively (published in Kaeuferle et al., 2022). **B** Frequency of TCR negative T cells assessed by flow cytometry analysis. Data show mean \pm SD of ≥ 3 independent experiments. **C** TCR KO efficiency on genetic level determined by sequence alignment of MOCK compared to untreated cells and CRISPR/Cas-edited samples compared to MOCK control. Data show mean \pm SD of 2 independent experiments. **D** INDEL pattern using TRAC and/or TRBC gRNA compared to MOCK. Data show mean \pm SD of 2 independent experiments. ** $p < 0.01$ *** $p < 0.001$

Cells were further characterized to evaluate the impact of TCR loss on primary human T cells. Therefore, the cellular composition after different treatments was analysed, as well as cell growth and T-cell phenotypes. Finally, the functionality of T cells with TCR KO was analysed. The cellular composition of cell products was evaluated by staining of characteristic surface markers and flow cytometric analysis (5.2.8). T cells were successfully enriched from 38% CD4⁺ and 16% CD8⁺ T cells among peripheral blood mononuclear cells (PBMCs) to 60% CD4⁺ and 28% CD8⁺ T cells *post* enrichment (**Figure 8 A**). CD14⁺ monocytes (18% in PBMCs) as well as CD19⁺ B cells (6% in PBMCs) could be completely removed (0% after T cell enrichment). CD56⁺ NK (T) cell frequencies could be decreased from 15% in PBMCs to 4% *post* enrichment. After one week of *in vitro* culture (untreated), electroporation (MOCK) or KO of the endogenous TCR (> 79% KO efficiency),

respectively, the samples were again analysed. High frequencies of CD8⁺ T cells were observed in the untreated control (44%), MOCK (50%) and in the TCR-KO sample (51%). CD4⁺ T-cell frequencies ranged from 40% to 44%. CD4⁺CD8⁺ double-positive cells were observed in all three cultured samples (2% each), whereas B cells and monocytes remained absent (0%). 7% CD56⁺ NK (T) cells were detected in the untreated sample and lower frequencies in MOCK control and TCR-KO sample (2% and 4%, respectively). During *in vitro* culture following initial T-cell enrichment, high frequencies of T cells (89% - 96%) were obtained, while frequencies of other populations decreased. However, the frequency of CD8⁺ T cells increased from 28% two days prior to electroporation to 44-51% eight days *post* electroporation. Of note, KO of the endogenous TCR did not influence the cellular composition compared to controls. After initial T-cell activation with CD3/CD28 Dynabeads two days prior to electroporation, cell expansion was comparable in untreated samples (from 1x10⁶ to 1.7x10⁸ cells), MOCK controls (from 1x10⁶ to 1.3x10⁸ cells) and TCR KO samples (from 1x10⁶ to 1.5x10⁸ cells) after 21 days (**Figure 8 B**). The frequency of TCR⁺ T cells within the TCR-KO sample remained stable within three weeks after electroporation, ranging from 80.7% on day 4 to 75.2% on day 21 *post* electroporation. (**Figure 8 C**).

In order to evaluate the functional impact of the TCR KO, cells were stimulated with the strong T-cell superantigen *Staphylococcus* enterotoxin B (SEB, 5.2.10). CD8⁺ T cells of untreated and MOCK controls secreted high amounts of IFN γ (24.2% and 22.7%, respectively) (**Figure 8 D**). In contrast, only 2.4% ($p = 0.0044$) IFN γ -secreting CD8⁺ T cells were observed in the TCR-KO sample, thus confirming the functional disruption of the TCR complex.

The phenotype of T cells was distinguished according to surface expression of CD45RO and CD62L at different time points during cultivation (5.2.8). Enrichment of T cells from PBMCs had no impact on the phenotype as well as T-cell activation (**Figure 8 E**). Most T cells showed a rather immature phenotype of naive (T_n) and stem cell-like T cells (T_{scm}, 44.3 – 60.9%), with smaller proportions of central memory (T_{cm}, 14.8 – 27.5%), effector memory (T_{em}, 16.1 – 18.2%), and effector T cells (T_{eff}, 7.6 – 14.3%). Eight days after genetic engineering T cells from untreated, MOCK control and TCR-KO samples mainly had a T_{cm} phenotype (85.1 – 87.4%). During *in vitro* culture, T cells from all three samples acquired a more matured phenotype with larger amounts of T_{em} cells, changing from 5.5 - 7.3% on day 8 to 22.6 - 50.9% on day 21. 21 days after electroporation TCR-KO samples had a higher proportion of T_{em} cells (50.9%) compared to untreated (24.5%) and MOCK controls (22.6%), though not significant ($p = 0.0611$).

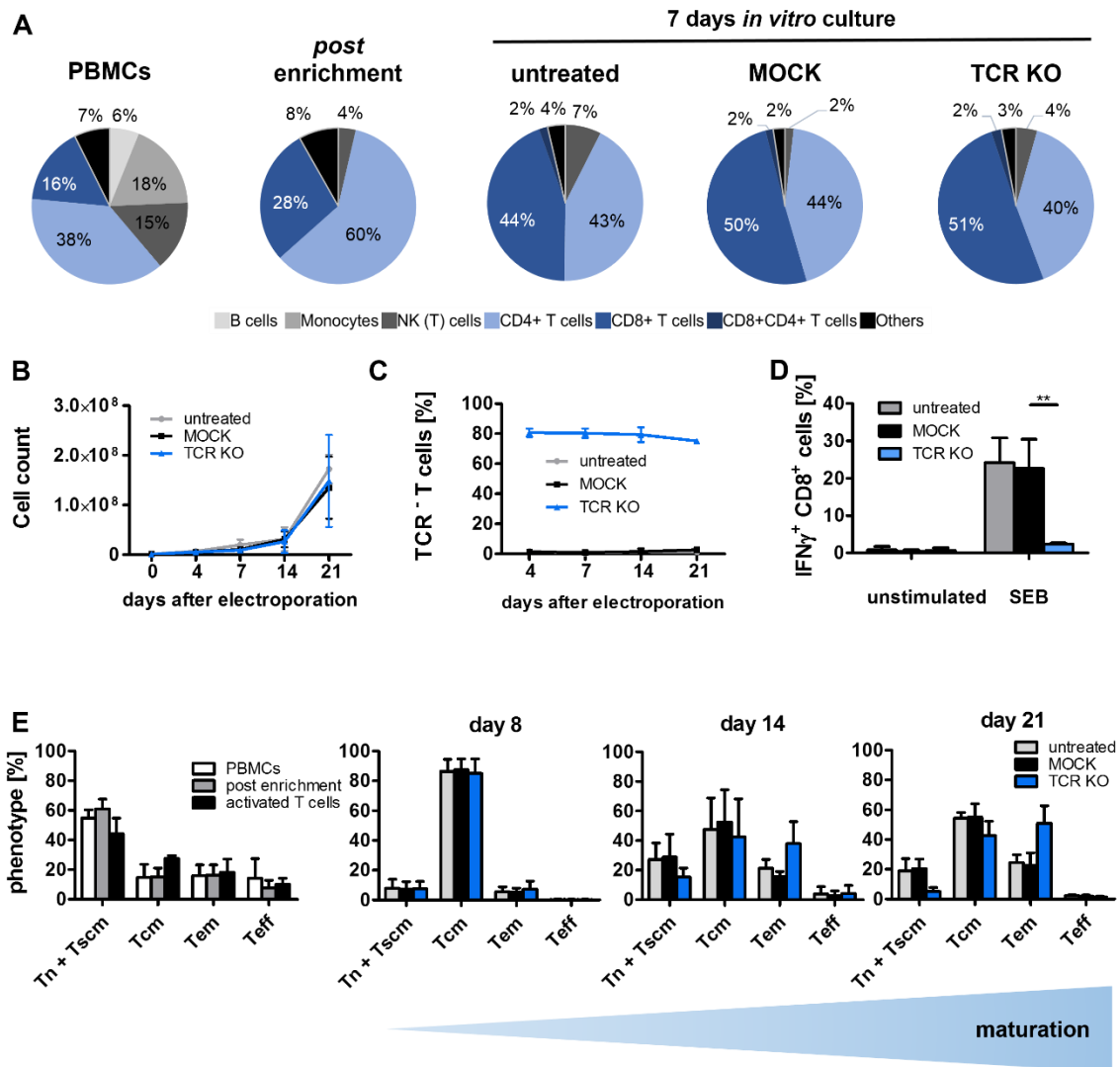


Figure 8: Stable and functionally disrupted TCR-KO samples maintain CD4/CD8 ratios, expansion characteristics, and T-cell phenotypes

Phenotypic and functional characterization of TCR-KO samples with high TCR KO efficiency. **A** Cellular composition two days prior to electroporation (PBMCs and *post* enrichment) and eight days *post* electroporation. Cells negative for all the indicated markers were determined as “others”. **B** Extrapolated cell numbers during *in vitro* cultivation. Data show mean \pm SD of 2 independent experiments. **C** Frequency of TCR⁺ T cells during *in vitro* cultivation. Data show mean \pm SD of 2 independent experiments. **D** Intracellular cytokine staining upon stimulation with or without SEB. Data show mean \pm SD of 5 independent experiments. **E** T-cell phenotypes in PBMCs, after enrichment and activation, and during *in vitro* cultivation. Data show mean \pm SD of ≥ 3 independent experiments. ** p < 0.01

Tn = naive T cells, Tscm = stem cell-like T cells, Tcm = central memory T cells, Tem = effector memory T cells, Teff = effector T cells.

6.2. Identification of CRISPR/Cas9-induced off-target events

Besides phenotypical and functional characterization of TCR-KO T cells, evaluation of the safety profile of CRISPR/Cas9-engineered cell products plays a crucial role, especially regarding clinical applications. Cas9-induced double-strand breaks (DSB) are dependent on the targeting gRNA which can bind not only to the on-target site but to identical off-target sequences, as well as sequences with some nucleotide mismatches. Whole-genome deep sequencing was performed in order to identify possible CRISPR/Cas9-mediated off-target events in TCR-KO samples (5.2.7).

Genomic DNA of bulk CRISPR/Cas9-treated samples as well as untreated and MOCK controls from two donors was harvested and sent for whole genome deep sequencing. Genome-wide variant calling revealed up to 3.6×10^6 single nucleotide polymorphisms (SNPs) in untreated, MOCK, *TRAC*- and *TRBC*-KO samples of both donors compared to hg19 reference genome (**Figure 9 A**). The frequency of INDELS was below 0.8×10^6 in all four samples of both donors. Surprisingly, neither the numbers of SNPs nor INDELS were significantly upregulated in CRISPR/Cas9-treated samples of both donors compared to untreated and MOCK control samples. In all four samples of each donor 98.7% SNPs occurred in non-coding regions, 0.7% were silent or missense mutations and $< 0.009\%$ were nonsense mutations (**Figure 9 B**). Insertion sizes ranged from 497 nucleotides in *TRAC* gRNA-treated samples to 645 nucleotides in *TRBC* gRNA-treated samples. Deletions were between 218 nucleotides (MOCK) and 313 (untreated) nucleotides long (**Figure 9 C**). Again, no significant difference between CRISPR/Cas9-edited and control samples could be observed.

So far, no difference in the total numbers of SNPs, INDELS or INDEL size between TCR-KO samples and controls could be detected. Therefore, an off-target prediction tool was used to search for potential off-target sites within the hg19 genome. The Cas-OFFinder algorithm considered mismatches of the gRNA and variations within the PAM sequence (Bae et al., 2014). 1,531,313 potential off-target events with up to nine mismatches were calculated for *TRAC* gRNA and 1,440,171 for *TRBC* gRNA. Predicted off-target sites with no more than four mismatches between gRNA and target sequence were further analysed using Integrative Genomics Viewer (Robinson et al., 2011).

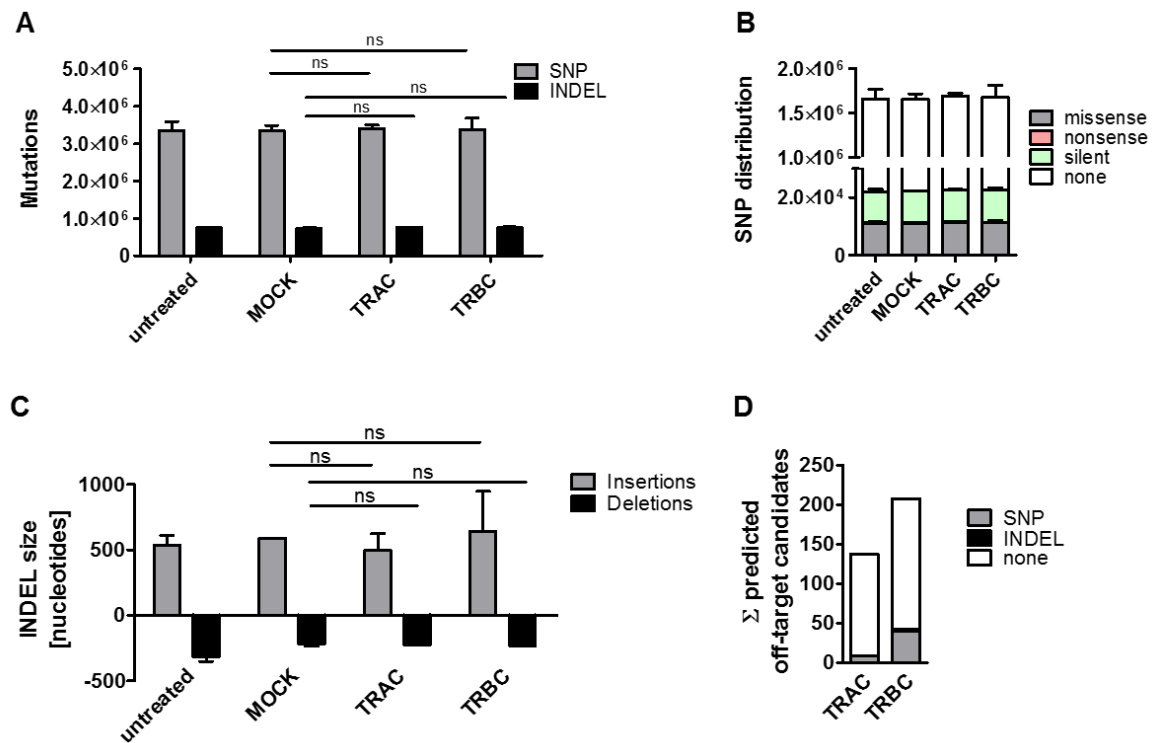


Figure 9: SNPs and INDELs detected by whole-genome sequencing

Presence and size of SNPs and INDELs of two individual samples compared to hg19 reference genome

A Total number of SNPs and INDELs in whole-genome sequences compared to hg19 genome. Data show mean \pm SD of two different donors. **B** Functional influence of detected SNPs compared to hg19 reference genome. Data show mean \pm SD of two different donors. **C** Size of detected insertions and deletions. Data show mean \pm SD of two different donors. **D** Identification of off-target events in regions close to predicted sites with up to four nucleotide mismatches between gRNA and off-target sequence. Data show mean \pm SD of two different donors. ns = not significant, $p > 0.05$

First, on-target mutations at *TRAC* and *TRBC* loci were validated (**Figure 10**). Therefore, a window of 20 nucleotides on either side of the Cas9 cut site – between nucleotide 3 and 4 upstream of the PAM sequence – was analysed. While sequences of untreated and MOCK control cells showed stable read frequencies in the analysed region, a clear drop in read frequencies was detected for *TRAC*-KO samples in both donors due to various deleted nucleotides next to the DSB site. A corresponding pattern could be observed for *TRBC*-KO samples at the *TRBC* locus. While stable read frequencies in untreated and MOCK controls were observed, read frequencies decreased in the *TRBC*-KO sample at the expected DSB site in donor 1. In donor 2, a strong increase of reads next to the DSB site was observed due to overlapping reads at one position. Of note, the positions predicted by Cas OFFinder were 6 nucleotides upstream of the observed DSB for *TRAC* gRNA and 17 nucleotides upstream for *TRBC* gRNA.

Next, predicted off-target sites with up to four nucleotide mismatches between gRNA and the targeted sequence were analysed. Importantly, none of the predicted off-target site could be confirmed on the exact predicted position. Hence, the analysed region was increased spanning 40 nucleotides around a possible DSB site next to the predicted position. Off-target candidates were defined as mutations that were only present in TCR-KO samples of both donors but not in the respective untreated and/or MOCK controls. 138 *in silico* predicted off-target sites were further analysed for TRAC gRNA and none of them could be confirmed. However, 9 SNPs up to 28 nucleotides downstream of predicted off-target positions with frequencies below 12% were observed in 6.5% of analysed regions (**Figure 9 D**). All of them were in non-coding or intronic regions according to IGV annotation (**Table 2**).

Table 2: Identification of TRAC gRNA-dependent mutations

Chr.	predicted position	mm	mutated reads [%]		mutation	distance	gene
7	105740489	4	2.3	2.3	SNP	21	SYPL1 Intron
5	132813873	4	3.1	3.3	SNP	25	FSTL4 Intron
2	126724956	4	3.8	2.3	SNP	3	Non-coding
2	163748315	4	2.7	2.3	SNP	6	Non-coding
6	157813089	4	2.9	3	SNP	5	ZDHHC14 Intron
14	53208454	4	1.8	2.10	SNP	19	STYX Intron
14	55263186	4	3.2	4.3	SNP	19	Non-coding
20	59697803	4	7.7	11.8	SNP	28	Non-coding
X	67375464	4	11.1	6.5	SNP	6	OPHN1 Intron

Chr. = chromosome; position of potential off-target event as predicted by Cas-OFFinder; mm = mismatches between gRNA and target sequence; percentage of mutated reads in each donor but not in controls; identified mutation: SNP = single nucleotide polymorphism, INDEL = insertions and/or deletions; Distance = genomic distance between predicted off-target position and identified mutation; affected gene according to IGV

For TRBC gRNA, 208 off-target candidates with up to four nucleotide mismatches were analysed and 42 mutations were detected. None of those were detected at the exact predicted off-target position. 40 of 42 mutations were SNPs and 34 of these SNPs were in intronic or non-coding regions according to IGV annotation (**Table 3, Figure 9 D**). 6 SNPs affected exons of *CHRNA3*, *HIC2*, *ISX-AS1*, and *RAB12*. *CHRNA3* is a cholinergic receptor nicotinic gamma subunit of the acetylcholine receptor protein and involved in movement, as

acetylcholine receptors transmit signals between nerve and muscle cells. Here, SNPs in 3.2.% of reads in exon 12 were observed following treatment with TRBC gRNA and Cas9. 3 SNPs were found in less than 5% of reads in the third exon of *HIC2* (Hypermethylated In Cancer 2 Protein), which is a transcriptional repressor. One SNP in 2.8% reads of exon 5 of *ISX-AS1* was found, which is also called long intergenic non-protein coding RNA 2885. *RAB12* (Ras-related protein Rab-12) controls autophagy as well as protein degradation and one SNP in up to 5.9% reads in its first exon was detected. In total, SNPs were found in 19.2% of analysed regions of TRBC gRNA treated cells.

Table 3: Identification of TRBC gRNA-dependent mutations

Chr.	predicted position	mm	mutated reads [%]		mutation	distance	gene
13	81600523	2	2.7	13.3	INDEL	7	LINC00377 Intron
12	48838860	3	9	4.1	SNP	5	Non-coding
16	67155182	3	4	5.2	SNP	10	C16orf70 Intron
22	42110228	3	7.9	5.6	SNP	-7	MEI1 Intron
19	55458599	3	4.5	4.3	SNP	14	NLRP7 Intron
15	64854338	3	4.8	17.5	INDEL	6	ZNF609 Intron
13	23387879	4	5.9	3.8	SNP	25	Non-coding
2	233410251	4	3.2	3.2	SNP	33	CHRNA3 Exon 12
9	72036758	4	2.7	5.4	SNP	33	Non-coding
11	886055	4	8.3	7.1	SNP	7	CHID1 Intron
11	118787195	4	3.2	3	SNP	-11	Non-coding
16	85917083	4	7.9	2.9	SNP	-7	Non-coding
22	21803056	4	4.8	2.9	SNP	25	HIC2 Exon 3
22	21803056	4	4.9	2.9	SNP	27	HIC2 Exon 3
22	21803056	4	2.4	2.9	SNP	37	HIC2 Exon 3
22	35155013	4	2.8	2.4	SNP	14	ISX-AS1 Exon 5
19	6326226	4	9.1	7.1	SNP	-9	ACER1 Intron
19	6326226	4	3.8	5.9	SNP	17	ACER1 Intron
19	37597638	4	2.8	2.6	SNP	13	ZNF420 Intron
19	52750112	4	2.9	3.1	SNP	14	Non-coding
17	74727093	4	4.2	4.3	SNP	5	METTL23 Intron
17	74727093	4	4.5	6.3	SNP	34	METTL23 Intron
17	74727093	4	6.7	5.6	SNP	37	METTL23 Intron
17	77248887	4	2.9	5	SNP	7	RBFOX3 Intron

20	24599991	4	2.9	2.4	SNP	-4	SYNDIG1 Intron
20	37397707	4	2.4	3.1	SNP	21	ACTR5 Intron
20	62696378	4	4	3.3	SNP	5	TCEA2 Intron
X	104402946	4	7.1	4.5	SNP	-1	IL1RAPL2 Intron
X	138364716	4	6.3	3.7	SNP	25	Non-coding
X	139911558	4	11.1	12.5	SNP	17	Non-coding
X	153697911	4	3.7	3.4	SNP	7	PLXNA3 Intron
18	8609509	4	4.8	5.9	SNP	31	RAB12 Exon 1
18	45480226	4	2.7	2.6	SNP	2	Non-coding
18	45480226	4	2.6	2.4	SNP	9	Non-coding
18	45480226	4	2.8	2.4	SNP	29	Non-coding
18	45480226	4	2.8	5	SNP	34	Non-coding
18	48478141	4	6.3	10	SNP	12	Non-coding
9	92232519	4	3	2.9	SNP	18	Non-coding
9	92232519	4	3,1	3.1	SNP	25	Non-coding
9	113018452	4	2.8	2.7	SNP	-9	TXN Intron
9	116141432	4	2.6	5	SNP	15	Non-coding
9	116141432	4	2.6	4.5	SNP	21	Non-coding

Chr. = chromosome; position of potential off-target event as predicted by Cas-OFFinder; mm = mismatches between gRNA and target sequence; percentage of mutated reads present in each donor at predicted regions but not in controls; identified mutation: SNP = single nucleotide polymorphism, INDEL = insertions and/or deletions; Distance = genomic distance between predicted off-target position and identified mutation; affected gene according to IGV

Of note, 2 of 42 mutations were INDELS located within introns of non-coding RNA LINC00377 on chromosome 13, position 81,600,530 and Zink Finger protein ZNF609 on chromosome 15, position 64,854,344, thereby identifying these two off-targets experimentally (**Figure 11**).

In summary, none of the *in silico* predicted off-target sites could be confirmed neither for TRAC nor for TRBC gRNA experimentally. However, 2 INDELS in TRBC gRNA treated cells of two different donors were experimentally identified as off-target events.

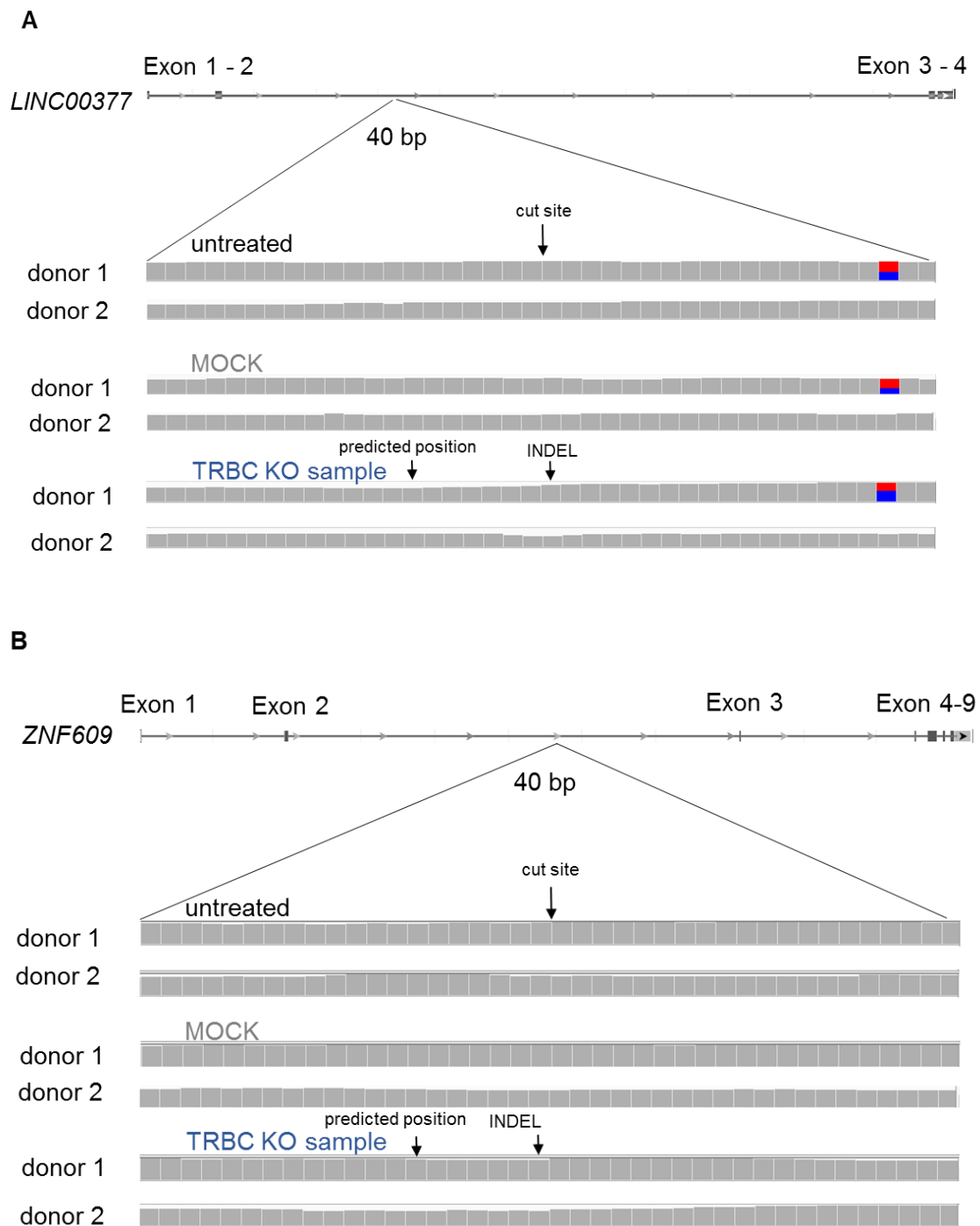


Figure 11: TRBC gRNA-dependent off-target events

Genomic DNA of untreated, MOCK control and CRISPR/Cas9-edited cells were investigated using whole-genome sequencing. Sequences of two different donors were compared to hg19 reference genome and analysed using IGV tool. **A** Identified off-target site for TRBC gRNA within the intronic region of *LINC00377*. **B** Identified off-target site for TRBC gRNA within an intron of *ZNF609*. Displayed are read frequencies of two donors for untreated, MOCK and TRBC gRNA and Cas9 treated *TRBC*-KO sample. Expected DSB sites, predicted off-target position and identified mutations are indicated with arrows. Red/blue bar indicates donor-dependent single nucleotide variants compared to hg19 reference genome.

6.3. Highly functional and target-specific LTDL-specific T-cell receptors

Two novel LTDLGQNLLY (LTDL)-specific TCRs were isolated *ex vivo* from a patient, who successfully controlled systemic, drug-refractory AdV infection after adoptive T-cell transfer with LTDL-specific T cells (Stief et al., 2022). These TCRs were functionally characterized *in vitro* to evaluate their specificity towards their cognate antigen. Therefore, coding vectors were introduced into primary human T cells using a retroviral delivery system (5.2.2, 5.2.4). In order to prevent TCR mispairing, both endogenous TCR chains were knocked out prior to transduction using CRISPR/Cas9 as described above (5.2.3.). Expression of effector markers and cytokines, as well as target-specific proliferation and cytotoxic activity of transduced cells upon stimulation with the cognate antigen were evaluated.

One week after transduction mean editing rates of 25.6% ($p = 0.0255$) and 29% ($p = 0.0077$) (**Figure 12 B**) with up to 51.7% and 50.4% LTDL-specific CD8⁺ T cells (**Figure 12 A**) were observed for TCR_1 and 2 by flow cytometric analysis, respectively (5.2.5). While the KO of the endogenous TCR also downregulates CD3 surface expression, the introduction of recombinant TCRs reversed this effect (**Figure 12 C**). In order to evaluate the specific effector functions of these TCRs, recombinant T cells were incubated with their cognate antigen LTDL or negative-control peptide GSEELRSLY (GSEE) (5.2.9). Although not significant, the degranulation marker CD107a was upregulated 7.7-fold among CD8⁺ T cells in TCR_1 samples and 7.3-fold in TCR_2 samples upon stimulation with LTDL, compared to unspecific stimulation with GSEE. Additionally, the expression of effector cytokines IFN γ (17.1- and 35.3-fold, $p = 0.0040$ for TCR_1 and 2) and TNF α (5.7-fold, $p = 0.0052$ and 6.8-fold for TCR_1 and TCR_2) increased in CD8⁺ T cells as response to LTDL-specific stimulation (**Figure 12 D**).

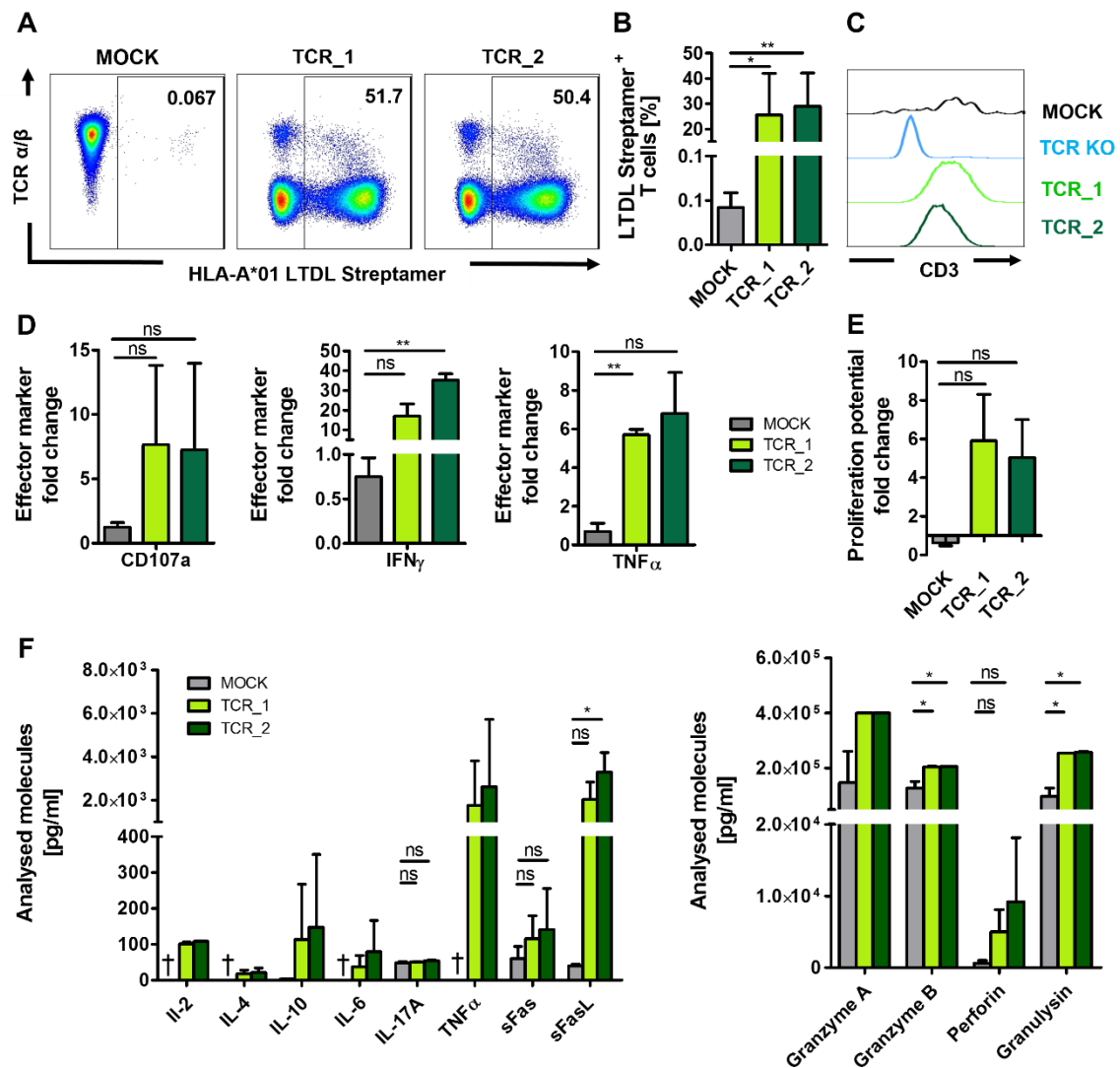


Figure 12: Recombinant T cells demonstrate high LTDL-specific functionality

TCR-KO T cells were retrovirally transduced with the respective TCRs and stimulated with their cognate antigen for functional analysis. **A** Representative flow cytometry data show percentage of LTDL-specific cells among CD8⁺ T cells one week after retroviral transduction. **B** Mean editing rates one week after genetic engineering display flow cytometric data of LTDL⁺ cells among CD8⁺ T cells. Data show mean ± SD of 5 independent experiments. **C** Expression of CD3 within LTDL⁺ CD8⁺ T cells or CD8⁺ T cells of TCR⁻ T cells. **D** Expression of effector markers after stimulation with LTDL peptide compared to GSEE stimulation. Data show mean ± SD of 2 independent experiments. **E** Proliferative potential of LTDL – MHC I Streptamer⁺ T cells upon co-culture with autologous LTDL-pulsed APCs compared to GSEE-pulsed APCs. Data show mean ± SD of 2 – 3 independent experiments. **F** Molecule secretion induced by co-culture with LTDL-pulsed autologous APCs displayed in pg/ml. Data show mean ± SD of 2 independent experiments. Granzyme A exceeded detection maximum of 400ng/ml. Data points marked with † were below detection threshold.

Furthermore, the proliferative potential of the transduced T cells as response to target-specific stimulation was assessed (5.2.13). Upon co-culture with irradiated, LTDL-pulsed PHA blasts for three days TCR_1 and 2 transduced T cells show an increased proliferative potential of 5.9- and 5.0-fold change, respectively, compared to unspecific stimulation with

GSEE-pulsed PHA blasts (**Figure 12 E**). Additionally, supernatants of these co-cultures were harvested after six days to analyse the secreted molecules (5.2.13). Very low levels of T_H2 cytokines IL-4, IL-6 and IL-10 could be detected after stimulation. Additionally, IL-2, IL-17A and sFas were poorly secreted. In contrast, Th1-specific cytokines like TNF α (1752.5 pg/ml and 2626.0 pg/ml for TCR_1 and TCR_2 transduced T cells, respectively) as well as sFas ligand (2033.2 pg/ml and 3289.0 pg/ml, $p = 0.0368$), Granzyme A (> 400 ng/ml each) and B (205.1 ng/ml, $p = 0.0483$ and 206.4 ng/ml, $p = 0.0467$), perforin (5.0 ng/ml and 9.2 ng/ml) and granulysin (254.4 ng/ml, $p = 0.0184$ and 258.4 ng/ml, $p = 0.0177$) were strongly expressed. Of note, Granzyme A secretion exceeded the detection limits of 8000 pg/ml even at high dilutions of 1:50. The value of secreted cytokines was thus set to a maximum of 400,000 pg/ml (**Figure 12 F**).

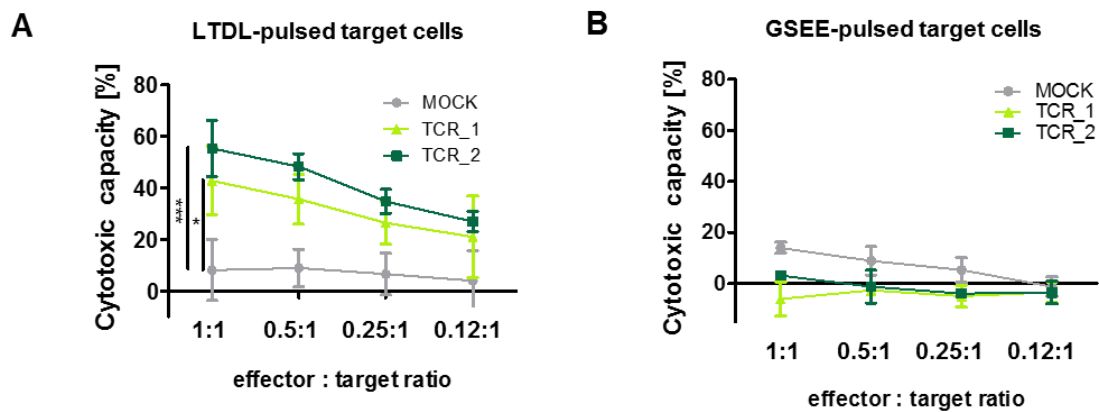


Figure 13: Cytotoxic capacity of transduced LTDL-specific T cells

CTL-mediated lysis of peptide pulsed target cells in different effector to target ratios. **A** Effector cells were co-cultured with LTDL-pulsed blasts. Data show mean \pm SD of 3 independent experiments (published in Stief et al., 2022). **B** Effector cells were co-cultured with GSEE-pulsed control cells. Data show mean \pm SD of 1 representative experiment in technical triplicates, * $p < 0.05$; *** $p < 0.001$

Cytotoxic capacity of enriched LTDL-specific T cells (5.2.11) was evaluated by co-culture with LTDL-pulsed target cells and determination of target-specific lysis (5.2.12). MOCK control was magnetically enriched for CD8 $^+$ cells, to have a comparable population of cytotoxic CD8 $^+$ T cells. 42.8% ($p = 0.0421$) and 55.3% ($p = 0.0005$) specific target cell lysis at an effector to target ratio of 1:1 was observed for TCR_1 and TCR_2-transduced T cells, respectively (**Figure 13 A**). Furthermore, target cell lysis was observed in an effector to target ratio-dependent manner. MOCK cells showed background killing of LTDL-pulsed

blasts below 10%. Unspecific killing of GSEE-pulsed, irradiated blasts was below 15% for MOCK control as well as for both TCR-transduced cells (**Figure 13 B**).

6.4. Functional TCR replacement using virus-free CRISPR/Cas9 engineering generates LTDL-specific T cells

To overcome retroviral-mediated random integration of transgenic TCRs into the host genome, homology-directed targeted integration was established. An orthotopic LTDL-specific TCR was designed with 5' and 3' homology arms for seamless integration into endogenous *TRAC* locus, thereby disrupting the TCR α chain. To avoid mispairing with the remaining endogenous β chain, *TRBC* was disrupted additionally. KI efficacy was determined by LTDL-MHC I Streptamer staining followed by characterization of these recombinant cells.

A DNA template of LTDL TCR_1 with 5' and 3' homology arms was designed *in silico* in order to repair the CRISPR/Cas-mediated double-strand break at *TRAC* locus by homology-directed repair (HDR) (**Figure 14 A**). The 5' homology arm (370bp) was followed by a P2A linker, followed by the complete β chain of LTDL TCR_1. A T2A linker separates the variable elements of the LTDL-specific α chain. 73 nucleotides upstream of Cas9-induced DSB within the first *TRAC* exon were incorporated, while the remaining endogenous *TRAC* sequence served as 3' homology arm (280bp) (5.2.2, 5.2.3). The targeted integration of the template within the endogenous *TRAC* locus was confirmed by PCR (5.2.6). Therefore, primers were chosen to bind upstream of the left homology arm and within the variable region of the LTDL-specific β chain. Correct integration of the HDR template revealed a specific PCR product of 1kb (**Figure 14 B**). KI efficacy was also determined on protein level by flow cytometric analysis (5.2.5). Up to 7.3% LTDL – MHC I Streptamer⁺ T cells among CD8⁺ T cells were observed in the KI sample (**Figure 14 C**). The flow cytometric quantification of LTDL – MHC I Streptamer⁺ T cells among CD8⁺ T cells revealed a significant ($p = 0.0040$) increase in LTDL-specific T cells with a mean editing efficacy of 4.8% LTDL – MHC I Streptamer⁺ T cells (**Figure 14 D**). Restored TCR expression correlated with CD3 surface expression, which was abolished in the TCR-KO sample but recovered in samples with CRISPR/Cas-mediated TCR KI (**Figure 14 E**).

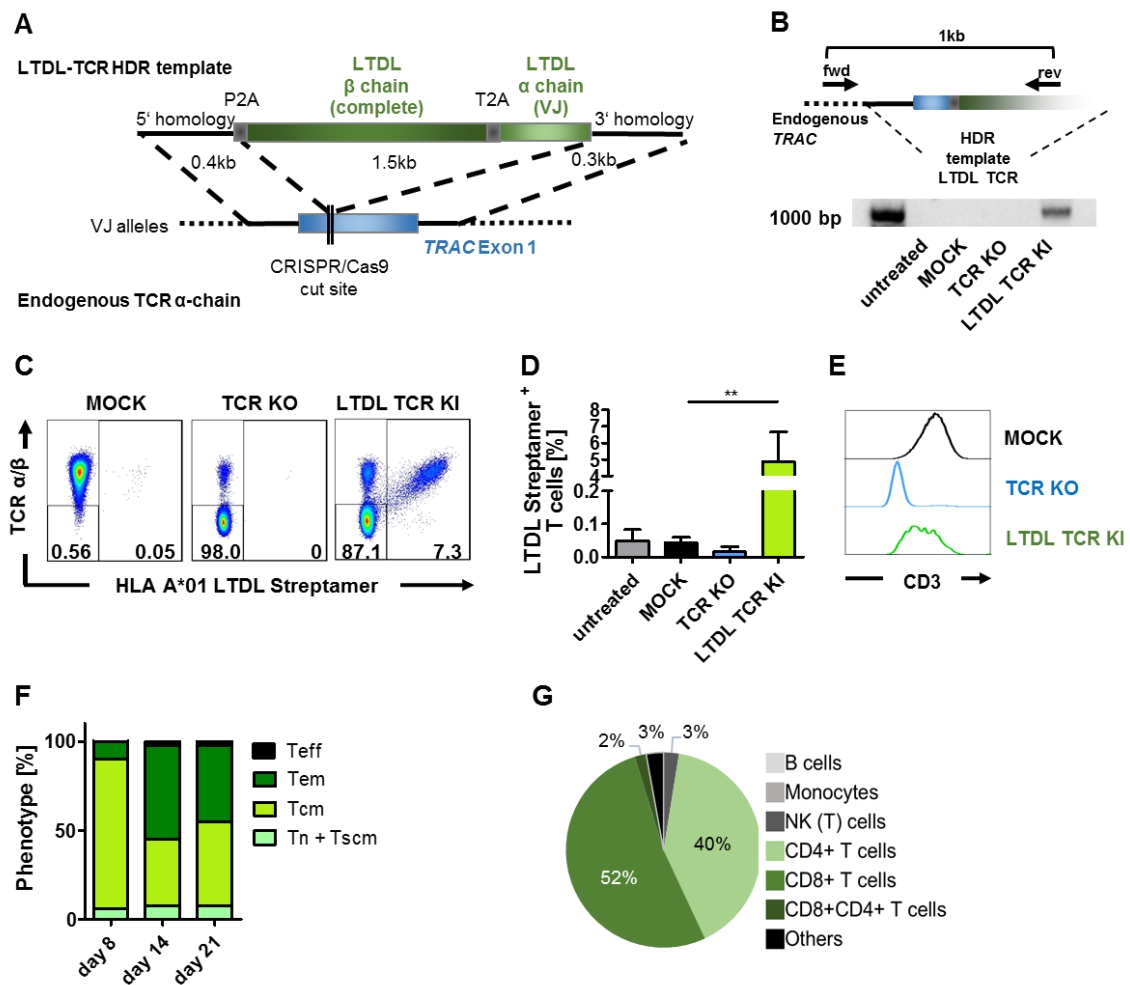


Figure 14: CRISPR/Cas9-mediated TCR replacement

T cells were electroporated with Cas9, TRAC and TRBC gRNA, and HDR template simultaneously for targeted integration of LTDL-specific TCR into the *TRAC* locus, thereby disrupting the complete endogenous TCR

A LTDL-specific TCR template for homology-directed repair (HDR) into the endogenous *TRAC* locus (published in Stief et al., 2022). **B** Integration of the HDR template into endogenous *TRAC* locus confirmed by PCR (published in Stief et al., 2022). **C** Representative dot plots of LTDL-MHC I Streptamer⁺ CD8⁺ T cells one week after electroporation (published in Stief et al., 2022). **D** Quantification of LTDL-MHC I Streptamer⁺ cells among CD8⁺ T cells one week after electroporation. Data show mean ± SD of 5 independent experiments (published in Stief et al., 2022). **E** Correlation of TCR and CD3 surface expression (published in Stief et al., 2022). **F** T cell phenotypes of TCR-KI samples. Data show mean ± SD of ≥ 3 independent experiments. **G** Cellular composition of TCR-KI sample one week after electroporation. ** p < 0.01

Analysis of the T-cell phenotypes *via* flow cytometry in the KI sample revealed a stable frequency of Tn and Tscm cells over time (6% on day 8, 7.9% on day 14 and 7.5% on day 21 post electroporation) among CD8⁺ T cells (**Figure 14 F**, 5.2.8). In contrast, the frequency of Tcm cells decreased (from 84.2% on day 8 post electroporation to 47% on day 21) while the percentage of Tem cells increased (from 9.6% to 43.3%). Additionally, a small

population of Teff cells comes up during *in vitro* cultivation (2.2% on day 21). These phenotypes are comparable to those of TCR-KO samples, which have more matured Tem cells than untreated and MOCK controls (**Figure 8 E**). Flow cytometric analysis of the cellular composition within the TCR-KI sample eight days *post* electroporation revealed similar distribution of CD8⁺ (52%) and CD4⁺ (40%) T cells (**Figure 14 G**) as in the TCR-KO and MOCK samples (**Figure 8 A**). While CD14⁺ monocytes and CD19⁺ B cells were still absent (0% each), low frequencies of CD56⁺ NK (T) cells (3%) and CD4⁺CD8⁺ (3%) were detected.

Next, the LTDL-specific functionality of these CRISPR/Cas-mediated TCR-KI cells upon stimulation with their cognate antigen was evaluated. Expression of effector markers and cytokines, as well as target-specific proliferation and cytotoxic activity of transduced cells upon stimulation with the cognate antigen were assessed. KI cells were co-cultured with cells that present the peptide in the context of HLA A*01:01 (5.2.10). In the KI sample 70.9% of LTDL – MHC I Streptamer⁺ cells produced IFN γ upon stimulation with LTDL-presenting cells, while unspecific stimulation with non-immunogenic FSECNALGSY-presenting cells did not result in any IFN γ production (0.1%, $p = 0.0005$, **Figure 15 A**). No LTDL – MHC I Streptamer⁺ IFN γ ⁺ cells were present in the MOCK control. Compared to unspecific stimulation with GSEE peptide, CD107a expression did not increase (1.3-fold in the MOCK control and 1.4-fold in TCR KI sample) following stimulation with LTDL peptide. TNF α expression increased 2.5-fold, but not significantly (**Figure 15 B**, 5.2.9). To assess the proliferative potential of the recombinant cells and secretion of molecules, CD56-depleted cells were co-cultured with irradiated, LTDL-pulsed PHA blasts and analysed in an immunobead-based assay (5.2.13). LTDL – MHC I Streptamer⁺ cells within the TCR-KI sample proliferated 1.9-fold ($p = 0.0507$) upon co-culture with LTDL-pulsed PHA blasts compared to GSEE-pulsed blasts, while the frequency of CD8⁺ T cells in the MOCK control slightly decreased (**Figure 15 C**).

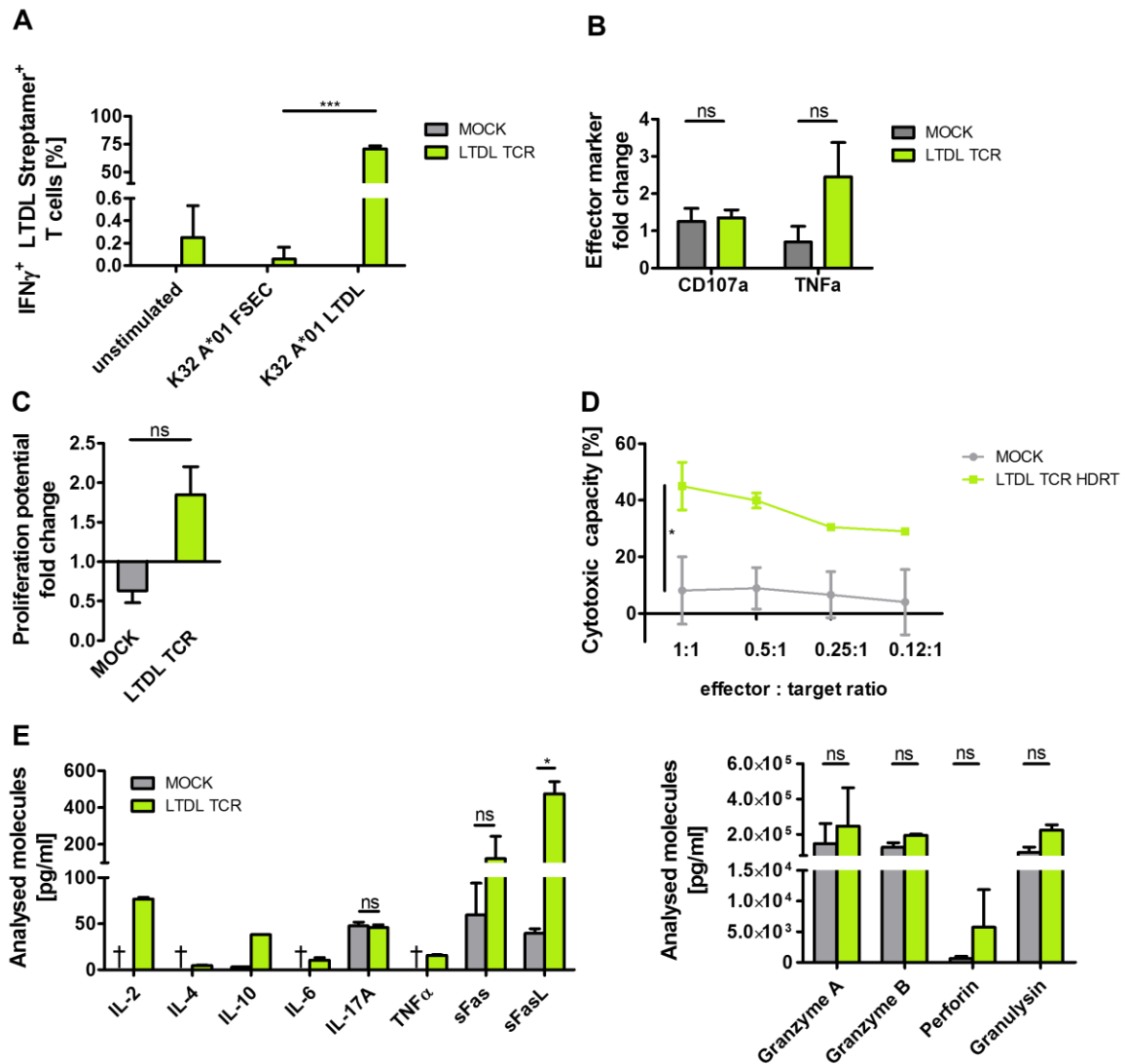


Figure 15: Functional LTDL-specific T-cell response after CRISPR/Cas9-mediated TCR replacement

T cells with CRISPR/Cas-mediated KI of LTDL TCR and KO of both endogenous TCR chains were stimulated with cognate antigen to evaluate their functionality. **A** Intracellular cytokine staining after co-culture with peptide-presenting cell line. Data show mean \pm SD of 3 independent experiments. **B** Expression of effector markers upon LTDL peptide stimulation displayed as fold change compared to unspecific GSEE stimulation. Data show mean \pm SD of 2 independent experiments. **C** Proliferation potential of LTDL – MHC I Streptamer⁺ T cells upon co-culture with autologous LTDL-pulsed APCs compared to GSEE-pulsed APCs. Data show mean \pm SD of 2 independent experiments. **D** Lysis of LTDL-pulsed target cells. Data show mean \pm SD of 2 independent experiments. **E** Secreted molecules after co-culture with LTDL-pulsed autologous APCs. Data show mean \pm SD of 2 independent experiments. Data points marked with † were below detection threshold. *** $p < 0.001$, * $p < 0.05$. ns = not significant, $p > 0.05$

In the supernatant of the co-culture low levels of IL-2 (76.9 pg/ml in TCR KI samples, MOCK below detection limit), IL-10 (38.0 pg/ml and 3.0 pg/ml), IL-6 (10.6 pg/ml, MOCK below detection limit), IL-17A (45.8 pg/ml and 47.7 pg/ml), TNF α (15.6 pg/ml, MOCK below detection limit), sFas (123.4 pg/ml and 59.5 pg/ml) and sFas ligand (475.1 pg/ml and

39.5 pg/ml, $p = 0.0114$) were detected. For Granzyme A (247 ng/ml and 147 ng/ml), Granzyme B (195 ng/ml and 127 ng/ml), perforin (5 ng/ml and 0.6 ng/ml) and granulysin (224 ng/ml and 97 ng/ml) much higher concentrations were observed (**Figure 15 E**). These findings indicate that effector cytokines of CTLs were strongly secreted while Th2 and anti-inflammatory cytokines are poorly expressed, although cytokines in TCR-KI samples were not significantly elevated compared to MOCK.

The cytotoxic activity of TCR-KI cells was determined by co-cultivation of CD56-depleted, LTDL – MHC I Streptamer sorted T cells with LTDL-pulsed PHA blasts (5.2.12). Up to 45% target cells lysis ($p = 0.0339$) was observed in an effector to target ratio dependent manner for TCR-KI cells, while background killing for MOCK control was below 10% (**Figure 15 D**).

In summary, these findings indicate strong target-specific effector functions of CRISPR/Cas9-engineered LTDL-specific T cells in terms of IFN γ secretion, proliferation and cytotoxic activities, although other CTL-specific markers were not significantly increased.

7. Discussion

7.1. Safe and highly efficient KO of TCRs in primary human T cells using virus-free CRISPR/Cas9

Genetic engineering of T cells for adoptive T-cell therapy (ACT) is a major milestone in immunotherapy, thus providing novel treatment strategies for a variety of diseases, including viral infections and cancer. A current instance is the approval of chimeric-antigen receptor (CAR) T cells, targeting CD19 which is expressed in B-cell-derived malignancies such as acute lymphoblastic leukaemia in 2017. Commonly used gene editing strategies use retroviral delivery systems for transgene submission. Retroviral vectors lead to random integration of the transgene into the host genome and provided viral promoters induce strong transgene expression (Engels et al., 2003). This approach offers high editing rates and in the example of CD19-CAR-T cells sustained anti-tumour effects could be achieved in patients suffering from B-cell leukaemia (Porter et al., 2011, Lee et al., 2015). However, few cases have been described of retroviral vectors which caused leukaemia in transduced haematopoietic stem cells (Cavazzana et al., 2016). These findings triggered improvement of viral vector systems as well as the development of alternative virus-free editing approaches (Rivière et al., 2012). Zinc finger nucleases (ZFN), transcription-activator like effector nucleases (TALENs), and the clustered regularly interspaced short palindromic repeats/Cas9 nuclease (CRISPR/Cas) system can be provided as plasmids, proteins, and mRNA and are capable to induce double-strand breaks at targeted loci which can be repaired subsequently by providing DNA templates for homologous repair (Porteus and Carroll, 2005, Gaj et al., 2013). ZFNs are engineered heterodimeric proteins composed of zinc-finger sequence-specific binding domains coupled to *FokI* restriction enzyme, that induce double-strand breaks (DSB) at predestined loci. At least two zinc fingers are required, each of them recognizing 3 bp of a DNA sequence, thus initialising dimerization of *FokI* cleavage domains at the targeted locus to induce a DSB. Although investigated in clinical trials, comparable low editing frequencies, limited zinc-finger specificity and reported off-target effects limit the broad application of ZFNs (Provasi et al., 2012, Delhove and Qasim, 2017). Transcription-activator like effectors (TALE) are bacterial-derived proteins which are fused to a DNA-cutting nuclease. Two pairs of TALEs are required for predestined DNA binding, dimerization of *FokI* nuclease and DNA cleavage (Miller et al., 2011). TALENs generate higher editing efficacies with increased specificity compared to ZFNs but are larger in size, thus limiting delivering vectors. The CRISPR/Cas9 system uses a short guideRNA

(gRNA) and the bacterial derived Cas9 nuclease cuts the DNA double strand at the predestined target site. In contrast to protein-dependent systems of ZFN and TALEN, CRISPR/Cas9 is guided by a 20-nucleotide short nucleotide sequence, complementary to the targeted DNA sequence. Based on the easy and flexible gRNA design and smaller size compared to protein-guided approaches, CRISPR/Cas components can be generated fast and are easily delivered to human cells. All three editing approaches have been successfully applied to disrupt the T-cell receptor (TCR) in order to prevent mispairing with subsequently introduced transgenic TCRs and GvHD due to alloreactivity, though with varying efficacy. Provasi et al. used integrase-defective lentiviral vector delivered ZFNs to disrupt the TCR β chain in human T cells and achieved 7% TCR/CD3-negative T cells (Provasi et al., 2012). A TALEN-mediated KO of the TCR, delivered by mRNA transfection resulted in 59% TCR-negative T cells targeting the TCR α chain and 41% TCR-negative T cells when TCR β chain was targeted (Berdien et al., 2014). Osborn et al. were first to apply the CRISPR/Cas system to induce a TCR KO in primary human T cells, thereby outperformed TALEN-mediated editing efficacy. TALEN mediated TCR KO in Jurkat cells achieved 60% CD3-negative cells, but in contrast to Berdien et al. the efficacy in primary T lymphocytes dramatically decreased and caused severe toxicity. However, 85% CD3-negative T cells were obtained using Cas9 and gRNA targeting *TRAC* (Osborn et al., 2016).

One aim of this thesis was to further increase TCR disruption rates using CRISPR/Cas9, in order to generate best possible prerequisites for subsequent TCR replacement. TCR KO was demonstrated on genetic level using TIDE analysis, by comparing DNA sequences of bulk edited cells with electroporated-only cells (MOCK). These results were confirmed on protein level by evaluation of TCR surface expression using flow cytometry analysis. TCR-KO efficiencies up to 94% and 96% TCR⁻ T cells were obtained for *TRAC* and *TRBC* gRNA, respectively, peaking in 98% TCR⁻ T cells for combined *TRAC* and *TRBC* KO, demonstrating high CRISPR/Cas9-mediated gene editing efficacy. KO of the TCR correlated with loss of CD3 surface expression, indicating complete disruption of the TCR complex, which was proven functionally by abrogated IFN γ expression upon unspecific TCR stimulation. Of note, CRISPR/Cas-mediated KO of the TCR did not impair T-cell phenotypes, CD4/CD8 ratios or expansion potential, which confirms observations from ZFN-mediated TCR disruption (Berdien et al., 2014). Functional TCR-KO T cells were capable to expand *in vitro* due to TCR-independent initial stimulation *via* CD3 and CD28. The procedure caused no toxicity in terms of viability to TCR-KO T cells and the frequency of TCR⁻ T cells within the TCR-KO sample remained stable during expansion with supplemented IL-7 and IL-15, thus indicating neglectable disadvantages of TCR⁻ T cells at

least after initial, TCR-independent activation *via* CD3/CD28. Long-term *in vitro* culture supports a more matured effector memory T-cell phenotype, which was elevated in TCR-KO samples. Different studies demonstrated IL-15 to promote memory phenotypes in CD8⁺ T cells and to be capable to induce TCR-independent activation of CD8⁺ memory T cells (Zhang et al., 1998, Liu et al., 2002). The absence of TCRs probably made cells more susceptible to IL-15 than their TCR-bearing counterparts, thus promoting a more matured phenotype in the TCR-KO sample during long-term cultivation.

Although mature T cells are less susceptible for oncogenic transformation than hematopoietic stem cells (Newrzela et al., 2008) and CRISPR/Cas-mediated gene editing is expected to induce less unwanted side effects than randomly integrating viral vectors, off-target activities can't be precluded (Lu et al., 2020). However, safe and predictable gene-editing strategies are strongly preferable regarding clinical applications and previous publications are rather contradictory (Veres et al., 2014, Fu et al., 2013). In order to identify potential Cas9-induced off-target effects whole-genome deep-sequencing was performed from *TRAC*-KO and *TRBC*-KO samples and compared to hg19 reference genome. No difference in the cumulative number of SNPs or INDELS, INDEL size or SNP effects were observed in CRISPR/Cas9-engineered samples compared to controls. Hence, off-target sites predicted by sequence similarity of the applied gRNA were analysed. Previous studies assumed that off-target events are limited by up to 3 nucleotide mismatches (Schwank et al., 2013, Mali et al., 2013). In the present study, sequences with up to 4 mismatches were considered as off-target candidates. Importantly, none of the predicted off-target candidates could be confirmed for the exact predicted positions. For this reason, regions spanning 40 nucleotides around possible Cas9 cut sites (3 nucleotides upstream of PAM sequences (Gasiunas et al., 2012)), including the predicted positions, were investigated. 9 SNPs in non-coding or intronic regions were detected for TRAC gRNA in proximity to predicted positions with 4 mismatches. For TRBC gRNA 42 mutations were observed, including 2 INDELS in intronic regions. Intronic variants can be responsible for different human diseases due to activation of alternative splicing sites, disruption of transcription regulatory motives and inactivation of intronic RNA genes (Vaz-Drago et al., 2017). The effect of these specific intronic mutations would need further investigation. Hence, most of the SNPs were observed for regions with 4 nucleotide mismatches to the applied crRNA.

Cas9-induced blunt-end DSB induce error prone non-homologous end-joining (NHEJ), thus mediating insertions and deletions of nucleotides rather than SNPs, that rather arise during culture or randomly accumulate due to technical artefacts (van Overbeek et al., 2016). Of

note, both TRBC gRNA-dependent INDELS did not pass high-quality call filters applied to unbiased genome-wide variant calling in a second approach, but revealed 3 intronic INDELS for TRAC and 6 intronic INDELS for TRBC gRNA, respectively (Kaeuferle et al., 2022). This confirms previous investigations for both gRNAs which reported neglectable off-target activity (Ren et al., 2017, Knipping et al., 2017).

In this project, a distinct, donor-independent INDEL pattern at the on-target site was identified by TIDE analysis for each gRNA applied. This gRNA pattern was preserved in the presence of both gRNAs. This finding presumes predictive, definite mutational events depending on the respective gRNA, the presence of adequate PAM and target sequences, rather than random mutations. This assumption is supported by findings from van Overbeek et al., who demonstrated that the repair of DSB is non-random and emerging INDEL patterns depend on the target-site sequence, whereby cell lines could be utilized to determine DNA repair profiles. (van Overbeek et al., 2016). Interestingly, they reported rather small INDEL sizes (< 40 base pairs) which is strongly opposing to large deletions (up to 6 kilobases) and genomic rearrangements reported by Kosicki et al. when applying intronic and exonic gRNAs to human differentiated cell lines, mouse embryonic and haematogenic stem cells (Kosicki et al., 2018). Short-read sequences as obtained in the current study would therefore be a limitation. The sequencing of bulk T cells may also underestimate the frequency of rare variations compared to monoclonal sequencing (Smith et al., 2020), but better reflects administered cell populations as for therapeutic applications. Accordingly, extensive characterization of gRNAs is an essential prerequisite for genome editing using CRISPR/Cas9, thus providing important information for precise prediction of possible unwanted side effects. Furthermore, a new generation of high-fidelity Cas nucleases has been developed in order to further decrease off-target activities which contributes to highly specific and safe genetic engineering (Slaymaker et al., 2016, Vakulskas et al., 2018). A direct comparison of respective WGS data, generated with Cas9 and the high-fidelity Cas could reveal possible advantages of the improved nucleases. Nevertheless, long-term follow ups in clinical settings with large patient cohorts will be required to ensure clinical safety of applied gRNAs and Cas nucleases.

7.2. Redirecting human T cells towards highly functional LTDL-specific CTLs for adoptive T-cell transfer

Stem cell transplantations (SCT) are a widely used treatment strategy for a variety of diseases. CD3-depleted grafts from allogeneic donors can avoid T-cell mediated GvHD, however, driving the patient into transient deficient T-cell immunity. The lack of virus-specific T cells leads to vulnerability to primary viral infections as well as the reactivation of persistent viruses like Cytomegalovirus, Epstein-Barr virus, and adenoviruses (AdVs). The presence of AdV-specific antibodies in the peripheral blood prior to infection can predetermine possible reactivation of the virus during immunodeficiency (Veltrop-Duits et al., 2011). Paediatric patients face higher risks for AdV infections compared to adult patients, that is also associated with higher morbidity and mortality rates (van Tol et al., 2005a, George et al., 2012, Baldwin et al., 2000). Infections with species C and B are predominant in paediatric patients, maybe due to their latency potential (Zheng et al., 2008, Baldwin et al., 2000, Flomenberg et al., 1994). But infections with other species and combinations of different species also occur, affecting different body sites (Zheng et al., 2008). AdV infections in patients following SCT are associated with gastrointestinal disease, infections of the respiratory tract, haemorrhagic cystitis, and hepatitis and progression into disseminated, life-threatening disease in the absence of virus-specific T cells (Chakrabarti et al., 2004, Feuchtinger et al., 2005). Adoptively transferred AdV-specific T cells are capable to reconstitute the recipient's cell-mediated immunity and to control viral infection (Leen et al., 2009, Feucht et al., 2015, Geyeregger et al., 2014, Feuchtinger et al., 2006). The AdV hexon-derived peptide LTDLGQNNLY has been shown to be highly conserved throughout different AdV species and to mediate cross-reactive protection, suggesting this epitope to be dominant in AdV immunity (Leen et al., 2004, Geyeregger et al., 2013, Keib et al., 2019). About 20% of stem cell donors are lacking protective hexon-specific T cells (Feuchtinger et al., 2008) and therefore would not be suitable donors for adoptive T-cell transfer. This limitation can be overcome by introduction of hexon-specific TCRs, thereby redirecting T-cell specificity and providing new means for adoptive T-cell therapy (Dörrie et al., 2014, Provasi et al., 2012, Oh et al., 2011, Stadtmauer et al., 2020).

Here, 2 novel LTDL-specific TCRs were functionally characterized *in vitro* after they have been isolated from a patient where adoptive transfer of LTDL-specific T cells mediated immunity against refractory, systemic AdV infection (Stief et al., 2022). As a proof-of-concept study, one of these highly functional TCRs was transferred into primary human T

cells using ribonucleoprotein transfection of CRISPR/Cas9 reagents, therefore redirecting T cells towards highly LTDL-specific T cells.

Both LTDL-specific TCRs were retrovirally transduced into primary human T cells in order to determine their cytotoxic effector functions like cytokine secretion, proliferation and cytotoxic potential upon stimulation with their cognate antigen. To prevent mispairing with human endogenous TCR chains additional KO of both endogenous TCR chains using CRISPR/Cas9 was performed. Retroviral transduction resulted in high LTDL-TCR expression and both TCRs demonstrated strong LTDL-specific effector functions. Secretion of effector cytokines CD107a, TNF α and IFN γ was elevated upon stimulation with LTDL. Upon co-culture with LTDL-presenting cells transduced LTDL-specific T cells demonstrated proliferative potential as well cytotoxic killing of target cells. Molecules analysed in the supernatant of transduced cells revealed elevated secretion of TNF α , FasL, Granzyme A and B, and Granulysin. These findings indicate that effector cytokines of cytotoxic T cells are secreted rather than Th2 cytokines, which is in line with the results obtained from cytotoxic killing assay. Similar response to antigen-specific stimulation of both TCRs is probably due to their highly similar CDR3 regions. Both TCRs demonstrated strong LTDL-specific effector functions and may therefore mediate protection *in vivo*, thereby being promising targets for recombinant expression in donor T cells in order to treat AdV infections in immunocompromised patients.

Since both TCRs showed similar effector functions, LTDL TCR_1 was selected for subsequent investigations using CRISPR/Cas9-mediated introduction into T cells. For homology-directed repair of the Cas9 nuclease-induced DSB within the TCR α chain constant region (*TRAC*) a template with homology arms covering 300 – 400 base pairs flanking the DSB was designed. Homology arms ensure in-frame integration of the DNA template into the endogenous *TRAC* locus. The template is coding for the complete LTDL TCR_1 β chain, the α chain variable region, and the first part of the constant region up to the CRISPR/Cas9-induced cut site in the endogenous sequence. This shortened TCR sequence was seamlessly integrated into the endogenous *TRAC* locus *via* CRISPR/Cas9 and utilized the endogenous *TRAC* sequence downstream of the DSB that enables functional, full-length TCR expression. LTDL-MHC I Streptamer staining confirmed stable surface expression of LTDL-TCR_1 that correlated with CD3 surface expression, which demonstrates complete TCR complex expression. The phenotypical characteristics of LTDL-TCR KI samples were comparable to those observed for MOCK samples. One week after genetic engineering, CD8/CD4 ratios showed a higher frequency of CD8⁺ T cells and

cells mainly had a central memory phenotype. Central memory phenotypes were previously shown to be more beneficial for adoptive T-cell therapy compared to other T-cell phenotypes (Berger et al., 2008). *Ex vivo* expanded antigen-specific CD8⁺ central memory T cells demonstrated proliferative potential, effector functions, and long-term persistence *in vivo* following adoptive transfer in primates (Berger et al., 2008).

Functional characterization of CRISPR/Cas-mediated LTDL-TCR KI samples was performed to evaluate their effector potential. The effector cytokine IFN γ was strongly expressed in LTDL-TCR expressing CD8⁺ T cells. In contrast to transduced LTDL-specific T cells, CRISPR/Cas-engineered LTDL-specific T cells showed no elevated expression of TNF α following peptide stimulation. The proliferative potential of CRISPR/Cas-engineered LTDL-specific T cells was also lower compared to transduced T cells. Expression of degranulation markers CD107a was conserved, however, LTDL-specific T cells showed high cytotoxic killing capacity against autologous LTDL-pulsed target cells. Although not significant, enhanced effector functions of transduced LTDL-specific T cells could be due to strong transgene expression mediated by the constitutive active viral promoter. CRISPR/Cas-engineered LTDL-specific T cells are controlled by the endogenous TCR promoter because of the targeted and seamless integration into the endogenous *TRAC* locus, which provides physiological regulation of the TCR. Following antigen-specific stimulation, TCR surface expression is downregulated to prevent excessive T-cell stimulation (Schrum et al., 2003, Eyquem et al., 2017). This mechanism is perturbed in retrovirally transduced T cells, where TCR downregulation is diminished but subsequent upregulation occurs faster (van Loenen et al., 2011, Schober et al., 2019). Regarding clinical applications, physiological TCR expression seems to be desirable but if this is superior *in vivo* has to be elucidated. The targeted integration of the LTDL-TCR into the endogenous *TRAC* locus does not only provide physiological TCR expression but eliminates expression of the endogenous TCR α chain, simultaneously. Although the disruption of only one element of the TCR complex is sufficient to abolish TCR surface expression (Schrum et al., 2003), mispairing of the transgenic TCR with the remaining endogenous β chain will occur (Schober et al., 2019). This results in reduced expression of the transgenic TCR, diminished antigen sensitivity, and formation of new TCRs with unknown specificity that potentially induce lethal GvHD by alloreactive T cells (Schober et al., 2019, Provasi et al., 2012, Poirot et al., 2015, Morton et al., 2020). Therefore, an additional KO of the endogenous β chain was performed as well. Although high TCR KO efficiencies were obtained with the established protocol, the introduction of a new TCR could still result in a small proportion of β -chain mispaired TCRs and double-specific T

cells, that cannot be fully excluded. Of note, Stenger et al. observed reduced alloreactivity of T cells with CRISPR/Cas9-mediated KO of the TCR β chain upon co-culture with PBMCs from 6 different donors (Stenger et al., 2020).

With few exceptions, bulk T-cell populations have been analysed in this study. This was possible due to high TCR-KO efficiencies and LDTL-Streptamer staining for detection of LDTL-specific T cells in flow cytometric analysis. However, isolation of engineered T cells using pMHC Streptamers has to be performed to obtain a purified fraction of LDTL-specific T cells for clinical applications. Direct isolation using antigen-specific Streptamers was already successfully used for good manufacturing practice (GMP)-compliant isolation of virus-specific T cells to high purities and with maintained phenotypes and functionality (Freimüller et al., 2015, Neuenhahn et al., 2017, Schmitt et al., 2011). Low-dose transfer of Streptamer-sorted virus-specific CD8⁺ T cells (3750 cells/kg body weight) isolated from haploidentical parents was demonstrated to mediate viral clearance but not GvHD in two paediatric allogeneic HSCT patients (Stemberger et al., 2014). Though no additional upscale of the manufacturing process will be required for this already in a GMP-compatible manner established procedure.

The protective and highly conserved epitope LTDLGQNLLY is restricted to HLA A*01:01, that is expressed by about 25% of individuals in Europe (González-Galarza et al., 2015). The identification of additional TCRs, directed against protective AdV-derived epitopes restricted to the remaining HLA types, would be required for the generation of “off-the-shelf” protective TCR banks. Thereby, the here presented proof-of-concept procedure would facilitate the HLA-dependent generation of AdV-specific T cells from seronegative stem cell donors for the treatment of refractory AdV infections of different subgroups in SCT recipients. This approach will circumvent the need of seropositive stem cell donors as well as seropositive HLA-identical 3rd party donors. The completely virus-free approach allows fast and flexible generation of templates and crRNAs and is more likely for approval by regulatory authorities than viral vector systems.

In conclusion, CRISPR/Cas9-mediated genetic engineering of primary human T cells was proven to be highly specific with neglectable off-target activity and stable editing efficacies. Replacing the endogenous TCR in primary human T cells with a LDTL-specific TCR using CRISPR/Cas9 is feasible, and characterization of these engineered T cells reveals highly functional and specific cytotoxic T cells. Simultaneous knock out of both endogenous TCR chains will prevent harmful TCR mispairing and therefore GvHD mediated by alloreactive TCRs. Redirecting primary human T cells from seronegative donors by CRISPR/Cas-

mediated replacement of the TCR is a powerful tool for treatment of refractory viral infections in the immunocompromised host. This approach could be transferred for treatment of other persistent viruses, emerging infectious and malignant diseases that would benefit from adoptively transferred specific T cells.

References

- AHMADI, M., KING, J. W., XUE, S.-A., VOISINE, C., HOLLER, A., WRIGHT, G. P., WAXMAN, J., MORRIS, E. & STAUSS, H. J. 2011. CD3 limits the efficacy of TCR gene therapy in vivo. *118*, 3528-3537.
- AKTAS, E., KUCUKSEZER, U. C., BILGIC, S., ERTEN, G. & DENIZ, G. 2009. Relationship between CD107a expression and cytotoxic activity. *Cellular Immunology*, *254*, 149-154.
- AL QURASHI, Y. M. A., GUIVER, M. & COOPER, R. J. 2011. Sequence typing of adenovirus from samples from hematological stem cell transplant recipients. *83*, 1951-1958.
- ANDERSEN, M. H., SCHRAMA, D., THOR STRATEN, P. & BECKER, J. C. 2006. Cytotoxic T Cells. *Journal of Investigative Dermatology*, *126*, 32-41.
- AYROLDI, E., ZOLLO, O., CANNARILE, L., D' ADAMIO, F., GROHMANN, U., DELFINO, D. V. & RICCARDI, C. 1998. Interleukin-6 (IL-6) Prevents Activation-Induced Cell Death: IL-2–Independent Inhibition of Fas/fasL Expression and Cell Death. *Blood*, *92*, 4212-4219.
- BAE, S., PARK, J. & KIM, J.-S. 2014. Cas-OFFinder: a fast and versatile algorithm that searches for potential off-target sites of Cas9 RNA-guided endonucleases. *Bioinformatics*, *30*, 1473-1475.
- BAHCECI, E., EPPERSON, D., DOUEK, D. C., MELENHORST, J. J., CHILDS, R. C. & BARRETT, A. J. 2003. Early reconstitution of the T-cell repertoire after non-myeloablative peripheral blood stem cell transplantation is from post-thymic T-cell expansion and is unaffected by graft-versus-host disease or mixed chimaerism. *122*, 934-943.
- BALDWIN, A., KINGMAN, H., DARVILLE, M., FOOT, A. B. M., GRIER, D., CORNISH, J. M., GOULDEN, N., OAKHILL, A., PAMPHILON, D. H., STEWARD, C. G. & MARKS, D. I. 2000. Outcome and clinical course of 100 patients with adenovirus infection following bone marrow transplantation. *Bone Marrow Transplantation*, *26*, 1333-1338.
- BARRANGOU, R., FREMAUX, C., DEVEAU, H., RICHARDS, M., BOYAVAL, P., MOINEAU, S., ROMERO, D. A. & HORVATH, P. 2007. CRISPR Provides Acquired Resistance Against Viruses in Prokaryotes. *Science*, *315*, 1709-1712.
- BENDLE, G. M., LINNEMANN, C., HOOIJKAAS, A. I., BIES, L., DE WITTE, M. A., JORRITSMA, A., KAISER, A. D. M., POUW, N., DEBETS, R., KIEBACK, E., UCKERT, W., SONG, J.-Y., HAANEN, J. B. A. G. & SCHUMACHER, T. N. M. 2010. Lethal graft-versus-host disease in mouse models of T cell receptor gene therapy. *Nature Medicine*, *16*, 565-570.
- BENNETT, J. E., DOLIN, R. & BLASER, M. J. 2014. *Mandell, Douglas, and Bennett's Principles and Practice of Infectious Diseases: 2-Volume Set*, Elsevier Health Sciences.
- BERDIEN, B., MOCK, U., ATANACKOVIC, D. & FEHSE, B. 2014. TALEN-mediated editing of endogenous T-cell receptors facilitates efficient reprogramming of T lymphocytes by lentiviral gene transfer. *Gene Therapy*, *21*, 539-548.
- BERDIEN, B., REINHARD, H., MEYER, S., SPÖCK, S., KRÖGER, N., ATANACKOVIC, D. & FEHSE, B. 2013. Influenza virus-specific TCR-transduced T cells as a model for adoptive immunotherapy. *Human vaccines & immunotherapeutics*, *9*, 1205-1216.
- BERESFORD, P. J., ZHANG, D., OH, D. Y., FAN, Z., GREER, E. L., RUSSO, M. L., JAJU, M. & LIEBERMAN, J. 2001. Granzyme A Activates an Endoplasmic Reticulum-associated Caspase-independent Nuclease to Induce Single-stranded DNA Nicks. *276*, 43285-43293.
- BERGER, C., JENSEN, M. C., LANSDORP, P. M., GOUGH, M., ELLIOTT, C. & RIDDELL, S. R. 2008. Adoptive transfer of effector CD8+ T cells derived from central memory cells establishes persistent T cell memory in primates. *The Journal of Clinical Investigation*, *118*, 294-305.

- BETTS, M. R., BRENCHELEY, J. M., PRICE, D. A., DE ROSA, S. C., DOUEK, D. C., ROEDERER, M. & KOUP, R. A. 2003. Sensitive and viable identification of antigen-specific CD8⁺ T cells by a flow cytometric assay for degranulation. *Journal of Immunological Methods*, 281, 65-78.
- BOLLARD, C. M., KUEHNLE, I., LEEN, A., ROONEY, C. M. & HESLOP, H. E. 2004. Adoptive immunotherapy for posttransplantation viral infections. *Biology of Blood and Marrow Transplantation*, 10, 143-155.
- BRINKMAN, E. K., CHEN, T., AMENDOLA, M. & VAN STEENSEL, B. 2014. Easy quantitative assessment of genome editing by sequence trace decomposition. *Nucleic Acids Research*, 42, e168-e168.
- BROUNS, S. J. J., JORE, M. M., LUNDGREN, M., WESTRA, E. R., SLIJKHUIS, R. J. H., SNIJDERS, A. P. L., DICKMAN, M. J., MAKAROVA, K. S., KOONIN, E. V. & VAN DER OOST, J. 2008. Small CRISPR RNAs guide antiviral defense in prokaryotes. *Science (New York, N.Y.)*, 321, 960-964.
- BURNETT, R. M. 1985. The structure of the adenovirus capsid: II. The packing symmetry of hexon and its implications for viral architecture. *Journal of Molecular Biology*, 185, 125-143.
- CALL, M. E., PYRDOL, J. & WUCHERPFENNIG, K. W. 2004. Stoichiometry of the T-cell receptor-CD3 complex and key intermediates assembled in the endoplasmic reticulum. 23, 2348-2357.
- CAVAZZANA, M., SIX, E., LAGRESLE-PEYROU, C., ANDRÉ-SCHMUTZ, I. & HACEIN-BEY-ABINA, S. 2016. Gene Therapy for X-Linked Severe Combined Immunodeficiency: Where Do We Stand? *Human gene therapy*, 27, 108-116.
- CHAKRABARTI, S., MILLIGAN, D. W., MOSS, P. A. H. & MAUTNER, V. 2004. Adenovirus Infections in Stem Cell Transplant Recipients: Recent Developments in Understanding of Pathogenesis, Diagnosis and Management. *Leukemia & Lymphoma*, 45, 873-885.
- CHAKUPURAKAL, G., ONION, D., BONNEY, S., COBBOLD, M., MAUTNER, V. & MOSS, P. 2013. HLA-Peptide Multimer Selection of Adenovirus-specific T Cells For Adoptive T-Cell Therapy. 36, 423-431.
- CHICAYBAM, L., SODRE, A. L., CURZIO, B. A. & BONAMINO, M. H. 2013. An Efficient Low Cost Method for Gene Transfer to T Lymphocytes. *PLOS ONE*, 8, e60298.
- CHO, S. W., KIM, S., KIM, J. M. & KIM, J.-S. 2013. Targeted genome engineering in human cells with the Cas9 RNA-guided endonuclease. *Nature Biotechnology*, 31, 230-232.
- COHEN, C. J., LI, Y. F., EL-GAMIL, M., ROBBINS, P. F., ROSENBERG, S. A. & MORGAN, R. A. 2007. Enhanced antitumor activity of T cells engineered to express T-cell receptors with a second disulfide bond. *Cancer research*, 67, 3898-3903.
- COUPER, K. N., BLOUNT, D. G. & RILEY, E. M. 2008. IL-10: The Master Regulator of Immunity to Infection. *The Journal of Immunology*, 180, 5771-5777.
- CRADDOCK, C. 2000. Haemopoietic stem-cell transplantation: recent progress and future promise. *The Lancet Oncology*, 1, 227-234.
- DE MEZERVILLE, M. H., TELLIER, R., RICHARDSON, S., HÉBERT, D., DOYLE, J. & ALLEN, U. 2006. Adenoviral Infections in Pediatric Transplant Recipients: A Hospital-Based Study. *The Pediatric Infectious Disease Journal*, 25, 815-818.
- DELHOVE, J. M. K. M. & QASIM, W. 2017. Genome-Edited T Cell Therapies. *Current Stem Cell Reports*, 3, 124-136.
- DHINGRA, A., HAGE, E., GANZENMUELLER, T., BÖTTCHER, S., HOFMANN, J., HAMPRECHT, K., OBERMEIER, P., RATH, B., HAUSMANN, F., DOBNER, T. & HEIM, A. 2019. Molecular Evolution of Human Adenovirus (HAdV) Species C. *Scientific Reports*, 9, 1039.
- DÖRRIE, J., KRUG, C., HOFMANN, C., MÜLLER, I., WELLNER, V., KNIPPERTZ, I., SCHIERER, S., THOMAS, S., ZIPPERER, E., PRINTZ, D., FRITSCH, G., SCHULER, G., SCHAFT, N. & GEYEREGGER, R. 2014. Human Adenovirus-Specific γ/δ and CD8⁺ T Cells Generated by T-Cell Receptor Transfection to Treat Adenovirus Infection after Allogeneic Stem Cell Transplantation. *PLOS ONE*, 9, e109944.

- DÖSSINGER, G., BUNSE, M., BET, J., ALBRECHT, J., PASZKIEWICZ, P. J., WEIßBRICH, B., SCHIEDEWITZ, I., HENKEL, L., SCHIEMANN, M., NEUENHAHN, M., UCKERT, W. & BUSCH, D. H. 2013. MHC Multimer-Guided and Cell Culture-Independent Isolation of Functional T Cell Receptors from Single Cells Facilitates TCR Identification for Immunotherapy. *PLOS ONE*, 8, e61384.
- ENGELS, B., CAM, H., SCHÜLER, T., INDRACCOLO, S., GLADOW, M., BAUM, C., BLANKENSTEIN, T. & UCKERT, W. 2003. Retroviral Vectors for High-Level Transgene Expression in T Lymphocytes. *Human Gene Therapy*, 14, 1155-1168.
- EYQUEM, J., MANSILLA-SOTO, J., GIAVRIDIS, T., VAN DER STEGEN, S. J. C., HAMIEH, M., CUNANAN, K. M., ODAK, A., GÖNEN, M. & SADELAIN, M. 2017. Targeting a CAR to the TRAC locus with CRISPR/Cas9 enhances tumour rejection. *Nature*, 543, 113.
- FEDERMANN, B., HÄGELE, M., PFEIFFER, M., WIRTHS, S., SCHUMM, M., FAUL, C., VOGEL, W., HANDGRETINGER, R., KANZ, L. & BETHGE, W. A. 2010. Immune reconstitution after haploidentical hematopoietic cell transplantation: impact of reduced intensity conditioning and CD3/CD19 depleted grafts. *Leukemia*, 25, 121.
- FEUCHT, J., OPPERK, K., LANG, P., KAYSER, S., HARTL, L., BETHGE, W., MATTHES-MARTIN, S., BADER, P., ALBERT, M. H., MAECKER-KOLHOFF, B., GREIL, J., EINSELE, H., SCHLEGEL, P.-G., SCHUSTER, F. R., KREMENS, B., ROSSIG, C., GRUHN, B., HANDGRETINGER, R. & FEUCHTINGER, T. 2015. Adoptive T-cell therapy with hexon-specific Th1 cells as a treatment of refractory adenovirus infection after HSCT. 125, 1986-1994.
- FEUCHTINGER, T., LANG, P. & HANDGRETINGER, R. 2007. Adenovirus infection after allogeneic stem cell transplantation. *Leukemia & Lymphoma*, 48, 244-255.
- FEUCHTINGER, T., LÜCKE, J., HAMPRECHT, K., RICHARD, C., HANDGRETINGER, R., SCHUMM, M., GREIL, J., BOCK, T., NIETHAMMER, D. & LANG, P. 2005. Detection of adenovirus-specific T cells in children with adenovirus infection after allogeneic stem cell transplantation. 128, 503-509.
- FEUCHTINGER, T., MATTHES-MARTIN, S., RICHARD, C., LION, T., FUHRER, M., HAMPRECHT, K., HANDGRETINGER, R., PETERS, C., SCHUSTER, F. R., BECK, R., SCHUMM, M., LOTFI, R., JAHN, G. & LANG, P. 2006. Safe adoptive transfer of virus-specific T-cell immunity for the treatment of systemic adenovirus infection after allogeneic stem cell transplantation. 134, 64-76.
- FEUCHTINGER, T., OPPERK, K., BETHGE, W. A., TOPP, M. S., SCHUSTER, F. R., WEISSINGER, E. M., MOHTY, M., OR, R., MASCHAN, M., SCHUMM, M., HAMPRECHT, K., HANDGRETINGER, R., LANG, P. & EINSELE, H. 2010. Adoptive transfer of pp65-specific T cells for the treatment of chemorefractory cytomegalovirus disease or reactivation after haploidentical and matched unrelated stem cell transplantation. *Blood*, 116, 4360-4367.
- FEUCHTINGER, T., RICHARD, C., JOACHIM, S., SCHEIBLE, M. H., SCHUMM, M., HAMPRECHT, K., MARTIN, D., JAHN, G., HANDGRETINGER, R. & LANG, P. 2008. Clinical Grade Generation of Hexon-specific T Cells for Adoptive T-cell Transfer as a Treatment of Adenovirus Infection After Allogeneic Stem Cell Transplantation. *Journal of Immunotherapy*, 31, 199-206.
- FLOMENBERG, P., BABBITT, J., DROBYSKI, W. R., ASH, R. C., CARRIGAN, D. R., SEDMAK, G. V., MCAULIFFE, T., CAMITTA, B., HOROWITZ, M. M., BUNIN, N. & CASPER, J. T. 1994. Increasing Incidence of Adenovirus Disease in Bone Marrow Transplant Recipients. *The Journal of Infectious Diseases*, 169, 775-781.
- FREIMÜLLER, C., STEMBERGER, J., ARTWOHL, M., GERMEROOTH, L., WITT, V., FISCHER, G., TISCHER, S., EIZ-VESPER, B., KNIPPERTZ, I., DÖRRIE, J., SCHAFT, N., LION, T., FRITSCH, G. & GEYEREGGER, R. 2015. Selection of adenovirus-specific and Epstein-Barr virus-specific T cells with major histocompatibility class I streptamers under Good Manufacturing Practice (GMP)-compliant conditions. *Cytotherapy*, 17.

- FU, Y., FODEN, J. A., KHAYTER, C., MAEDER, M. L., REYON, D., JOUNG, J. K. & SANDER, J. D. 2013. High-frequency off-target mutagenesis induced by CRISPR-Cas nucleases in human cells. *Nature biotechnology*, 31, 822-826.
- GAJ, T., GERSBACH, C. A. & BARBAS, C. F., 3RD 2013. ZFN, TALEN, and CRISPR/Cas-based methods for genome engineering. *Trends in biotechnology*, 31, 397-405.
- GARNETT, C. T., ERDMAN, D., XU, W. & GOODING, L. R. 2002. Prevalence and Quantitation of Species C Adenovirus DNA in Human Mucosal Lymphocytes. *Journal of Virology*, 76, 10608-10616.
- GARNETT, C. T., TALEKAR, G., MAHR, J. A., HUANG, W., ZHANG, Y., ORNELLES, D. A. & GOODING, L. R. 2009. Latent Species C Adenoviruses in Human Tonsil Tissues. *Journal of Virology*, 83, 2417-2428.
- GASCOIGNE, N. R. J. 2008. Do T cells need endogenous peptides for activation? *Nature Reviews Immunology*, 8, 895-900.
- GASIUNAS, G., BARRANGOU, R., HORVATH, P. & SIKSNYS, V. 2012. Cas9-crRNA ribonucleoprotein complex mediates specific DNA cleavage for adaptive immunity in bacteria. *Proceedings of the National Academy of Sciences*, 109, E2579-E2586.
- GEORGE, D., EL-MALLAWANY, N. K., JIN, Z., GEYER, M., DELLA-LATTA, P., SATWANI, P., GARVIN, J. H., BRADLEY, M. B., BHATIA, M., VAN DE VEN, C., MORRIS, E., SCHWARTZ, J. & CAIRO, M. S. 2012. Adenovirus infection in paediatric allogeneic stem cell transplantation recipients is a major independent factor for significantly increasing the risk of treatment related mortality. 156, 99-108.
- GEYEREGGER, R., FREIMÜLLER, C., STEMBERGER, J., ARTWOHL, M., WITT, V., LION, T., FISCHER, G., LAWITSCHKA, A., RITTER, J., HUMMEL, M., HOLTER, W., FRITSCH, G. & MATTHES-MARTIN, S. 2014. First-in-Man Clinical Results With Good Manufacturing Practice (GMP)-compliant Polypeptide-expanded Adenovirus-specific T Cells After Haploidentical Hematopoietic Stem Cell Transplantation. *Journal of Immunotherapy*, 37, 245-249.
- GEYEREGGER, R., FREIMÜLLER, C., STEVANOVIC, S., STEMBERGER, J., MESTER, G., DMYTRUS, J., LION, T., RAMMENSEE, H.-G., FISCHER, G., EIZ-VESPER, B., LAWITSCHKA, A., MATTHES, S. & FRITSCH, G. 2013. Short-term in-vitro expansion improves monitoring and allows affordable generation of virus-specific T-cells against several viruses for a broad clinical application. *PloS one*, 8, e59592-e59592.
- GHEBREMEDHIN, B. 2014. Human adenovirus: Viral pathogen with increasing importance. *European journal of microbiology & immunology*, 4, 26-33.
- GONZÁLEZ-GALARZA, F. F., TAKESHITA, L. Y. C., SANTOS, E. J. M., KEMPSON, F., MAIA, M. H. T., DA SILVA, A. L. S., TELES E SILVA, A. L., GHATTAORAYA, G. S., ALFIREVIC, A., JONES, A. R. & MIDDLETON, D. 2015. Allele frequency net 2015 update: new features for HLA epitopes, KIR and disease and HLA adverse drug reaction associations. *Nucleic acids research*, 43, D784-D788.
- GRAKOU, A., BROMLEY, S. K., SUMEN, C., DAVIS, M. M., SHAW, A. S., ALLEN, P. M. & DUSTIN, M. L. 1999. The Immunological Synapse: A Molecular Machine Controlling T Cell Activation. 285, 221-227.
- GRATWOHL, A., BRAND, R., FRASSONI, F., ROCHA, V., NIEDERWIESER, D., REUSSER, P., EINSELE, H., CORDONNIER, C., FOR THE, A., CHRONIC LEUKEMIA WORKING, P., THE INFECTIOUS DISEASES WORKING PARTY OF THE EUROPEAN GROUP FOR, B. & MARROW, T. 2005. Cause of death after allogeneic haematopoietic stem cell transplantation (HSCT) in early leukaemias: an EBMT analysis of lethal infectious complications and changes over calendar time. *Bone Marrow Transplantation*, 36, 757-769.
- GU, C., WU, L. & LI, X. 2013. IL-17 family: cytokines, receptors and signaling. *Cytokine*, 64, 477-485.

- GUNTHER, P. S. P., JANET K.; FAIST, BENJAMIN; KAYSER, SIMONE; HARTL, LENA; FEUCHTINGER, TOBIAS; JAHN, GERHARD; NEUENHAHN, MICHAEL; BUSCH, DIRK H.; STEVANOVIC, STEFAN; DENNEHY, KEVIN M 2015. Identification of a Novel Immunodominant HLA-B*07: 02-restricted Adenoviral Peptide Epitope and Its Potential in Adoptive Transfer Immunotherapy. *Journal of Immunotherapy*, 38, 267-275.
- HANSEN, T. H. & BOUVIER, M. 2009. MHC class I antigen presentation: learning from viral evasion strategies. *Nature Reviews Immunology*, 9, 503-513.
- HEEMSKERK, B., VAN VREESWIJK, T., VELTROP-DUITS, L. A., SOMBROEK, C. C., FRANKEN, K., VERHOOSSEL, R. M., HIEMSTRA, P. S., VAN LEEUWEN, D., RESSING, M. E., TOES, R. E. M., VAN TOL, M. J. D. & SCHILHAM, M. W. 2006. Adenovirus-Specific CD4⁺ T Cell Clones Recognizing Endogenous Antigen Inhibit Viral Replication In Vitro through Cognate Interaction. *The Journal of Immunology*, 177, 8851-8859.
- HSU, P. D., SCOTT, D. A., WEINSTEIN, J. A., RAN, F. A., KONERMANN, S., AGARWALA, V., LI, Y., FINE, E. J., WU, X., SHALEM, O., CRADICK, T. J., MARRAFFINI, L. A., BAO, G. & ZHANG, F. 2013. DNA targeting specificity of RNA-guided Cas9 nucleases. *Nature biotechnology*, 31, 827-832.
- IRMLER, M., HERTIG, S., MACDONALD, H. R., SADOUL, R., BECHERER, J. D., PROUDFOOT, A., SOLARI, R. & TSCHOPP, J. 1995. Granzyme A is an interleukin 1 beta-converting enzyme. 181, 1917-1922.
- ISHINO, Y., SHINAGAWA, H., MAKINO, K., AMEMURA, M. & NAKATA, A. 1987. Nucleotide sequence of the iap gene, responsible for alkaline phosphatase isozyme conversion in Escherichia coli, and identification of the gene product. *Journal of bacteriology*, 169, 5429-5433.
- JANEWAY, C., TRAVERS, P. & WALPORT, M. 2001. *Immunobiology: The Immune System in Health and Disease* [Online]. New York: Garland Science. Available: <https://www.ncbi.nlm.nih.gov/books/NBK27130> [Accessed 2019].
- JINEK, M., CHYLINSKI, K., FONFARA, I., HAUER, M., DOUDNA, J. A. & CHARPENTIER, E. 2012. A Programmable Dual-RNA-Guided DNA Endonuclease in Adaptive Bacterial Immunity. *Science*, 337, 816-821.
- JINEK, M., EAST, A., CHENG, A., LIN, S., MA, E. & DOUDNA, J. 2013. RNA-programmed genome editing in human cells. *eLife*, 2, e00471-e00471.
- KAEUFERLE, T., STIEF, T. A., CANZAR, S., KUTLU, N. N., WILLIER, S., STENGER, D., FERRADA-ERNST, P., HABJAN, N., PETERS, A. E., BUSCH, D. H. & FEUCHTINGER, T. 2022. Genome-wide off-target analyses of CRISPR/Cas9-mediated T-cell receptor engineering in primary human T cells. *Clinical & Translational Immunology*, 11, e1372.
- KAGI, D., LEDERMANN, B., BURKI, K. & SEILER, P. J. N. 1994. Oder matt B., Olsen KJ, Podack ER, Zinkernagel RM, Hengartner H. Cytotoxicity mediated by T cells and natural killer cells is greatly impaired in perforin-deficient mice. 369, 31-37.
- KÁLLAY, K., KASSA, C., RÉTI, M., KARÁSZI, É., SINKÓ, J., GODA, V., STRÉHN, A., CSORDÁS, K., HORVÁTH, O., SZEDERJESI, A., TASNÁDY, S., HARDI, A. & KRIVÁN, G. 2018. Early Experience With CliniMACS Prodigy CCS (IFN-gamma) System in Selection of Virus-specific T Cells From Third-party Donors for Pediatric Patients With Severe Viral Infections After Hematopoietic Stem Cell Transplantation. 41, 158-163.
- KASPAR, A. A., OKADA, S., KUMAR, J., POULAIN, F. R., DROUVALAKIS, K. A., KELEKAR, A., HANSON, D. A., KLUCK, R. M., HITOSHI, Y., JOHNSON, D. E., FROELICH, C. J., THOMPSON, C. B., NEWMAYER, D. D., ANEL, A., CLAYBERGER, C. & KRENSKY, A. M. 2001. A Distinct Pathway of Cell-Mediated Apoptosis Initiated by Granulysin. 167, 350-356.
- KEIB, A., MEI, Y.-F., CICIN-SAIN, L., BUSCH, D. H. & DENNEHY, K. M. 2019. Measuring Antiviral Capacity of T Cell Responses to Adenovirus. 202, 618-624.

- KNABEL, M., FRANZ, T. J., SCHIEMANN, M., WULF, A., VILLMOW, B., SCHMIDT, B., BERNHARD, H., WAGNER, H. & BUSCH, D. H. 2002. Reversible MHC multimer staining for functional isolation of T-cell populations and effective adoptive transfer. *Nature Medicine*, 8, 631-637.
- KNIPPING, F., OSBORN, M. J., PETRI, K., TOLAR, J., GLIMM, H., VON KALLE, C., SCHMIDT, M. & GABRIEL, R. 2017. Genome-wide Specificity of Highly Efficient TALENs and CRISPR/Cas9 for T Cell Receptor Modification. *Molecular Therapy - Methods & Clinical Development*, 4, 213-224.
- KOSICKI, M., TOMBERG, K. & BRADLEY, A. 2018. Repair of double-strand breaks induced by CRISPR-Cas9 leads to large deletions and complex rearrangements. *Nature biotechnology*, 36, 765-771.
- LEE, D. W., KOCHENDERFER, J. N., STETLER-STEVENSON, M., CUI, Y. K., DELBROOK, C., FELDMAN, S. A., FRY, T. J., ORENTAS, R., SABATINO, M., SHAH, N. N., STEINBERG, S. M., STRONCEK, D., TSCHERNIA, N., YUAN, C., ZHANG, H., ZHANG, L., ROSENBERG, S. A., WAYNE, A. S. & MACKALL, C. L. 2015. T cells expressing CD19 chimeric antigen receptors for acute lymphoblastic leukaemia in children and young adults: a phase 1 dose-escalation trial. *The Lancet*, 385, 517-528.
- LEEN, A. M., BOLLARD, C. M., MYERS, G. D. & ROONEY, C. M. 2006. Adenoviral Infections in Hematopoietic Stem Cell Transplantation. *Biology of Blood and Marrow Transplantation*, 12, 243-251.
- LEEN, A. M., CHRISTIN, A., MYERS, G. D., LIU, H., CRUZ, C. R., HANLEY, P. J., KENNEDY-NASSER, A. A., LEUNG, K. S., GEE, A. P., KRANCE, R. A., BRENNER, M. K., HESLOP, H. E., ROONEY, C. M. & BOLLARD, C. M. 2009. Cytotoxic T lymphocyte therapy with donor T cells prevents and treats adenovirus and Epstein-Barr virus infections after haploidentical and matched unrelated stem cell transplantation. 114, 4283-4292.
- LEEN, A. M., SILI, U., VANIN, E. F., JEWELL, A. M., XIE, W., VIGNALI, D., PIEDRA, P. A., BRENNER, M. K. & ROONEY, C. M. 2004. Conserved CTL epitopes on the adenovirus hexon protein expand subgroup cross-reactive and subgroup-specific CD8+ T cells. *Blood*, 104, 2432-2440.
- LEEN, A. M., TRIPIC, T. & ROONEY, C. M. 2010. Challenges of T cell therapies for virus-associated diseases after hematopoietic stem cell transplantation. *Expert opinion on biological therapy*, 10, 337-351.
- LEFRANC, M.-P., GIUDICELLI, V., DUROUX, P., JABADO-MICHALOUD, J., FOLCH, G., AOUINTI, S., CARILLON, E., DUVERGEY, H., HOULES, A., PAYSAN-LAFOSSE, T., HADI-SALJOQI, S., SASORITH, S., LEFRANC, G. & KOSSIDA, S. 2014. IMGT®, the international ImMunoGeneTics information system® 25 years on. *Nucleic Acids Research*, 43, D413-D422.
- LIANG, X., POTTER, J., KUMAR, S., RAVINDER, N. & CHESNUT, J. D. 2017. Enhanced CRISPR/Cas9-mediated precise genome editing by improved design and delivery of gRNA, Cas9 nuclease, and donor DNA. *Journal of Biotechnology*, 241, 136-146.
- LIN, R. & LIU, Q. 2013. Diagnosis and treatment of viral diseases in recipients of allogeneic hematopoietic stem cell transplantation. *Journal of hematology & oncology*, 6, 94-94.
- LION, T., KOSULIN, K., LANDLINGER, C., RAUCH, M., PREUNER, S., JUGOVIC, D., PÖTSCHGER, U., LAWITSCHKA, A., PETERS, C., FRITSCH, G. & MATTHES-MARTIN, S. 2010. Monitoring of adenovirus load in stool by real-time PCR permits early detection of impending invasive infection in patients after allogeneic stem cell transplantation. *Leukemia*, 24, 706-714.
- LIU, H., JIN, L., KOH, S. B. S., ATANASOV, I., SCHEIN, S., WU, L. & ZHOU, Z. H. 2010. Atomic structure of human adenovirus by cryo-EM reveals interactions among protein networks. *Science (New York, N.Y.)*, 329, 1038-1043.

- LIU, K., CATALFAMO, M., LI, Y., HENKART, P. A. & WENG, N.-P. 2002. IL-15 mimics T cell receptor crosslinking in the induction of cellular proliferation, gene expression, and cytotoxicity in CD8+ memory T cells. *Proceedings of the National Academy of Sciences of the United States of America*, 99, 6192-6197.
- LJUNGMAN, P. 2004. Treatment of adenovirus infections in the immunocompromised host. *European Journal of Clinical Microbiology and Infectious Diseases*, 23, 583-588.
- LJUNGMAN, P., URBANO-ISPIZUA, A., CAVAZZANA-CALVO, M., DEMIRER, T., DINI, G., EINSELE, H., GRATWOHL, A., MADRIGAL, A., NIEDERWIESER, D., PASSWEG, J., ROCHA, V., SACCARDI, R., SCHOUTEN, H., SCHMITZ, N., SOCIE, G., SUREDA, A., APPERLEY, J., FOR THE EUROPEAN GROUP FOR, B. & MARROW, T. 2006. Allogeneic and autologous transplantation for haematological diseases, solid tumours and immune disorders: definitions and current practice in Europe. *Bone Marrow Transplantation*, 37, 439-449.
- LOWIN, B., BEERMANN, F., SCHMIDT, A. & TSCHOPP, J. 1994. A null mutation in the perforin gene impairs cytolytic T lymphocyte- and natural killer cell-mediated cytotoxicity. 91, 11571-11575.
- LU, Y., XUE, J., DENG, T., ZHOU, X., YU, K., DENG, L., HUANG, M., YI, X., LIANG, M., WANG, Y., SHEN, H., TONG, R., WANG, W., LI, L., SONG, J., LI, J., SU, X., DING, Z., GONG, Y., ZHU, J., WANG, Y., ZOU, B., ZHANG, Y., LI, Y., ZHOU, L., LIU, Y., YU, M., WANG, Y., ZHANG, X., YIN, L., XIA, X., ZENG, Y., ZHOU, Q., YING, B., CHEN, C., WEI, Y., LI, W. & MOK, T. 2020. Safety and feasibility of CRISPR-edited T cells in patients with refractory non-small-cell lung cancer. *Nat Med*, 26, 732-740.
- MALI, P., AACH, J., STRANGES, P. B., ESVELT, K. M., MOOSBURNER, M., KOSURI, S., YANG, L. & CHURCH, G. M. 2013. CAS9 transcriptional activators for target specificity screening and paired nickases for cooperative genome engineering. *Nature Biotechnology*, 31, 833-838.
- MCILWAIN, D. R., BERGER, T. & MAK, T. W. 2013. Caspase Functions in Cell Death and Disease. *Cold Spring Harbor Perspectives in Biology*, 5.
- MILLER, J. C., TAN, S., QIAO, G., BARLOW, K. A., WANG, J., XIA, D. F., MENG, X., PASCHON, D. E., LEUNG, E., HINKLEY, S. J., DULAY, G. P., HUA, K. L., ANKOUDINOVA, I., COST, G. J., URNOV, F. D., ZHANG, H. S., HOLMES, M. C., ZHANG, L., GREGORY, P. D. & REBAR, E. J. 2011. A TALE nuclease architecture for efficient genome editing. *Nature Biotechnology*, 29, 143-148.
- MORTON, L. T., REIJMERS, R. M., WOUTERS, A. K., KWEEKEL, C., REMST, D. F. G., POTHAST, C. R., FALKENBURG, J. H. F. & HEEMSKERK, M. H. M. 2020. Simultaneous Deletion of Endogenous TCR $\alpha\beta$ for TCR Gene Therapy Creates an Improved and Safe Cellular Therapeutic. *Mol Ther*, 28, 64-74.
- NEUENHAHN, M., ALBRECHT, J., ODENDAHL, M., SCHLOTT, F., DÖSSINGER, G., SCHIEMANN, M., LAKSHMIPATHI, S., MARTIN, K., BUNJES, D., HARS DORF, S., WEISSINGER, E. M., MENZEL, H., VERBEEK, M., UHAREK, L., KRÖGER, N., WAGNER, E., KOBBE, G., SCHROEDER, T., SCHMITT, M., HELD, G., HERR, W., GERMEROOTH, L., BONIG, H., TONN, T., EINSELE, H., BUSCH, D. H. & GRIGOLEIT, G. U. 2017. Transfer of minimally manipulated CMV-specific T cells from stem cell or third-party donors to treat CMV infection after allo-HSCT. *Leukemia*, 31, 2161-2171.
- NEUMANN, R., GENERSCH, E. & EGGERS, H. J. 1987. Detection of adenovirus nucleic acid sequences in human tonsils in the absence of infectious virus. *Virus Research*, 7, 93-97.
- NEWRZELA, S., CORNILS, K., LI, Z., BAUM, C., BRUGMAN, M. H., HARTMANN, M., MEYER, J., HARTMANN, S., HANSMANN, M.-L., FEHSE, B. & VON LAER, D. 2008. Resistance of mature T cells to oncogene transformation. *Blood*, 112, 2278-2286.
- OH, H.-L. J., CHIA, A., CHANG, C. X. L., LEONG, H. N., LING, K. L., GROTENBREG, G. M., GEHRING, A. J., TAN, Y. J. & BERTOLETTI, A. 2011. Engineering T cells specific for a dominant severe

- acute respiratory syndrome coronavirus CD8 T cell epitope. *Journal of virology*, 85, 10464-10471.
- OSBORN, M. J., WEBBER, B. R., KNIPPING, F., LONETREE, C.-L., TENNIS, N., DEFEO, A. P., MCELROY, A. N., STARKER, C. G., LEE, C., MERKEL, S., LUND, T. C., KELLY-SPRATT, K. S., JENSEN, M. C., VOYTAS, D. F., VON KALLE, C., SCHMIDT, M., GABRIEL, R., HIPPEN, K. L., MILLER, J. S., SCHARENBERG, A. M., TOLAR, J. & BLAZAR, B. R. 2016. Evaluation of TCR Gene Editing Achieved by TALENs, CRISPR/Cas9, and megaTAL Nucleases. *Molecular Therapy*, 24, 570-581.
- ÖZDEMİR, E., SALIBA, R. M., CHAMPLIN, R. E., COURIEL, D. R., GIRALT, S. A., DE LIMA, M., KHOURI, I. F., HOSING, C., KORNBLAU, S. M., ANDERLINI, P., SHPALL, E. J., QAZILBASH, M. H., MOLLDREM, J. J., CHEMALY, R. F. & KOMANDURI, K. V. 2007. Risk factors associated with late cytomegalovirus reactivation after allogeneic stem cell transplantation for hematological malignancies. *Bone Marrow Transplantation*, 40, 125-136.
- PARDO, J., PÉREZ-GALÁN, P., GAMEN, S., MARZO, I., MONLEÓN, I., KASPAR, A. A., SUSÍN, S. A., KROEMER, G., KRENSKY, A. M., NAVAL, J. & ANEL, A. 2001. A Role of the Mitochondrial Apoptosis-Inducing Factor in Granulysin-Induced Apoptosis. 167, 1222-1229.
- POIROT, L., PHILIP, B., SCHIFFER-MANNIOUI, C., LE CLERRE, D., CHION-SOTINEL, I., DERNIAME, S., POTREL, P., BAS, C., LEMAIRE, L., GALETTO, R., LEBUHOTEL, C., EYQUEM, J., CHEUNG, G. W.-K., DUCLERT, A., GOUBLE, A., ARNOULD, S., PEGGS, K., PULE, M., SCHARENBERG, A. M. & SMITH, J. 2015. Multiplex Genome-Edited T-cell Manufacturing Platform for “Off-the-Shelf” Adoptive T-cell Immunotherapies. *Cancer Research*, 75, 3853-3864.
- PORTER, D. L., LEVINE, B. L., KALOS, M., BAGG, A. & JUNE, C. H. 2011. Chimeric Antigen Receptor-Modified T Cells in Chronic Lymphoid Leukemia. *New England Journal of Medicine*, 365, 725-733.
- PORTEUS, M. H. & CARROLL, D. 2005. Gene targeting using zinc finger nucleases. *Nature Biotechnology*, 23, 967-973.
- PROVASI, E., GENOVESE, P., LOMBARDO, A., MAGNANI, Z., LIU, P.-Q., REIK, A., CHU, V., PASCHON, D. E., ZHANG, L., KUBALL, J., CAMISA, B., BONDANZA, A., CASORATI, G., PONZONI, M., CICERI, F., BORDIGNON, C., GREENBERG, P. D., HOLMES, M. C., GREGORY, P. D., NALDINI, L. & BONINI, C. 2012. Editing T cell specificity towards leukemia by zinc finger nucleases and lentiviral gene transfer. *Nature Medicine*, 18, 807-815.
- REDDY, V. S., NATCHIAR, S. K., STEWART, P. L. & NEMEROW, G. R. 2010. Crystal structure of human adenovirus at 3.5 Å resolution. *Science (New York, N.Y.)*, 329, 1071-1075.
- REN, J., LIU, X., FANG, C., JIANG, S., JUNE, C. H. & ZHAO, Y. 2017. Multiplex Genome Editing to Generate Universal CAR T Cells Resistant to PD1 Inhibition. 23, 2255-2266.
- RIVIÈRE, I., DUNBAR, C. E. & SADELAIN, M. 2012. Hematopoietic stem cell engineering at a crossroads. *Blood*, 119, 1107-1116.
- ROBINSON, J. T., THORVALDSDÓTTIR, H., WINCKLER, W., GUTTMAN, M., LANDER, E. S., GETZ, G. & MESIROV, J. P. 2011. Integrative genomics viewer. *Nature Biotechnology*, 29, 24.
- ROSS, S. H. & CANTRELL, D. A. 2018. Signaling and Function of Interleukin-2 in T Lymphocytes. *Annual review of immunology*, 36, 411-433.
- ROTH, T. L., PUIG-SAUS, C., YU, R., SHIFRUT, E., CARNEVALE, J., LI, P. J., HIATT, J., SACO, J., KRYSOFINSKI, P., LI, H., TOBIN, V., NGUYEN, D. N., LEE, M. R., PUTNAM, A. L., FERRIS, A. L., CHEN, J. W., SCHICKEL, J.-N., PELLERIN, L., CARMODY, D., ALKORTA-ARANBURU, G., DEL GAUDIO, D., MATSUMOTO, H., MORELL, M., MAO, Y., CHO, M., QUADROS, R. M., GURUMURTHY, C. B., SMITH, B., HAUGWITZ, M., HUGHES, S. H., WEISSMAN, J. S., SCHUMANN, K., ESENSTEN, J. H., MAY, A. P., ASHWORTH, A., KUPFER, G. M., GREELEY, S. A. W., BACCHETTA, R., MEFFRE, E., RONCAROLO, M. G., ROMBERG, N., HEROLD, K. C., RIBAS, A., LEONETTI, M. D. & MARSON, A. 2018. Reprogramming human T cell function and specificity with non-viral genome targeting. *Nature*, 559, 405-409.

- RUNDE, V., ROSS, S., TRENSCHEL, R., LAGEMANN, E., BASU, O., RENZING-KÖHLER, K., SCHAEFER, U. W., ROGGENDORF, M. & HOLLER, E. 2001. Adenoviral infection after allogeneic stem cell transplantation (SCT): report on 130 patients from a single SCT unit involved in a prospective multi center surveillance study. *Bone Marrow Transplantation*, 28, 51-57.
- SALOMON, B. & BLUESTONE, J. A. 2001. Complexities of CD28/B7: CTLA-4 Costimulatory Pathways in Autoimmunity and Transplantation. 19, 225-252.
- SCHMITT, A., TONN, T., BUSCH, D. H., GRIGOLEIT, G. U., EINSELE, H., ODENDAHL, M., GERMEROOTH, L., RINGHOFFER, M., RINGHOFFER, S., WIESNETH, M., GREINER, J., MICHEL, D., MERTENS, T., ROJEWSKI, M., MARX, M., VON HARSDORF, S., DÖHNER, H., SEIFRIED, E., BUNJES, D. & SCHMITT, M. 2011. Adoptive transfer and selective reconstitution of streptamer-selected cytomegalovirus-specific CD8⁺ T cells leads to virus clearance in patients after allogeneic peripheral blood stem cell transplantation. 51, 591-599.
- SCHÖBER, K., MÜLLER, T. R., GÖKMEN, F., GRASSMANN, S., EFFENBERGER, M., POLTORAK, M., STEMBERGER, C., SCHUMANN, K., ROTH, T. L., MARSON, A. & BUSCH, D. H. 2019. Orthotopic replacement of T-cell receptor α - and β -chains with preservation of near-physiological T-cell function. *Nature Biomedical Engineering*.
- SCHRUM, A. G., TURKA, L. A. & PALMER, E. 2003. Surface T-cell antigen receptor expression and availability for long-term antigenic signaling. *Immunological Reviews*, 196, 7-24.
- SCHUMANN, K., LIN, S., BOYER, E., SIMEONOV, D. R., SUBRAMANIAM, M., GATE, R. E., HALIBURTON, G. E., YE, C. J., BLUESTONE, J. A., DOUDNA, J. A. & MARSON, A. 2015. Generation of knock-in primary human T cells using Cas9 ribonucleoproteins. *Proceedings of the National Academy of Sciences of the United States of America*, 112, 10437-10442.
- SCHWANK, G., KOO, B.-K., SASSELLI, V., DEKKERS, JOHANNA F., HEO, I., DEMIRCAN, T., SASAKI, N., BOYMANS, S., CUPPEN, E., VAN DER ENT, CORNELIS K., NIEUWENHUIS, EDWARD E. S., BEEKMAN, JEFFREY M. & CLEVERS, H. 2013. Functional Repair of CFTR by CRISPR/Cas9 in Intestinal Stem Cell Organoids of Cystic Fibrosis Patients. *Cell Stem Cell*, 13, 653-658.
- SILVA-FILHO, J. L., CARUSO-NEVES, C. & PINHEIRO, A. A. S. 2014. IL-4: an important cytokine in determining the fate of T cells. *Biophysical reviews*, 6, 111-118.
- SLAYMAKER, I. M., GAO, L., ZETSCHKE, B., SCOTT, D. A., YAN, W. X. & ZHANG, F. 2016. Rationally engineered Cas9 nucleases with improved specificity. *Science (New York, N.Y.)*, 351, 84-88.
- SMALL, T. N., PAPADOPOULOS, E. B., BOULAD, F., BLACK, P., CASTRO-MALASPINA, H., CHILDS, B. H., COLLINS, N., GILLIO, A., GEORGE, D., JAKUBOWSKI, A., HELLER, G., FAZZARI, M., KERNAN, N., MACKINNON, S., SZABOLCS, P., YOUNG, J. W. & O'REILLY, R. J. 1999. Comparison of Immune Reconstitution After Unrelated and Related T-Cell-Depleted Bone Marrow Transplantation: Effect of Patient Age and Donor Leukocyte Infusions. 93, 467-480.
- SMITH, C., GORE, A., YAN, W., ABALDE-ATRISTAIN, L., LI, Z., HE, C., WANG, Y., BRODSKY, R. A., ZHANG, K., CHENG, L. & YE, Z. 2014. Whole-genome sequencing analysis reveals high specificity of CRISPR/Cas9 and TALEN-based genome editing in human iPSCs. *Cell stem cell*, 15, 12-13.
- SMITH, R. H., CHEN, Y. C., SEIFUDDIN, F., HUPALO, D., ALBA, C., REGER, R., TIAN, X., ARAKI, D., DALGARD, C. L., CHILDS, R. W., PIROOZNIYA, M. & LAROCHELLE, A. 2020. Genome-Wide Analysis of Off-Target CRISPR/Cas9 Activity in Single-Cell-Derived Human Hematopoietic Stem and Progenitor Cell Clones. *Genes (Basel)*, 11.
- STADTMAUER, E. A., FRAIETTA, J. A., DAVIS, M. M., COHEN, A. D., WEBER, K. L., LANCASTER, E., MANGAN, P. A., KULIKOVSKAYA, I., GUPTA, M., CHEN, F., TIAN, L., GONZALEZ, V. E., XU, J., JUNG, I. Y., MELENHORST, J. J., PLESA, G., SHEA, J., MATLAWSKI, T., CERVINI, A., GAYMON, A. L., DESJARDINS, S., LAMONTAGNE, A., SALAS-MCKEE, J., FESNAK, A., SIEGEL, D. L., LEVINE, B. L., JADLOWSKY, J. K., YOUNG, R. M., CHEW, A., HWANG, W. T., HEXNER, E. O.,

- CARRENO, B. M., NOBLES, C. L., BUSHMAN, F. D., PARKER, K. R., QI, Y., SATPATHY, A. T., CHANG, H. Y., ZHAO, Y., LACEY, S. F. & JUNE, C. H. 2020. CRISPR-engineered T cells in patients with refractory cancer. *Science*, 367.
- STEMBERGER, C., GRAEF, P., ODENDAHL, M., ALBRECHT, J., DÖSSINGER, G., ANDERL, F., BUCHHOLZ, V. R., GASTEIGER, G., SCHIEMANN, M., GRIGOLEIT, G. U., SCHUSTER, F. R., BORKHARDT, A., VERSLUYS, B., TONN, T., SEIFRIED, E., EINSELE, H., GERMEROTH, L., BUSCH, D. H. & NEUENHAHN, M. 2014. Lowest numbers of primary CD8⁺ T cells can reconstitute protective immunity upon adoptive immunotherapy. 124, 628-637.
- STENGER, D., STIEF, T. A., KAEUFERLE, T., WILLIER, S., RATAJ, F., SCHOBER, K., VICK, B., LOTFI, R., WAGNER, B., GRÜNEWALD, T. G. P., KOBOLD, S., BUSCH, D. H., JEREMIAS, I., BLAESCHKE, F. & FEUCHTINGER, T. 2020. Endogenous TCR promotes in vivo persistence of CD19-CAR-T cells compared to a CRISPR/Cas9-mediated TCR knockout CAR. *Blood*, 136, 1407-1418.
- STERNBERG, SAMUEL H. & DOUDNA, JENNIFER A. 2015. Expanding the Biologist's Toolkit with CRISPR-Cas9. *Molecular Cell*, 58, 568-574.
- STIEF, T. A., KAEUFERLE, T., MÜLLER, T. R., DÖRING, M., JABLONOWSKI, L. M., SCHOBER, K., FEUCHT, J., DENNEHY, K. M., WILLIER, S., BLAESCHKE, F., HANDGRETINGER, R., LANG, P., BUSCH, D. H. & FEUCHTINGER, T. 2022. Protective T-cell receptor identification for orthotopic reprogramming of immunity in refractory virus infections. *Molecular Therapy*, 30, 198-208.
- SUKDOLAK, C., TISCHER, S., DIEKS, D., FIGUEIREDO, C., GOUDEVA, L., HEUFT, H.-G., VERBOOM, M., IMMENSCHUH, S., HEIM, A., BORCHERS, S., MISCHAK-WEISSINGER, E., BLASCZYK, R., MAECKER-KOLHOFF, B. & EIZ-VESPER, B. 2013. CMV-, EBV- and ADV-Specific T Cell Immunity: Screening and Monitoring of Potential Third-Party Donors to Improve Post-Transplantation Outcome. *Biology of Blood and Marrow Transplantation*, 19, 1480-1492.
- TANG, J., OLIVE, M., PULMANAUSAHAKUL, R., SCHNELL, M., FLOMENBERG, N., EISENLOHR, L. & FLOMENBERG, P. 2006. Human CD8⁺ cytotoxic T cell responses to adenovirus capsid proteins. *Virology*, 350, 312-322.
- TRAPANI, J. A., JANS, D. A., JANS, P. J., SMYTH, M. J., BROWNE, K. A. & SUTTON, V. R. 1998. Efficient Nuclear Targeting of Granzyme B and the Nuclear Consequences of Apoptosis Induced by Granzyme B and Perforin Are Caspase-dependent, but Cell Death Is Caspase-independent. 273, 27934-27938.
- TURNER, S. J., DOHERTY, P. C., MCCLUSKEY, J. & ROSSJOHN, J. 2006. Structural determinants of T-cell receptor bias in immunity. *Nature Reviews Immunology*, 6, 883-894.
- VAKULSKAS, C. A., DEVER, D. P., RETTIG, G. R., TURK, R., JACOBI, A. M., COLLINGWOOD, M. A., BODE, N. M., MCNEILL, M. S., YAN, S., CAMARENA, J., LEE, C. M., PARK, S. H., WIEBKING, V., BAK, R. O., GOMEZ-OSPINA, N., PAVEL-DINU, M., SUN, W., BAO, G., PORTEUS, M. H. & BEHLKE, M. A. 2018. A high-fidelity Cas9 mutant delivered as a ribonucleoprotein complex enables efficient gene editing in human hematopoietic stem and progenitor cells. *Nature Medicine*, 24, 1216-1224.
- VAN LOENEN, M. M., DE BOER, R., AMIR, A. L., HAGEDOORN, R. S., VOLBEDA, G. L., WILLEMZE, R., VAN ROOD, J. J., FALKENBURG, J. H. F. & HEEMSKERK, M. H. M. 2010. Mixed T cell receptor dimers harbor potentially harmful neoreactivity. *Proceedings of the National Academy of Sciences of the United States of America*, 107, 10972-10977.
- VAN LOENEN, M. M., HAGEDOORN, R. S., DE BOER, R., VAN EGMOND, E. H. M., FALKENBURG, J. H. F. & HEEMSKERK, M. H. M. 2011. Rapid Re-expression of Retrovirally Introduced Versus Endogenous TCRs in Engineered T cells After Antigen-specific Stimulation. *Journal of Immunotherapy*, 34, 165-174.
- VAN MONTFOORT, N., VAN DER AA, E. & WOLTMAN, A. M. 2014. Understanding MHC class I presentation of viral antigens by human dendritic cells as a basis for rational design of therapeutic vaccines. *Frontiers in immunology*, 5, 182-182.

- VAN TOL, M. J. D., CLAAS, E. C. J., HEEMSKERK, B., VELTROP-DUIITS, L. A., DE BROUWER, C. S., VAN VREESWIJK, T., SOMBROEK, C. C., KROES, A. C. M., BEERSMA, M. F. C., DE KLERK, E. P. A., EGELER, R. M., LANKESTER, A. C. & SCHILHAM, M. W. 2005a. Adenovirus infection in children after allogeneic stem cell transplantation: diagnosis, treatment and immunity. *Bone Marrow Transplantation*, 35, S73-S76.
- VAN TOL, M. J. D., KROES, A. C. M., SCHINKEL, J., DINKELAAR, W., CLAAS, E. C. J., JOL-VAN DER ZIJDE, C. M. & VOSSSEN, J. M. 2005b. Adenovirus infection in paediatric stem cell transplant recipients: increased risk in young children with a delayed immune recovery. *Bone Marrow Transplantation*, 36, 39-50.
- VAN OVERBEEK, M., CAPURSO, D., CARTER, MATTHEW M., THOMPSON, MATTHEW S., FRIAS, E., RUSS, C., REECE-HOYES, JOHN S., NYE, C., GRADIA, S., VIDAL, B., ZHENG, J., HOFFMAN, GREGORY R., FULLER, CHRISTOPHER K. & MAY, ANDREW P. 2016. DNA Repair Profiling Reveals Nonrandom Outcomes at Cas9-Mediated Breaks. *Molecular Cell*, 63, 633-646.
- VAZ-DRAGO, R., CUSTÓDIO, N. & CARMO-FONSECA, M. J. H. G. 2017. Deep intronic mutations and human disease. 136, 1093-1111.
- VELTROP-DUIITS, L. A., HEEMSKERK, B., SOMBROEK, C. C., VAN VREESWIJK, T., GUBBELS, S., TOES, R. E. M., MELIEF, C. J. M., FRANKEN, K. L. M. C., HAVENGA, M., VAN TOL, M. J. D. & SCHILHAM, M. W. 2006. Human CD4+ T cells stimulated by conserved adenovirus 5 hexon peptides recognize cells infected with different species of human adenovirus. *European Journal of Immunology*, 36, 2410-2423.
- VELTROP-DUIITS, L. A., VAN VREESWIJK, T., HEEMSKERK, B., THIJSSSEN, J. C. P., EL SEADY, R., JOL-VAN DER ZIJDE, E. M., CLAAS, E. C. J., LANKESTER, A. C., VAN TOL, M. J. D. & SCHILHAM, M. W. 2011. High Titers of Pre-existing Adenovirus Serotype-Specific Neutralizing Antibodies in the Host Predict Viral Reactivation After Allogeneic Stem Cell Transplantation in Children. *Clinical Infectious Diseases*, 52, 1405-1413.
- VERES, A., GOSIS, B. S., DING, Q., COLLINS, R., RAGAVENDRAN, A., BRAND, H., ERDIN, S., COWAN, C. A., TALKOWSKI, M. E. & MUSUNURU, K. 2014. Low incidence of off-target mutations in individual CRISPR-Cas9 and TALEN targeted human stem cell clones detected by whole-genome sequencing. *Cell stem cell*, 15, 27-30.
- WALSH, M. P., CHINTAKUNTLAWAR, A., ROBINSON, C. M., MADISCH, I., HARRACH, B., HUDSON, N. R., SCHNURR, D., HEIM, A., CHODOSH, J., SETO, D. & JONES, M. S. 2009. Evidence of molecular evolution driven by recombination events influencing tropism in a novel human adenovirus that causes epidemic keratoconjunctivitis. *PLoS one*, 4, e5635-e5635.
- WALTER, E. A., GREENBERG, P. D., GILBERT, M. J., FINCH, R. J., WATANABE, K. S., THOMAS, E. D. & RIDDELL, S. R. 1995. Reconstitution of Cellular Immunity against Cytomegalovirus in Recipients of Allogeneic Bone Marrow by Transfer of T-Cell Clones from the Donor. 333, 1038-1044.
- WEISS, A. & LITTMAN, D. R. 1994. Signal transduction by lymphocyte antigen receptors. *Cell*, 76, 263-274.
- WU, C.-A. M., ROTH, T. L., BAGLAENKO, Y., FERRI, D. M., BRAUER, P., ZUNIGA-PFLUCKER, J. C., ROSBE, K. W., WITHER, J. E., MARSON, A. & ALLEN, C. D. C. 2018. Genetic engineering in primary human B cells with CRISPR-Cas9 ribonucleoproteins. *Journal of immunological methods*, 457, 33-40.
- WUCHERPFENNIG, K. W., GAGNON, E., CALL, M. J., HUSEBY, E. S. & CALL, M. E. J. C. S. H. P. I. B. 2010. Structural biology of the T-cell receptor: insights into receptor assembly, ligand recognition, and initiation of signaling. 2, a005140.
- XU, S. & CAO, X. 2010. Interleukin-17 and its expanding biological functions. *Cellular & molecular immunology*, 7, 164-174.
- XUAN, L., JIANG, X., SUN, J., ZHANG, Y., HUANG, F., FAN, Z., GUO, X., DAI, M., LIU, C., YU, G., ZHANG, X., WU, M., HUANG, X. & LIU, Q. 2013. Spectrum of Epstein-Barr Virus-Associated

- Diseases in Recipients of Allogeneic Hematopoietic Stem Cell Transplantation. 96, 560-566.
- ZHANG, X., SUN, S., HWANG, I., TOUGH, D. F. & SPRENT, J. 1998. Potent and Selective Stimulation of Memory-Phenotype CD8⁺ T Cells In Vivo by IL-15. *Immunity*, 8, 591-599.
- ZHANG, Y., HUANG, W., ORNELLES, D. A. & GOODING, L. R. 2010. Modeling Adenovirus Latency in Human Lymphocyte Cell Lines. *Journal of Virology*, 84, 8799-8810.
- ZHENG, X., LU, X., ERDMAN, D. D., ANDERSON, E. J., GUZMAN-COTTRILL, J. A., KLETZEL, M. & KATZ, B. Z. 2008. Identification of adenoviruses in specimens from high-risk pediatric stem cell transplant recipients and controls. *Journal of clinical microbiology*, 46, 317-320.
- ZHENG, Y., STAMMINGER, T. & HEARING, P. 2016. E2F/Rb Family Proteins Mediate Interferon Induced Repression of Adenovirus Immediate Early Transcription to Promote Persistent Viral Infection. *PLOS Pathogens*, 12, e1005415.

Appendix

Abbreviations

ACT	Adoptive T-cell transfer
AdV	Adenovirus
APC	Antigen presenting cell
Bp	Base pair
Cas	CRISPR associated protein
CDR	Complementarity determining regions
Chr	Chromosome
CRISPR	Clustered regularly interspaced palindromic repeats
crRNA	CRISPR RNA
CTL	Cytotoxic T lymphocyte
CTV	CellTrace™ Violet
D	Diversity elements
DC	Dendritic cell
DSB	Double-strand break
FasL	Fas ligand
FSEC	FSECNALGSY
GMP	Good-manufacturing process
gRNA	Guide RNA
GSEE	GSEELRSLY
GvHD	Graft-versus-Host Disease
HAS	Human serum albumin
HDR	Homology-directed repair
HDRT	Homology-directed repair template
HLA	Human leucocyte antigen
HSCT	Hematopoietic stem cell transplantation
IFN	Interferon
IL	Interleukin
INDEL	Insertion and/or Deletion
ITAM	Immunoreceptor tyrosine-based activation motif
J	Joining elements
KO	Knock out
LTDL	LTDLGQNLLY
MHC	Major histocompatibility complex
NHEJ	Non-homologous end-joining

NK cell	Natural killer cell
PAM	Protospacer adjacent motives
PBMC	Peripheral blood mononuclear cell
pMHC	Peptide : major histocompatibility complex
RNP	Ribonucleoprotein complex
SEB	<i>Staphylococcus</i> enterotoxin B
SNP	Single nucleotide polymorphism
TALLEN	Transcription-activator like effector nuclease
Tcm	Central memory T cell
TCR	T-cell receptor
Teff	Effector T cell
Tem	Effector-memory T cell
Th cells	Helper T cells
Tn	Naïve T cell
TRAC	T-cell receptor alpha chain constant region
tracrRNA	Trans-activating CRISPR RNA
TRBC	T-cell receptor beta chain constant region
Tscm	Stem cell-like T cell
V	Variable region or elements
ZFN	Zink finger nucleases

Sequences

Sequence of LTDL-TCR_1 for CRISPR/Cas-mediated homology-directed repair:

The left homology arm is followed by a P2A linker, followed by TCR β chain variable region and the complete human TRBC. A T2A linker separates the TCR- α variable region that is followed by the right homology arm, which is part of the TCR α chain constant region. Mutated PAM sites are indicated in red.

```

CTGCCTTTACTCTGCCAGAGTTATATTGCTGGGGTTTTGAAGAAGATCCTATTAATA
AAAGAATAAGCAGTATTATTAAGTAGCCCTGCATTTTCAGGTTTCCTTGAGTGGCAGGC
CAGGCCTGGCCGTGAACGTTCACTGAAATCATGGCCTCTTGGCCAAGATTGATAGCT
TGTGCCTGTCCCTGAGTCCCAGTCCATCACGAGCAGCTGGTTTCTAAGATGCTATTT
CCCGTATAAAGCATGAGACCGTGACTTGCCAGCCCCACAGAGCCCCGCCCTTGTC
ATCACTGGCATCTGGACTCCAGCCTGGGTTGGGGCAAAGAGGGAAATGAGATCATG
TCCTAACCTGATCCTCTTGTCCCACAGATATCCAGAACCCTGACCCTGCCGTGTAC
CAGCTGAGAGACTCTAAATCCAGTGACAAGTCTGTCTGCCTATTCGGCAGCGGCCG
CACCAACTTCAGCCTGCTGAAGCAGGCCGGCGACGTGGAAGAGAACCCCGGGCCC
ATGGGCTCCAGGCTGCTCTGTTGGGTGCTGCTTTGTCTCCTGGGAGCAGGCCAGT
AAAGGCTGGAGTCACTCAAACCTCAAGATATCTGATCAAACGAGAGGACAGCAAGT
GACACTGAGCTGCTCCCCTATCTCTGGGCATAGGAGTGATCCTGGTACCAACAGAC
CCCAGGACAGGGCCTTCAGTTCCTCTTTGAATACTTCAGTGAGACACAGAGAAACAA
AGGAAACTTCCCTGGTTCGATTCTCAGGGCGCCAGTTCTCTAACTCTCGCTCTGAGAT
GAATGTGAGCACCTTGGAGCTGGGGGACTCGGCCCTTTATCTTTGCGCCAGCAGCT
TGGAGGGCCAAACCGCGGGGGGAGCAGTACTTCGGGCCGGGCACCAGGCTCACGGT
CACAGAGGACCTGAAAACGTGTTCCCACCCGAGGTGCTGTGTTTGAGCCATCAG
AAGCAGAGATCTCCACACCCAAAAGGCCACACTGGTGTGCCTGGCCACAGGCTTC
TACCCCGACCACGTGGAGCTGAGCTGGTGGGTGAATGGGAAGGAGGTGCACAGTG
GGGTCAGCACAGACCCGCAGCCCCTCAAGGAGCAGCCCGCCCTCAATGACTCCAGA
TACTGCCTGAGCAGCCGCCTGAGGGTCTCGGCCACCTTCTGGCAGAACCCCGCAA
CCACTTCCGCTGTCAAGTCCAGTTCTACGGGCTCTCGGAGAATGACGAGTGGACCC
AAGATAGGGCCAAACCTGTCACCCAGATCGTCAGCGCCGAGGCCTGGGGTAGAGCA
GACTGTGGCTTCACCTCCGAGTCTTACCAGCAAGGGGTCTGTCTGCCACCATCCTC
TATGAGATCTTGCTAGGGAAGGCCACCTTGTATGCCGTGCTGGTCAAGTGCCTCGTG
CTGATGGCCATGGTCAAGAGAAAGGATTCCAGAGGCGGCAGCGGGCAGGGCAGAG
GAAGTCTGCTAACATGCGGTGACGTGAGGAGAATCCTGGACCTATGGAGACCCTC
TTGGGCCTGCTTATCCTTTGGCTGCAGCTGCAATGGGTGAGCAGCAAACAGGAGGT
GACGCAGATTCTGCAGCTCTGAGTGTCCAGAAGGAGAAAACCTTGTTTCTCAACTG
CAGTTTCACTGATAGCGCTATTTACAACCTCCAGTGGTTTAGGCAGGACCCTGGGAA
AGGTctcacatctctgttcttATTCAAGTCAAGTCAAGAGAGAGCAAACAAGTGGAAAGACTTAAT
GCCTCGCTGGATAAATCATCAGGACGTAGTACTTTATAATTGCAGCTTCTCAGCCTG
GTGACTCAGCCACCTACCTCTGTGCTGTGATGACAACCTGACAGCTGGGGGAAATTGC
AGTTTGGAGCAGGGACCCAGGTTGTGGTCAACCCAGATATCCAGAACCCTGACCCT
GCCGTGTACCAGCTGAGAGACTCTAAATCCAGTGACAAGTCTGTCTGTCTATTACC
GATTTTGATTCTCAAACAAATGTGTCAAAAGTAAGGATTCTGATGTGTATATCACAG
ACAAAACCTGTGCTAGACATGAGGTCTATGGACTTCAAGAGCAACAGTGTGTGGCCT
GGAGCAACAAATCTGACTTTGCATGTGCAAACGCCTTCAACAACAGCATTATTCAGA
AGACACCTTCTTCCCAGCCCAGGTAAGGGCAGCTTTGGTGCCTTCGCAGGCTGTTT
CCTTGCTTCAGGAATGGCCAGGTTCTGCCAGAGCTCTGGTCAATGATG

```

Sequence of LTDL-TCR_1 for retroviral transduction:

The **human Kozac sequence** is followed by TCR β chain with murine *TRBC* with additional cysteine bridge. A subsequent P2A sequence is followed by TCR α chain including murine *TRAC* with additional cysteine bridge, cloned into pMP71 vector.

GCCGCCACCATGGGCTCCAGGCTGCTCTGTTGGGTGCTGCTTTGTCTCCTGGGAGC
 AGGCCAGTAAAGGCTGGAGTCACTCAAACCTCAAAGATATCTGATCAAACGAGAGG
 ACAGCAAGTGACTGAGCTGCTCCCCTATCTCTGGGCATAGGAGTGTATCCTGGTA
 CCAACAGACCCAGGACAGGGCCTTCAGTTCCTCTTTGAATACTTCAGTGAGACACA
 GAGAAACAAAGGAACTTCCCTGGTCGATTCTCAGGGCGCCAGTTCTCTAACTCTCG
 CTCTGAGATGAATGTGAGCACCTTGGAGCTGGGGGACTCGGCCCTTTATCTTTGCGC
 CAGCAGCTTGGAGGGCCAAACCGCGGGGGAGCAGTACTTCGGGCCGGGCACCAGG
 CTCACGGTCACAGAGGATCTGAGAAATGTGACTCCACCCAAGGTCTCCTTGTGGAG
 CCATCAAAGCAGAGATTGCAAACAAACAAAAGGCTACCCTCGTGTGCTTGGCCAGG
 GGCTTCTTCCCTGACCACGTGGAGCTGAGCTGGTGGGTGAATGGCAAGGAGGTCCA
 CAGTGGGGTCTGCACGGACCCTCAGGCCTACAAGGAGAGCAATTATAGCTACTGCC
 TGAGCAGCCGCTGAGGGTCTCTGCTACCTTCTGGCACAATCCTCGAAACCACTTCC
 GCTGCCAAGTGACAGTTCATGGGCTTTCAGAGGAGGACAAGTGGCCAGAGGGCTCA
 CCCAAACCTGTCACACAGAACATCAGTGCAGAGGCCTGGGGCCGAGCAGACTGTGG
 AATCACTTCAGCATCCTATCATCAGGGGGTTCTGTCTGCAACCATCCTCTATGAGATC
 TACTGGGGAAGGCCACCCTATATGCTGTGCTGGTCAAGTGGCCTGGTGCTGATGGC
 CATGGTCAAGAAAAAATTCCGGCAGCGGCCACCAACTTCAGCCTGCTGAAGC
 AGGCCGGCGACGTGGAAGAGAACCCTGGGCCCATGGAGACCCTCTTGGGCCTGCT
 TATCCTTTGGCTGCAGCTGCAATGGGTGAGCAGCAAACAGGAGGTGACGCAGATTC
 CTGCAGCTCTGAGTGTCCCAGAAGGAGAAAACCTTGGTTCTCAACTGCAGTTTCACTG
 ATAGCGCTATTTACAACCTCCAGTGGTTTAGGCAGGACCCTGGGAAAGGTCTCACAT
 CTCTGTTGCTTATTCAGTCAAGTCAGAGAGAGCAAACAAGTGGAAAGACTTAATGCCT
 CGCTGGATAAATCATCAGGACGTAGTACTTTATACATTGCAGCTTCTCAGCCTGGTGA
 CTCAGCCACCTACCTCTGTGCTGTGCATGACAACTGACAGCTGGGGGAAATTGCAGTT
 TGGAGCAGGGACCCAGGTTGTGGTCACCCAGATATCCAGAACCCAGAACCTGCTG
 TGTACCAGTTAAAAGATCCTCGGTCTCAGGACAGCACCTCTGCCTGTTACCGACT
 TTGACTCCCAAATCAATGTGCCGAAAACCATGGAATCTGGAACGTTTCATCACTGACAA
 ATGCGTGCTGGACATGAAAGCTATGGATTCCAAGAGCAATGGGGCCATTGCCTGGA
 GCAACCAGACAAGCTTCCCTGCCAAGATATCTTCAAAGAGACCAACGCCACCTACC
 CCAGTTCAGACGTTCCCTGTGATGCCACGTTGACTGAGAAAAGCTTTGAAACAGATA
 TGAACCTAACTTTCAAACCTGTCAGTTATGGGACTCCGAATCCTCCTGCTGAAAGT
 AGCCGGATTTAACCTGCTCATGACGCTGAGGCTGTGGTCCAGTTGA

Sequence of LTDL-TCR_2 for retroviral transduction:

The **human Kozac sequence** is followed by **TCR β chain** with murine *TRBC* with additional cysteine bridge. A subsequent **P2A sequence** is followed by **TCR α chain** including murine *TRAC* with additional cysteine bridge, cloned into pMP71 vector.

GCCGCCACCATGGGCTCCAGGCTGCTCTGTTGGGTGCTGCTTTGTCTCCTGGGAGC
 AGGCCCAGTAAAGGCTGGAGTCACTCAAACCTCAAAGATATCTGATCAAACGAGAGG
 ACAGCAAGTGACTGAGCTGCTCCCTATCTCTGGGCATAGGAGTGATCCTGGTA
 CCAACAGACCCAGGACAGGGCCTTCAGTTCCTCTTTGAATACTTCAGTGAGACACA
 GAGAAACAAAGGAACTTCCCTGGTTCGATTCTCAGGGCGCCAGTTCTCTAACTCTCG
 CTCTGAGATGAATGTGAGCACCTTGGAGCTGGGGGACTCGGCCCTTTATCTTTGCGC
 CAGCAGCTTGGAGGGACAGACAACGGGTGAGCAGTTCTTCGGGCCAGGGACACGG
 CTCACCGTGCTAGAGGATCTGAGAAATGTGACTCCACCCAAGGTCTCCTTGTTGAG
 CCATCAAAGCAGAGATTGCAAACAAACAAAAGGCTACCCTCGTGTGCTTGGCCAGG
 GGCTTCTTCCCTGACCACGTGGAGCTGAGCTGGTGGGTGAATGGCAAGGAGGTCCA
 CAGTGGGGTCTGCACGGACCCTCAGGCCTACAAGGAGAGCAATTATAGCTACTGCC
 TGAGCAGCCGCCTGAGGGTCTCTGCTACCTTCTGGCACAATCCTCGAAACCACTTCC
 GCTGCCAAGTGACAGTTCATGGGCTTTCAGAGGAGGACAAGTGGCCAGAGGGCTCA
 CCCAAACCTGTCACACAGAACATCAGTGCAGAGGCCTGGGGCCGAGCAGACTGTGG
 AATCACTTCAGCATCCTATCATCAGGGGGTTCTGTCTGCAACCATCCTCTATGAGATC
 CTAAGTGGGAAAGGCCACCCTATATGCTGTGCTGGTCAAGTGGCCTGGTGTGATGCC
 CATGGTCAAGAAAAAATTCCGGCAGCGGGCCACCAACTTCAGCCTGCTGAAGC
 AGGCCGGCGACGTGGAAGAGAACCCCGGGCCCATGGAGACCCTCTTGGGCCTGCT
 TATCCTTTGGCTGCAGCTGCAATGGGTGAGCAGCAAACAGGAGGTGACGCAGATTC
 CTGCAGCTCTGAGTGTCCCAGAAGGAGAAAACCTTGGTTCTCAACTGCAGTTTCACTG
 ATAGCGCTATTTACAACCTCCAGTGGTTTAGGCAGGACCCTGGGAAAGGTCTCACAT
 CTCTGTTGCTTATTCAGTCAAGTCAAGTCAAGTCAAGTCAAGTCAAGTCAAGTCAAGT
 CGCTGGATAAATCATCAGGACGTAGTACTTTATACATTGCAGCTTCTCAGCCTGGTGA
 CTCAGCCACCTACCTCTGTGCTGTGCATCCGAAGTGCAGCTGGGGGAAATTGCAGTT
 TGGAGCAGGGACCCAGGTTGTGGTCAACCCAGATATCCAGAACCCAGAACCTGCTG
 TGTACCAGTTAAAAGATCCTCGGTCTCAGGACAGCACCCCTCTGCCTGTTACCGACT
 TTGACTCCCAAATCAATGTGCCGAAAACCATGGAATCTGGAACGTTTCATCACTGACAA
 ATGCGTGCTGGACATGAAAGCTATGGATTCCAAGAGCAATGGGGCCATTGCCTGGA
 GCAACCAGACAAGCTTCACCTGCCAAGATATCTTCAAAGAGACCAACGCCACCTACC
 CCAGTTCAGACGTTCCCTGTGATGCCACGTTGACTGAGAAAAGCTTTGAAACAGATA
 TGAACCTAACTTTCAAACCTGTCAGTTATGGGACTCCGAATCCTCCTGCTGAAAGT
 AGCCGGATTTAACCTGCTCATGACGCTGAGGCTGTGGTCCAGTTGA

List of figures

Figure 1: T-cell receptor structure and diversity due to gene rearrangement.....	10
Figure 2: Cytotoxic capacities of cytotoxic T cells	11
Figure 3: Three major capsid proteins form the icosahedral shape of adenovirus capsid	14
Figure 4: Magnetic isolation of LTDL-specific T cells using pMHC I Streptamer	16
Figure 5: CRISPR/Cas9-mediated genome engineering	19
Figure 6: Adoptive transfer of LTDL-specific T cells controls AdV infection in vivo	21
Figure 7: Highly efficient TCR KO in primary human T cells.....	39
Figure 8: Stable and functionally disrupted TCR-KO samples maintain CD4/CD8 ratios, expansion characteristics, and T-cell phenotypes	41
Figure 9: SNPs and INDELS detected by whole-genome sequencing	43
Figure 10: On-target read frequencies decrease in CRISPR/Cas-edited samples.....	44
Figure 11: TRBC gRNA-dependent off-target events.....	48
Figure 12: Recombinant T cells demonstrate high LTDL-specific functionality	50
Figure 13: Cytotoxic capacity of transduced LTDL-specific T cells	51
Figure 14: CRISPR/Cas9-mediated TCR replacement	53
Figure 15: Functional LTDL-specific T-cell response after CRISPR/Cas9-mediated TCR replacement.....	55

Figure 1A is adapted by permission from Springer Nature Customer Service Centre GmbH: Springer Nature, *Nature Reviews Immunology* 8, pages 895–900 (2008), Do T cells need endogenous peptides for activation? Nicholas R. J. Gascoigne, Copyright © 2008, Nature Publishing Group. DOI: 10.1038/nri2431

Figure 1B is adapted by permission from Springer Nature Customer Service Centre GmbH: Springer Nature, *Nature Reviews Immunology* 6, pages 883–894 (2006), Structural determinants of T-cell receptor bias in immunity. Stephen J. Turner, Peter C. Doherty, James McCluskey & Jamie Rossjohn, Copyright © 2006, Nature Publishing Group. DOI: 10.1038/nri1977

Figure 2 is adapted from Elsevier open access, *Journal of Investigative Dermatology* Volume 126, ISSUE 1, P32-41, Cytotoxic T cells. Mads Hald Andersen, David Schrama, Per Thor Straten, Jürgen C. Becker. Copyright © 2006 The Society for Investigative Dermatology, Inc. DOI: 10.1038/sj.jid.5700001

Figure 3 is adapted from HHS Public Access author manuscript, *Science* Vol 329, Issue 5995, pp. 1071-1075 (2010), Crystal Structure of Human Adenovirus at 3.5 Å Resolution. Vijay S. Reddy S. Kundhavai NatchiarPhoebe L. Stewartand Glen R. Nemerow. Copyright © 2010, American Association for the Advancement of Science. DOI: 10.1126/science.1187292

Parts of the results and figure 7A are published by John Wiley and Sons open access, *Clinical & Translational Immunology* 11(1):e1372 (2022), Genome-wide off-target analyses of CRISPR/Cas9-mediated T-cell receptor engineering in primary human T cells. Theresa Kaeuferle , [Tanja A Stief](#) , Stefan Canzar, Nayad N Kutlu, Semjon Willier, Dana Stenger, Paulina Ferrada-Ernst, Nicola Habjan,

Annika E Peters, Dirk H Busch, Tobias Feuchtinger. Copyright © 2022 The Authors. Clinical & Translational Immunology published by John Wiley & Sons Australia, Ltd on behalf of Australian and New Zealand Society for Immunology, Inc. DOI: 10.1002/cti2.1372

Parts of the results including figures 6, 13A, 14A, 14B, 14C, 14D, and 14E are published by Elsevier, Molecular Therapy 30(1):198-208 (2022), Protective T cell receptor identification for orthotopic reprogramming of immunity in refractory virus infections. [Tanja A. Stief](#); Theresa Kaeuferle; Thomas R. Müller; Michaela Döring; Lena M. Jablonowski; Kilian Schober; Judith Feucht; Kevin M. Dennehy; Semjon Willier; Franziska Blaeschke; Rupert Handgretinger; Peter Lang; Dirk H. Busch; Tobias Feuchtinger. Copyright © 2022, Elsevier. DOI: 10.1016/j.ymthe.2021.05.021

List of tables

Table 1: Structure of protective LTDL-specific TCRs	21
Table 2: Identification of TRAC gRNA-dependent mutations	45
Table 3: Identification of TRBC gRNA-dependent mutations	46

Table 1 is published by John Wiley and Sons open access, Clinical & Translational Immunology 11(1):e1372 (2022), Genome-wide off-target analyses of CRISPR/Cas9-mediated T-cell receptor engineering in primary human T cells. Theresa Kaeuferle , [Tanja A Stief](#) , Stefan Canzar, Nayad N Kutlu, Semjon Willier, Dana Stenger, Paulina Ferrada-Ernst, Nicola Habjan, Annika E Peters, Dirk H Busch, Tobias Feuchtinger. Copyright © 2022 The Authors. Clinical & Translational Immunology published by John Wiley & Sons Australia, Ltd on behalf of Australian and New Zealand Society for Immunology, Inc. DOI: 10.1002/cti2.1372

Eidesstattliche Versicherung

Ich versichere hiermit an Eides statt, dass meine Dissertation selbständig und ohne unerlaubte Hilfsmittel angefertigt worden ist.

Die vorliegende Dissertation wurde weder ganz, noch teilweise bei einer anderen Prüfungskommission vorgelegt.

Ich habe noch zu keinem früheren Zeitpunkt versucht, eine Dissertation einzureichen oder an einer Doktorprüfung teilzunehmen.

München, den 07.10.2021

Tanja Stief

Danksagung

An dieser Stelle möchte ich mich bei allen Menschen bedanken, die mich während meiner Promotion auf unterschiedliche Art und Weise unterstützt haben. Auch wenn ich hier nicht alle aufzählen kann, habe ich doch niemanden vergessen.

An erster Stelle möchte ich mich bei Prof. Dr. Tobias Feuchtinger für die Möglichkeit bedanken, dass ich diese spannende Forschungsarbeit in seiner Arbeitsgruppe anfertigen durfte. Vielen Dank für Ihre fachliche Anleitung und Unterstützung, durch die ich viel dazugelernt habe.

Mein besonderer Dank gilt Prof. Dr. Heinrich Leonhardt für die Betreuung und Begutachtung meiner Arbeit seitens der Fakultät für Biologie der Ludwig-Maximilians-Universität, München.

Dem Deutschen Zentrum für Infektionsforschung (DZIF) und dem Ausbildungs-Programm des Elitenetzwerks Bayern – iTarget danke ich für die wissenschaftliche und finanzielle Förderung. Außerdem möchte ich mich bei allen Patienten und ihren Familien bedanken, die diese Forschung überhaupt erst möglich machen.

Mein größter Dank gilt Dr. Theresa Käuferle, die meine erste Anlaufstelle bei Fragen und Problemen war. Liebe Theresa, du hast mir so vieles beigebracht und mich immer unterstützt. Danke, dass du immer ein offenes Ohr für mich hattest und mir mit deinen vielen Ratschlägen oftmals neue Wege aufgezeigt hast. Du hast meine Arbeit in vielerlei Hinsicht bereichert.

Außerdem möchte ich mich bei Thomas Müller und Dr. Kilian Schober bedanken, die mir vor allem bei dem schwierigen Projektstart geholfen haben.

Vielen Dank auch allen Mitgliedern der AG Feuchtinger, die die Zeit im Labor aber auch außerhalb zu etwas ganz Besonderem gemacht haben. Danke für anregende Diskussionen, neue Impulse und großartige Gespräche. Besonders hervorheben möchte ich Dana Stenger, mit der ich in das Abenteuer Promotion gestartet bin. Aber auch Larissa Deisenberger und Lena Jablonowski waren wichtige Personen in den vergangenen Jahren.

Danke auch an Heidi, Gaby, Susi, Rafaele, Valerie, Pilar und so vielen mehr aus dem Kubus und dem Dr. von Hauner'schen Kinderspital.

Mein herzlichster Dank gilt meinen Eltern für ihre bedingungslose Unterstützung, durch die diese lange Ausbildung überhaupt erst möglich war. Danke für alles!